

AMERICAN UNIVERSITY OF BEIRUT

STRESS DISTRIBUTION ON THE TEMPORO-
MANDIBULAR JOINT (TMJ) IN UNILATERAL SAGITTAL
SPLIT OSTEOTOMY (USSO):
A FINITE ELEMENT ANALYSIS STUDY

By

CHRISTOPHER GEORGES KHAWAM

A thesis
submitted in partial fulfillment of the requirements
for the degree of Master of Science
to the Department of Dentofacial Medicine
of the Faculty of Medicine
at the American University of Beirut

Beirut, Lebanon
April, 2023

AMERICAN UNIVERSITY OF BEIRUT

STRESS DISTRIBUTION ON THE TEMPORO-
MANDIBULAR JOINT (TMJ) IN UNILATERAL SAGITTAL
SPLIT OSTEOTOMY (USSO):
A FINITE ELEMENT ANALYSIS STUDY

By

CHRISTOPHER GEORGES KHAWAM


Approved by:


Dr. Joseph G. Ghafari, Professor and Chairman
Department of Dentofacial Medicine


Chairman of Committee


Dr. Ramzi V. Haddad, Associate Professor
Department of Dentofacial Medicine


Advisor and Member of Committee


Dr. Samir A. Mustapha, Associate Professor
Department of Mechanical Engineering

Member of Committee


Dr. Najj Y. Abou Chebel, Clinical Instructor
Department of Dentofacial Medicine

Member of Committee


Dr. Makram J. Ammourey, Adjunct Clinical Instructor
Department of Dentofacial Medicine

Member of Committee

Date of thesis defense: April 27, 2023

AMERICAN UNIVERSITY OF BEIRUT

THESIS RELEASE FORM

Student Name: Khawam Christopher Georges

I authorize the American University of Beirut, to: (a) reproduce hard or electronic copies of my thesis; (b) include such copies in the archives and digital repositories of the University; and (c) make freely available such copies to third parties for research or educational purposes:

- As of the date of submission
- One year from the date of submission of my thesis.
- Two years from the date of submission of my thesis.
- Three years from the date of submission of my thesis.



May 9, 2023

Signature

Date

ACKNOWLEDGEMENTS

I would like to express my deepest gratitude to all those who have helped me during my thesis journey.

First and foremost, I would like to thank my thesis advisor, Dr. Ramzi Haddad, for his guidance, expertise, and unwavering support throughout this process. His insightful feedback, constructive criticism, and endless encouragement have been invaluable in shaping the direction of my research.

I would also like to thank the Head of the Department of Dentofacial Medicine at the American University of Beirut, Pr. Joseph Ghafari for his dedication to academic excellence and his unwavering commitment to providing students with the resources and support necessary to succeed, and for giving me the opportunity to be in this second to none program.

I would also like to thank Dr. Makram Ammouy and Dr. Kinan Zeno for their constant help and guidance throughout my residency years with the clinical education as well as the finite element process for my thesis.

I would also like to thank Dr. Naji Abou Chebel the extraordinary maxillofacial surgeon for his teachings and contributions which helped greatly with my clinical education.

Furthermore, I am deeply grateful to my family and friends and my love Kiona Ghawi for their constant encouragement and support. Their unwavering belief in me and my abilities has been a source of inspiration and motivation throughout my academic journey.

In conclusion, I would like to express my heartfelt thanks to all those who have contributed to my thesis in one way or another. Your support and encouragement have been instrumental in helping me achieve my academic goals.

ABSTRACT OF THE THESIS OF

Christopher George Khawam

for

Master of Science

Major: Orthodontics

Title: Stress distribution on the temporo-mandibular joint (TMJ) in unilateral sagittal split osteotomy (USSO): A finite element analysis study

Introduction:

Bilateral sagittal split osteotomy (BSSO) is a standard technique in mandibular orthognathic surgery to correct facial asymmetries. Unilateral SSO was introduced as a less aggressive alternative limited to only one side of the mandible and with a narrow range of movement. Stress distribution on the condyles in USSO has not been addressed to determine symmetry of balance in this asymmetric procedure.

Hypothesis/aims:

The aims of this study are to evaluate: 1. the stress distribution on and displacement of the contralateral and ipsilateral neck of the condyles and menisci in simulated models of patients treated with USSO following graded movements of the mandible in advancement and setback; 2. the effect of condylar volume variation on stress distribution. The main hypothesis was that minimal stress would be registered on the operated condyle, and that a threshold should exist at which either advancement or setback mandibular movements should not be detrimental to condylar position and function.

Methods:

This retrospective study was conducted on 8 pretreatment CT scans of patients who presented for the surgical correction of mandibular asymmetry and who qualified for the USSO based on established inclusion criteria. USSO 3D movements (unilateral advancement and setback) in increments of 2 mm (from 4 to 12mm) were simulated in a finite element (FE) model and the corresponding stresses measured at the level of the temporomandibular structures (condyles and their respective discs and glenoid fossae). Stress distributions and displacements were analyzed for the different surgical movements through analyses of variance for group comparisons between advancement and setback and within the USSO variables, and correlation tests for associations among variables.

Results:

Stress and displacement at the condyle were higher on the non-operated than the operated side: highest on the anterior, posterior and lateral condylar surfaces, at the medial surface of the condylar neck, on the anterior condylar surface during setback, and posterior surface during advancement. The pattern of stress distribution suggested a lateral outward rotation of the condyle on the non-operated side. More displacement (up to 1.3mm) occurred at the

non-operated than operated condyle. When condylar volume increased the displacement decreased. A balance of stress and displacement was observed at 6mm of advancement or setback before a new cycle of stress increase and decline. Increase in displacement was associated with increase in stress.

Conclusions:

1. This study was the first to contribute FE modeling and findings based on the individual variations among 8 human subjects who underwent USSO surgery.
2. With increased surgical movements, statistically significant increase in stress was observed at the level of the condyles, condylar necks, and menisci on the operated and non-operated sides.
3. The non-operated side disclosed most differences with incremental surgical movements.
4. Individual velocity changes suggested a balance of stress between operated and non-operated sides between 4 and 6 mm of mandibular advancement or setback, which corresponded to the actual amount of surgical movement in the 8 patients under study.
5. This research yielded a clinically testable hypothesis that should be explored in future FE models and direct clinical investigations.

Significance:

The significance of this research is the determination of the range of the surgical movements with the least and most stress on the temporomandibular structures thus the limits of mandibular displacement using the USSO.

TABLE OF CONTENTS

ACKNOWLEDGEMENTS	1
ABSTRACT	2
ILLUSTRATIONS	9
TABLES	11
INTRODUCTION	12
A. History of orthognathic surgery	12
B. Engineering influence in orthodontics: orthognathic surgery and 3D virtual planning	16
LITERATURE REVIEW	18
A. The Temporo-Mandibular Joint (TMJ).....	18
1. Anatomy.....	18
2. Articular Dynamics	19
3. Pathologies of the TMJ	20
B. Combined orthodontic-surgical treatment of Class II and CL III malocclusion.....	21
1. Incisor Decompensation	23
a. Sagittal (anteroposterior) plane.....	23
b. Transverse plane	24
c. Vertical plane.....	25
2. Double Jaw surgery Vs mandibular only surgery.....	26

C.	BSSO vs USSO.....	27
D.	Finite Element Analysis (FEA).....	29
1.	Definition.....	30
2.	3D imaging	31
a.	Evolution towards 3D imaging.....	31
b.	CBCT vs CT scans.....	33
3.	Development of FEA in dentistry	34
4.	Limitations and inaccurate assumptions	35
a.	Generalizability of results.....	37
b.	3D Modeling of human tissues	39
5.	FEA in orthodontics.....	41
6.	Significance	43
E.	Specific aims.....	46
F.	Hypothesis	46
MATERIAL AND METHODS.....		47
A.	Material.....	47
1.	Anatomical record.....	47
B.	Methods	48
1.	3D model.....	48
a.	Model segmentation.....	48
i.	Bone/teeth masks	49
ii.	Articular disk/Meniscus Mask.....	51

iii. Smoothing.....	51
iv. Surgical cut	52
b. Meshing Process	56
2. Finite Element Analysis (FEA).....	58
a. Definition of material properties.....	58
b. Interactions.....	59
c. Loading setups	61
i. Load	61
ii. Boundary conditions	62
a. Data collection	63
i. Measures	63
3. Statistical analysis.....	66
RESULTS	69
A. PART 1: change in stress and displacement relative to surgical movement: case series.....	69
1. Stress at the neck of the condyles	70
2. Stress at the anterior surface of the meniscus	71
3. Stress at the different condylar surfaces	73
4. Displacement at the condyles and condylar necks.....	78
B. PART 2: Comparisons of the outcome variables between surgical groups, degree of movements and sides	79
1. Difference between advancement and setback	80
2. Effect of ammount of surgical movement and side (operated vs non-operated)	81

a. Stress at the condylar necks	83
b. Stress at the medial surface of the menisci	86
c. Stress at the lateral surface of the menisci	86
d. Stress at the anterior surface of the menisci	88
e. Stress at the posterior surface of the menisci	89
f. Displacement of the condyles.....	94
g. Displacement of the neck of the condyles	94
C. Correlations	96
1. Correlation between displacement and stress with the incremental surgical movements (4, 6, 8, 10, 12 mm) at the neck of the condyle	96
2. Correlation between displacement and condylar volume with the incremental surgical movements (4, 6, 8, 10, 12 mm)	96
DISCUSSION	98
A. Strengths	99
1. Individual variation.....	99
2. Complete 3D model	Error! Bookmark not defined.
B. FEA studies	100
C. Assessment of the methods	Error! Bookmark not defined.
D. Assessment of the findings	107
E. Clinical implications.....	107
F. Limitations and research considerations.....	107
CONCLUSION	109
APPENDIX	111

REFERENCES 113

ILLUSTRATIONS

Figure

1.1. HULLIHEN'S MANDIBULAR BODY OSTECTOMY (FONSECA R.J., 2017).	13
1.2. CALDWELL AND LETTERMAN'S VERTICAL SUBSIGMOID OSTECTOMY (FONSECA R.J., 2017).	14
1.3. OBWEGESER-DAL PONT BILATERAL SAGITTAL SPLIT OSTECTOMY (BÖCKMANN ET AL., 2014).	15
1.4. ORTHOGNATHIC SURGERY 3D VIRTUAL PLANNING (CHOI JONG-WOO & LEE JANG YEOL, 2021)..	17
2.1. ANATOMY OF THE TEMPORO-MANDIBULAR JOINT (NETTER, FRANK H; NORTON, NEIL SCOTT; MACHADO, 2017).....	19
2.2. NORMAL TEMPORO-MANDIBULAR JOINT DYNAMICS(AMINI B., 2015)	20
2.3. PRESURGICAL INCISORS DECOMPENSATION IN CL III PATIENT (K. J. LEE, 2014).....	24
2.4. PRESURGICAL TRANSVERSE DENTAL DECOMPENSATION (K. J. LEE, 2014).	25
3.1. MASK CREATION FROM A SKULL CT SCAN IN SIMPLEWARE SCAN IP.....	49
3.2. PAINT WITH THRESHOLD TOOL FOR THE CREATION OF THE MANDIBULAR MASK.....	50
3.3. MASKS OF THE MENISCI	51
3.4. MANDIBULAR MODEL WITH THE DIFFERENT MASKS (TEMPORAL, MENISCUS, MANDIBLE).	52
3.5. SIMULATION OF THE UNILATERAL SAGITTAL SPLIT OSTECTOMY.	54
3.6. FINITE ELEMENT MODEL OF THE 8 DIFFERENT CT SCANS. A: PATIENTS THAT UNDERWENT ADVANCEMENT SURGERY. B: PATIENTS THAT UNDERWENT SETBACK SURGERY.....	55
3.7. MESHED MODEL OF THE MANDIBLE.....	58
3.8. TANGENTIAL AND NORMAL BEHAVIOR CONTACT PROPERTIES.....	60
3.9. HINGE TYPE CONNECTORS AT THE LEVEL OF THE CONDYLES.	61
3.10. DIRECTION VECTORS OF THE DISPLACEMENT WITH THE DATUM AXIS.	62
3.11. BOUNDARY CONDITIONS SETTINGS.....	63
3.12. SEPARATION METHOD FOR THE DIFFERENT SURFACE OF THE MENISCUS AND CONDYLES.	65
3.13. CONDYLAR VOLUME CALCULATION IN SIMPLEWARE SCAN IP.	66
4.1. FINITE ELEMENT ANALYSIS VISUAL REPRESENTATION OF THE STRESS INCREASE AT THE LEVEL OF THE NECK OF THE CONDYLES IN ONE PATIENT WHOSE USSO INVOLVED MANDIBULAR ADVANCEMENT, AND ANOTHER WITH MANDIBULAR SETBACK. NOTE THE HIGHER STRESSES ON THE NON-OPERATED SIDE, MORE INTENSE AND DIFFUSED IN THE SETBACK OPERATION.....	70
4.2. VELOCITY CURVES ILLUSTRATING STRESS (Y AXIS) AT THE NECK OF THE CONDYLES RELATIVE TO INCREMENTAL SURGICAL ADVANCEMENT (A) AND SETBACK (B) MOVEMENTS (X AXIS) ON THE OPERATED AND NON-OPERATED SIDES.....	71
4.3. FINITE ELEMENT ANALYSIS VISUAL REPRESENTATION OF THE STRESS INCREASE AT THE LEVEL OF THE MENISCI IN ONE PATIENT WITH ADVANCEMENT USSO AND ANOTHER WITH MANDIBULAR SETBACK. NOTE THE HIGHER STRESSES ON THE NON-OPERATED SIDE INCREASED WITH THE SURGICAL MOVEMENT AND MORE INTENSE IN THE SETBACK OPERATION.....	72
4.4. VELOCITY CURVES ILLUSTRATING STRESS (Y AXIS) AT THE ANTERIOR SURFACE OF THE MENISCUS RELATIVE TO INCREMENTAL SURGICAL ADVANCEMENT (A) AND SETBACK (B) MOVEMENTS (X AXIS) ON THE OPERATED AND NON-OPERATED SIDES.....	73
4.5. FINITE ELEMENT ANALYSIS VISUAL REPRESENTATION OF THE STRESS INCREASE AT THE LEVEL OF THE NON-OPERATED CONDYLE IN ONE PATIENT WITH ADVANCEMENT USSO AND ANOTHER WITH MANDIBULAR SETBACK. NOTE THE HIGHER STRESSES ON THE NON-OPERATED SIDE INCREASED WITH THE SURGICAL MOVEMENT.....	74

4.6. Velocity curves of individual advancement patients plotting stress at the condyles relative to the incremental surgical movements ranges with the black arrow showing actual surgical movements done by the surgeon.....	75
4.7. Velocity curves of individual setback patients plotting stress at the condyles relative to the incremental surgical movements ranges with the black arrow showing actual surgical movements done by the surgeon.....	76
4.8. Graphs representing the velocity curves of mean stresses at various condylar surfaces relative to incremental surgical advancement and setback movements.....	77
4.9. Graphs representing the velocity curve of the displacement at the condyles relative to surgical advancement (A) and setback (B) movements.....	78
4.10. Graph representing the velocity curve of the displacement at the neck of the condyles relative to surgical advancement (A) and setback (B) movements.....	78
4.11. Stress at the level of the neck of the condyle: A. Advancement; B: Setback, Side 1= operated, Side 2= non-operated.(Amount 1 = 4mm; 2= 6mm; 3= 8mm; 4= 10mm; 5= 12mm).....	83
4.12. Von mises stresses (y axis) at the level of the medial surface of the meniscus in the advancement (A) and setback (B) groups.Amounts of movements (x axis): 1 = 4mm; 2= 6mm; 3= 8mm; 4= 10mm; 5= 12mm.Condylar sides: 1- operated, 2- non-operated.....	85
4.15. Von mises stresses (y axis) at the level of the lateral surface of the meniscus in the advancement (A) and setback (B) groups.Amounts of movements (x axis): 1 = 4mm; 2= 6mm; 3= 8mm; 4= 10mm; 5= 12mm.Condylar sides: 1- operated, 2- non-operated.....	87
4.14. Von mises stresses (y axis) at the level of the anterior surface of the meniscus in the advancement (A) and setback (B) groups.Amounts of movements (x axis): 1 = 4mm; 2= 6mm; 3= 8mm; 4= 10mm; 5= 12mm.Condylar sides: 1- operated, 2- non-operated.....	89
4.15. Von mises stresses (y axis) at the level of the posterior surface of the meniscus in the advancement (A) and setback (B) groups.Amounts of movements (x axis): 1 = 4mm; 2= 6mm; 3= 8mm; 4= 10mm; 5= 12mm.Condylar sides: 1- operated, 2- non-operated.....	91
4.16. Displacement at the level of the condyles in the advancement (A) and setback (B) groups.Amounts of movements (x axis): 1 = 4mm; 2= 6mm; 3= 8mm; 4= 10mm; 5= 12mm.Condylar sides: 1- operated, 2- non-operated.....	93
4.17. Displacement at the level of the neck of the condyles in the advancement (A) and setback (B) groups.Amounts of movements (x axis): 1 = 4mm; 2= 6mm; 3= 8mm; 4= 10mm; 5= 12mm.Condylar sides: 1- operated, 2- non-operated.....	95

TABLES

Table

3.1. Material properties of the different components of the models.....	59
4.1. Three-way mixed ANOVA interactions for the different variables.	80
4.2. Comparison of the outcome variables between advancement and setback	81
4.3. Stress at the condylar neck in the advancement group (n=4).....	82
4.4. Stress at the condylar neck in the setback group (n=4)	83
4.5. Stress at the medial surface of the menisci in the advancement group (n=4).....	84
4.6. Stress at the medial surface of the menisci in the setback group (n=4).....	85
4.7. Stress at the lateral surface of the menisci in the advancement group (n=4).....	86
4.8. Stress at the lateral surface of the menisci in the setback group (n=4).....	87
4.9. Stress at the anterior surface of the menisci in the advancement group (n=4)	88
4.10. Stress at the anterior surface of the menisci in the setback group (n=4)	89
4.11. Stress at the posterior surface of the menisci in the advancement group (n=4)	90
4.12. Stress at the posterior surface of the menisci in the setback group (n=4)	90
4.13. Displacement of the condyle in the advancement group (n=4)	92
4.14. Displacement of the condyle in the setback group (n=4).	93
4.15. Displacement of the neck of the condyle in the advancement group (n=4).	94
4.16. Displacement of the neck of the condyle in the setback group (n=4).....	95
4.17. Pearson's correlation coefficients between displacement and stress with the incremental surgical movements (4,6,8,10,12mm) at the neck of the condyles.....	96
4.18. Pearson's correlation coefficients between displacement and condylar volume in operated and non-operated sides.....	97
5.1. Summary of aims and conclusions from articles on post BSSO condylar changes. ...	105

CHAPTER I

INTRODUCTION

A. History of orthognathic surgery

Teeth crowding and malposition have been perceived as problematic since the primitive civilizations that dates back at least to 1000 BC. Early attempts of adjustment and modification of this condition have been seen in the Etruscan and the Greeks who designed primitive orthodontic appliances.(Proffit, W.R., Fields Jr, H. W. & Sarver, 2012)

In more severe cases where no orthodontic treatment can offer a solution for the correction of extreme malocclusions and dentofacial discrepancies, surgery to readjust and well align the jaws at fault is the only answer. A proper coordination between surgery and orthodontics should be maintained in order to reach a favorable treatment outcome with stable functional and esthetic results to enhance the quality of life of the patient.(Bell, 2018)

Many pioneers contributed to the development and refinement of the modern orthognathic techniques after the early 18th century period of surgery without orthodontics which had a large number of unsuccessful and compromised treatments. The first mandibular body ostectomy and osteotomy was performed in 1849 at the hands of the father of American orthognathic and maxillofacial surgery Simon P. Hüllihen from wheeling, West Virginia and it was used mainly for the correction of skeletal anterior open bite (Figure1.1). His technique comprised a wedge ostectomy at the level of the premolars

for backward repositioning of the mandible and the use of silver-plated occlusal splints for bony consolidation.

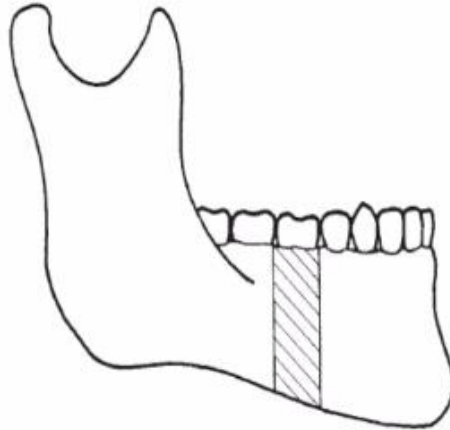


Figure 1.1. Hullihen's mandibular body osteotomy (Fonseca R.J., 2017).

The father of American plastic surgery Wilbur P. Blair not only modified Hullihen's technique by executing segmental mandibular body osteotomy as proposed by the pioneer orthodontist Edward H. Angle, but also, he integrated his horizontal osteotomy of the ramus, situated between the mandibular foramen and the sigmoid notch. He also highlighted the value of the symbiotic orthodontist-surgeon relationship in the success of treatment. In 1906, Anton Freiherr von Eiselsberg designed the step osteotomy for mandibular set-back in order to increase the bony contact surface area.

William M. Harsha was the first to note the importance of inferior alveolar nerve preservation in 1912. Meanwhile in Europe, Paul Berger from France introduced the bilateral condylectomy for mandibular prognathism via a periauricular incision in 1897, but this procedure resulted in weak occlusal effects. In 1928, Frantisek Kostecka from Prague modified Dufourmentel's subcondylar osteotomy technique with an extraoral approach

using Gigli saw and popularized it to be widely used. The same year, Alexander Limberg a Russian surgeon introduced the posterior oblique vertical ramus osteotomy technique for skeletal open bite correction. The vertical subsigmoid osteotomy via an extraoral approach was first described by Caldwell and Letterman which consists of an inferior bone cut extending to the anterior gonial angle.

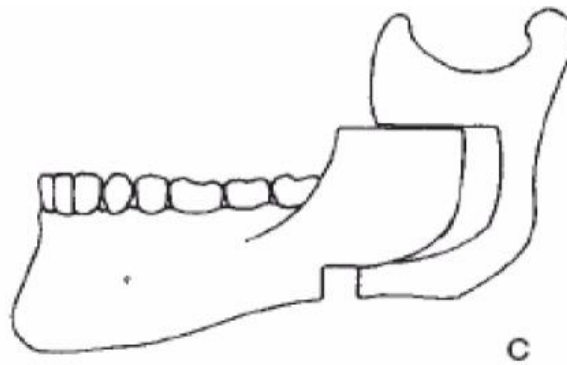


Figure 1.2. Caldwell and Letterman's vertical subsigmoid osteotomy (Fonseca R.J., 2017).

The famous inverted-L osteotomy which was used for mandibular advancement via transcervical incision accompanied by interpositional bone grafting was portrayed by Martin Wassmund in 1927 and Hans Pichler in 1928. In 1955 the famous and widely used bilateral sagittal split osteotomy technique was first described by the German surgeon Hugo Obwegeser which was favored over other techniques because of its predictability and functional and esthetic results. In 1958, The Italian surgeon Dal Pont modified Obwegeser's technique allowing more mandibular advancement with an anterior extension. "Genioplasty" or the intraoral horizontal osteotomy of the inferior border surfaced with Obwegeser and Trauner in 1955.

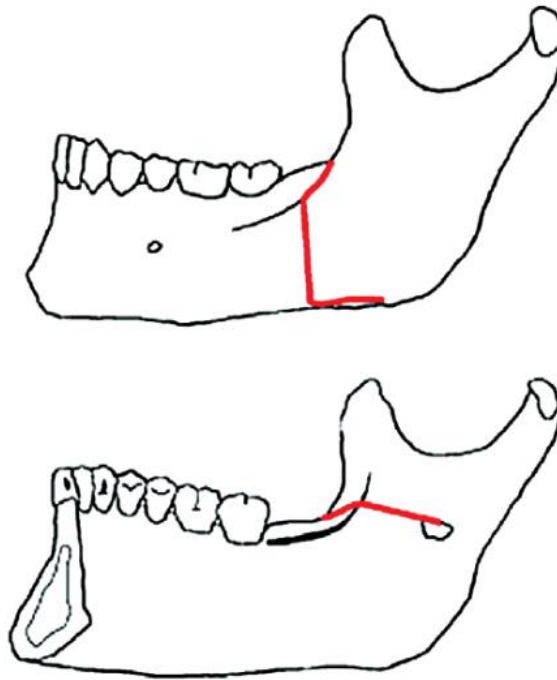


Figure 1.3. Obwegeser-Dal Pont bilateral sagittal split osteotomy (Böckmann et al., 2014).

As the increase in the innovative mandibular surgery techniques the maxillary surgery procedure did not follow the same rate, until the German surgeon Bernard Von Langenbeck which introduced the first maxillary osteotomy surgery in 1859 which was unilateral and for tumor removal. In 1867, David W. Cheever modified Billroth le Fort I maxillary down-fracture technique for tumor removal purposes which paved the way for the well know le Fort I procedure. In 1935, Martin Wassmund introduced the first true anterior maxillary osteotomy, which was used mainly for anterior openbites. Later, in 1955 posterior osteotomy was presented by Karl Schucahrdt which was Wassmund's student. In 1934, the first le Fort I osteotomy mobilization was led by George Axhausen.

In the United Sated, all the body ostectomy procedures were deserted due to technological limitations and biological complications; and most procedures targeted the

mandibule as subcondylar osteotomy or extraoral vertical ramus osteotomy via an extraoral approach. Obwegeser acknowledged the importance of the interpositional bone grafts and their impact on stability and the need to separate the pterygoid plates in order to move the maxillary complex freely without any impediment.

After the year 1985, technological advances in the rigid and semi-rigid fixations to stabilize the bony counterparts surfaced. The Bavarian oral and maxillofacial surgeon Bernd Spiessl was the first to use rigid internal fixation to mandibular sagittal split osteotomy and the initial materials used were exceedingly stiff stainless steel or other types of rigid metals but then titanium plates were introduced which would revolutionize the fixation techniques. (Bell, 2018)

The gathered knowledge from the previous experiences, successes and failures of the orthognathic surgery pioneers has led to a scaffold of information and various different techniques which paved the way for all future generations of oral and maxillofacial surgeons. (Wang, 2002)

B. Engineering influence in orthodontics: orthognathic surgery and 3D virtual planning

The advancement of the orthodontics field was profoundly related to the incorporation of the 3D technology and the digital design tools implemented by biomedical engineering and the reverse engineering systems. Such technologies consist of 3D model scanning and superimposition, digital diagnostic setup and 3D soft tissue facial analysis and many more (Ghafoor, 2018). Surgical planning is a crucial step prior to the surgical

procedure, it allows the oral and maxillofacial surgeon to prepare the proper movements and visualize how the teeth would occlude and how the face would be affected. Thus, an accurate surgical plan and technique contribute to the success of orthognathic surgery. With the influence of the 3D technology and the engineering programs which incorporated software analysis, advanced imaging and virtual planning using 3D scans of the maxillofacial skeleton and dental arches; more accurate, precise and predictable outcomes can be achieved. 3D virtual planning retains several benefits such as:

- Visualization of the skeleton and dental arch in a unique digital model, as well as a clear view of all the discrepancies and deformities with all the accurate measurements.
- Easy access and storage of all virtual models
- Production of surgical splints using the computer aided-design and computer-aided manufacturing (CAD/CAM) methods
- Accurate prediction of postoperative facial soft tissue changes. (Stokbro et al., 2014)

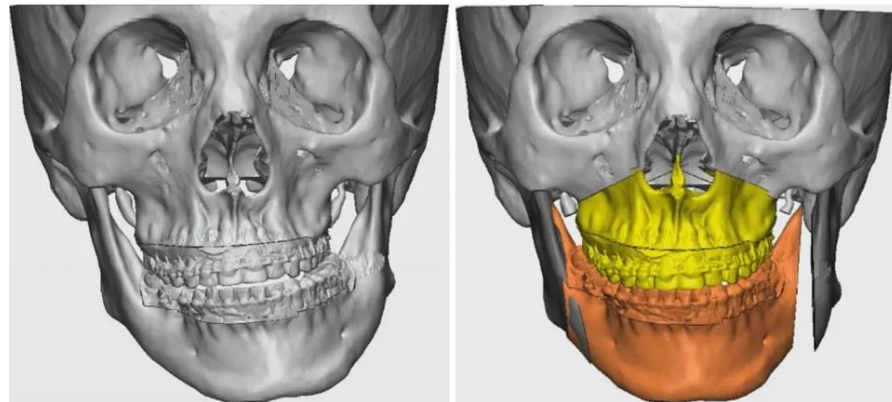


Figure 1.4. Orthognathic surgery 3D virtual planning (Choi Jong-Woo & Lee Jang Yeol, 2021).

CHAPTER II

LITERATURE REVIEW

A. The Temporo-Mandibular Joint (TMJ)

1. Anatomy

The Temporo-Mandibular Joint is a diarthrosis uniting the ramus of the mandible to the skull. It consists of : (1) two bony articular surfaces, covered with fibro-cartilage comprising on top the posterior slope of the condyle of the temporal and down the anterior slope of the mandibular condyle. (2) A fibrous disc (meniscus) interposed between the temporal bone and the mandibular condyle, which completely separates the joint into two non-communicating articular spaces, inferior (meniscus-condylar) and superior (meniscus-temporal). (3) The disc has the shape of a biconcave lens, the fine central part (intermediate zone) separating two anterior and posterior thickenings (anterior and posterior bands). The superior articular space is about 3 times larger than the inferior one, which is itself divided arbitrarily into anterior and posterior recesses.

There are several means of union, such as: (a) the capsule, a fibrous sleeve inserted at the periphery of the articular surfaces and the meniscus, and common to the two articular cavities, (b) the synovial lining the inside of the two articular cavities, (c) the posterior meniscal-temporal frenum, or bilaminar zone, consists of two avascular fibrous layers (in continuity with the posterior band of the disc) within a richly vascularized fibrous tissue, which is inserted posteriorly on the Glaser fissure and anteriorly on the posterior surface of

the neck of the mandibular condyle, (d) distant ligaments, (e) the mandible suspension system consisting of the masticatory muscles (masseter, temporal, medial and lateral pterygoids among which the superior head inserted on the antero-internal part of the meniscus and plays a fundamental role in the mechanism of opening of the mouth).(Netter, Frank H; Norton, Neil Scott; Machado, 2017)

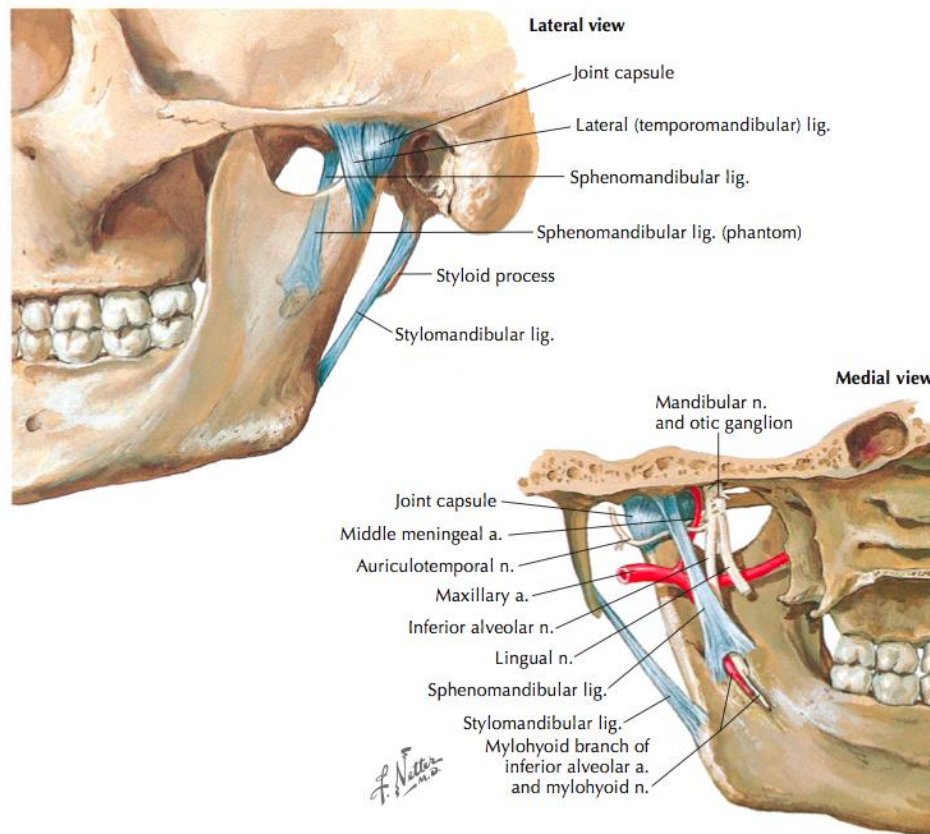


Figure 2.1. Anatomy of the temporo-mandibular joint (Netter, Frank H; Norton, Neil Scott; Machado, 2017).

2. Articular Dynamics

The movement of the meniscus occurs in close coordination with that of the condyle. In the closed mouth position the normal position of the disc is such that the apex

of the condyle is located directly below the posterior bulge of the meniscus. The opening of the mouth simultaneously associates translation and rotation, so that in the closed mouth position, the posterior band of the disc covers the apex of the mandibular condyle and in the open mouth position, the mandibular condyle is placed facing the temporal condyle, the intermediate zone of the disk being placed between these two bony structures.(Richard, Drake; Vogl, A. Wayne; Mitchell, 2020)

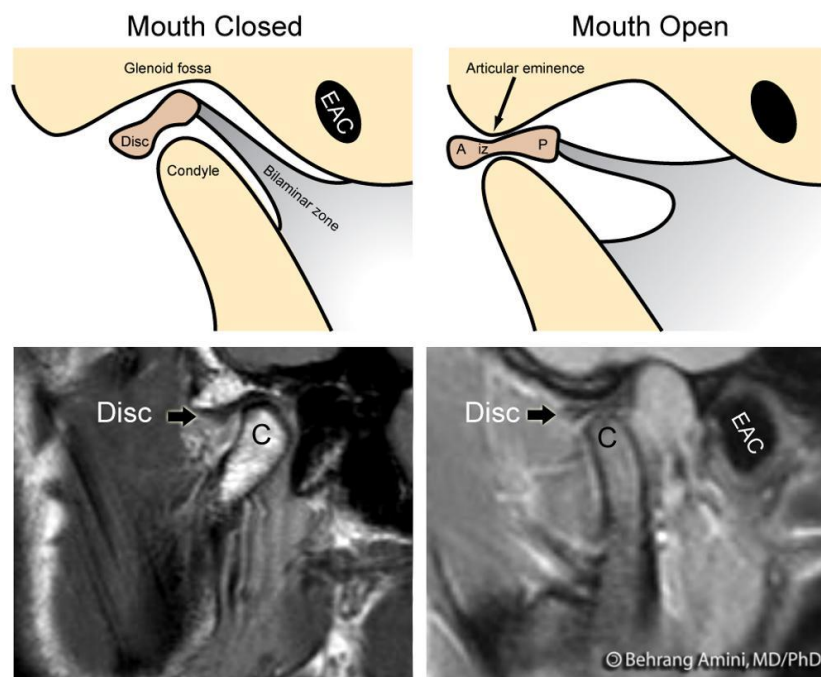


Figure 2.2. Normal temporomandibular joint dynamics(Amini B., 2015)

3. Pathologies of the TMJ

Temporomandibular joint pain (TMJ) affects 30-50% of the adult population at some point in their lives.(de Leeuw, 2018) The TMJ may be the site of several pathologies such as: (1) developmental pathologies for example aplasia or agenesis (absence),

hypoplasia (defect), dysplasia (duplication) or hyperplasia (excess) which leads to facial asymmetry.(2) Traumatic pathologies such as simple joint contusions, condylar fractures and dislocations with or without meniscal lesions. (3) Inflammatory pathologies such infectious, rheumatic and degenerative arthritis. (4) tumoral pathologies such as primary bony, cartilaginous or synovial tumors; benign osteoma, eosinophilic granuloma, chondromatosis and synovial cysts; malignant tumors like osteosarcoma and synovial sarcoma. (5) Articular dysfunction, which is the most common TMJ pathology, It is defined by an abnormal relative position of the disc with respect to the mandibular condyle and the temporal articular surfaces and which prevents a harmonious mechanical coordination of its movements. Internal disturbances of TMJ can be divided into three functional categories which are displacement or dislocation of the disk with or without reduction and anterior disc displacement with perforation. (Wright, 2014)

B. Combined orthodontic-surgical treatment of Class II and CL III malocclusion

Class II or distocclusion: Mandibular molars distally positioned relative to the maxillary molars. It could be accompanied with disturbance of the line of occlusion. (Angle, 1899) Class II malocclusion treatment is difficult, because it depends on a combination of controlled mechanics, growth, and patient cooperation. When accompanied with a substantial skeletal abnormality, various treatment options can be used, ranging from orthopedic intervention to encourage differential growth to orthodontic treatment combined with orthognathic surgery. Each method has its own advantages and disadvantages, as well as distinct outcomes. (Ammoury et al., 2019) There are failure characteristics that dictates

the unfavorable outcome of orthodontic treatment without orthognathic surgery, such as increased overjet of more than 10 mm, ANB $\geq 7^\circ$, mandibular plane angle larger than 40° , mandibular posterior rotation.(Berg, 1979)

Class II malocclusions with underlying severe skeletal abnormalities may not be resolved by growth modification or orthodontic camouflage. The ideal treatment is orthognathic surgery, which repositions the jaws in the appropriate relationship.

Class III or mesiocclusion: Mandibular molars mesially positioned relative to the maxillary molars. It could be accompanied by disturbance of the line of occlusion. (Angle, 1899) Class III malocclusion has a diverse and complicated etiology. It's linked to both hereditary and environmental variables.(Jaradat, 2018) There is no escaping the fact that heredity has a significant impact on facial appearance. (Proffit, W.R., Fields Jr, H. W. & Sarver, 2012)Environmental influences have a transforming effect on an individual's constitution. Environmental influences on the growth and development of the face, jaws, and teeth are mostly pressures and forces associated to physiological activity.(Moss & Salentijn, 1969)

Growth modification or orthodontic camouflage may not be enough to correct Class III malocclusions with serious underlying skeletal defects. The ideal treatment in patient these patients is orthognathic surgery which places the jaws in their ideal position.

Surgery in both skeletal CL II and CL III patients does not replace orthodontic treatment; rather, it is a supplement that requires collaboration between the orthodontist and the maxillofacial surgeon to produce the best outcomes.(A K Hegtvedt, M L Ollins, R P White Jr, 1987)

1. Incisor Decompensation

The three components of pre-surgical orthodontic treatment are arch alignment, arch coordination, and arch decompensation.(McNeil et al., 2014) The total disruption of the natural dental compensation of the dysgnathic jaw relation in all three axes, ideally ending in an orthoaxial incisor inclination, is required for combined orthodontic-surgical treatment. (Raposo et al., 2018) The pre-surgical occlusion directs and, in the worst-case setup, restricts surgical movements. This not only leads to unpredictability in results and prolonged postoperative treatment durations, but also to patient and treatment team discomfort. (Klein et al., 2020) In orthognathic patients, intra-arch mechanics should be planned to accomplish the ideal postsurgical interdigitation and allow for the development of Class I canine and molar relationship after surgery. To achieve these goals, the maxillary and mandibular teeth must be positioned in as close to "ideal" relationships to their underlying osseous bases as possible; thus, leading the malocclusion and the facial esthetics to look worse.(Jacobs & Sinclair, 1983)

a. Sagittal (anteroposterior) plane

To overcome the underlying skeletal discrepancies, the teeth compensate to achieve occlusal contact and interdigitation. In skeletal CL II patients, proclined mandibular incisors and retroclined or upright maxillary incisors are often seen. Therefore, to achieve insignificant interferences during the surgery, normalization using CL III mechanics to advance maxillary molars and retrude mandibular molars to increase significantly the overjet to allow the mandible to advance more forward.

In skeletal CL III patients, retroclined mandibular incisors and proclined or upright maxillary incisors are often seen. Therefore, to achieve insignificant interferences during the surgery, normalization using CL II mechanics to advance mandibular molars and retrude maxillary molars to increase significantly the underjet to allow the more efficient surgical positioning of the jaws. (Jacobs & Sinclair, 1983)

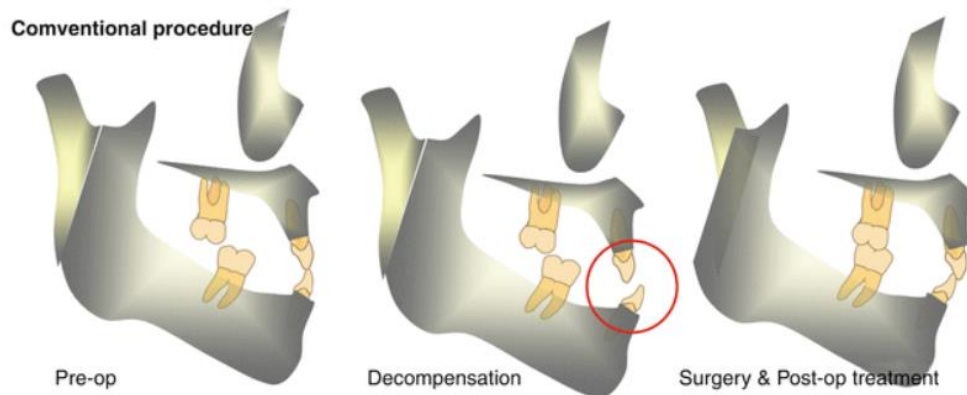


Figure 2.3. Presurgical incisors decompensation in CL III patient (K. J. Lee, 2014)

b. Transverse plane

It is important to establish the origin of the transverse problem, whether it is from dental or skeletal nature. The patient's diagnostic casts in their original centric occlusion relationship cannot be used to make this determination. In order to accurately diagnose transverse dimension anomalies, the research models must be hand articulated into the predicted postsurgical Class I canine connection. In their pretreatment centric relationship, many people with skeletal Class II malocclusion will not have transverse difficulties. However, when the casts are adjusted to a Class I canine relationship, bilateral palatal crossbite may be seen, which must be addressed. However, in CL III patients exhibiting

clinically a bilateral crossbite, when the casts are adjusted to a CL I canine relationship, correction of the crossbite can be seen. Dental compensations should not mask the skeletal discrepancies.(Jacobs et al., 1980)

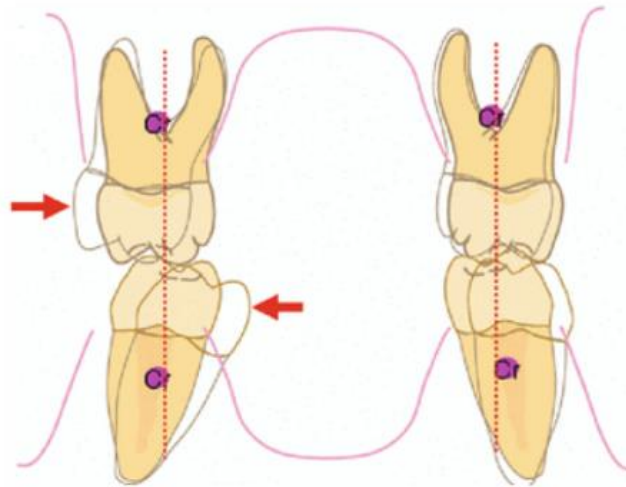


Figure 2.4. Presurgical transverse dental decompensation (K. J. Lee, 2014).

c. Vertical plane

In open bite cases where the anterior facial height needs to be reduced and minimal to moderate curves in any of the arches are present, presurgical leveling and the use of a continuous arch wire are considered. Any extrusion of the maxillary molars after surgery may result in the return of an open bite. The minimization of intrusive mechanics in the posterior region, as well as any extrusive mechanics in the anterior region, will facilitate in the surgical correction of the deformity to the greatest extent possible. Whereas in severely reversed or accentuated curve of Spee, the use of segmental archwires technique is indicated to correct each occlusal plane separately and later correct them surgically.

In deep bite cases with a decreased anterior facial height, the majority of the orthodontic mechanics, particularly the leveling of the mandibular occlusal plane, should be postponed until after the surgery, whereas the leveling of the maxillary arch can be done in the presurgical phase, since the postsurgical occlusion will be mainly on the molars and incisors, the challenging leveling process in the mandible can be easily achieved mechanically after surgery using vertical elastics. It would be more difficult to do the leveling in the presurgical phase due to the heavy occlusal forces.(Henderson, 1981)

Class III malocclusions with a closed mandibular plane angle are characterized by inadequate vertical growth of the maxillary posterior segment, resulting in a vertical dimension deficit posteriorly. In such circumstances, the occlusal plane rotates clockwise in the posterior area, with a loss of proportion between vertical maxillary growth and the mandibular ramus, and the mandible rotates excessively counterclockwise. As a result, an anterior crossbite with a negative overbite is possible. The primary goal of treating class III malocclusion with horizontal growth is to reestablish skeletal harmony by occlusal plane control and obtaining an appropriate posterior vertical dimension, therefore improving the balance between the posterior maxillary vertical dimension mandibular ramus height and the mandibular ramus height. (Sevillano et al., 2020)

2. Double Jaw surgery Vs mandibular only surgery

To determine whether the surgery targets one jaw or both jaws, the underlying skeletal discrepancy and the facial measurements must be considered. In facial skeletal distortion such as midfacial hypoplasia and hyperplasia of the lower part of the face and in

unilateral asymmetry cases, it is crucial to operate on both jaws to correct the soft tissue integuments and the adjust the occlusion. (Lindorf & Steinhäuser, 1978) Double jaw surgery is also recommended in severe TMJ disorders and moderate to severe obstructive sleep apnea. In skeletal CL II patients with an orthognathic maxilla, retrognathic mandible and a normal nasolabial angle with absence of any anterior or posterior increased gingival display or maxillary canting, one jaw surgery of the mandible is considered. In case the maxilla is at fault, or the facial esthetics require any maxillary surgical correction such as advancement, clockwise or counterclockwise rotation, both jaws are considered. In skeletal CL III patients, approximately 25% have a maxillary retrusion, 25% have mandibular prognathism and 50% have a combination of these two relationships.(Guyer et al., 1986) Therefore, in CL III cases the majority of the patients undergo double jaw surgery with maxillary advancement and limited mandibular setback not to impinge on the airways. Regarding bimaxillary surgery stability, mandibular stability is not as excellent as maxillary stability and considerable setback and inferior repositioning of the posterior maxilla are the key risk factors for mandibular relapse.(Jakobsone et al., 2011)

C. BSSO vs USSO

Bilateral sagittal split osteotomy (BSSO) as described by Obwegeser and modified by Dal Pont is the most commonly used osteotomy for the advancement and setback of the mandible during the treatment of malocclusions.(Möhlhenrich et al., 2016) Performing SSO on bilateral mandibular rami (bilateral SSO, BSSO) to reduce unexpected stress or torsion in the temporomandibular joint (TMJ) was considered a standard technique in mandibular

orthognathic surgeries. Previously, it was believed that only bilateral mandibular approaches could be used to separate the tooth-bearing distal mandible segment from both TMJ- attached proximal segments, allowing free repositioning of the proximal segments into neutral condyle positions and fixing the distal segment with minimal TMJ tension. However, in a recent report, unilateral SSO (USSO) was used to correct lateral deviation of the mandible and yielded favorable outcomes. If unilateral surgery could guarantee long-term postoperative stability, as well as favorable results in correcting facial asymmetry, operation time and the incidence of postoperative complications, including inferior alveolar nerve damage, hemorrhage, or a bad split, could be reduced compared to those observed in bilateral mandibular surgeries. (S.G. Lee et al., 2015) Skeletal mandibular asymmetry is usually corrected by BSSO. However, USSO should be considered for patients who require maxillary advancement for the correction of a Class III malocclusion when there is relatively little mandibular asymmetry with a dental midline discrepancy of <5 mm. Operating on only one side of the mandible reduces possible mandibular complications by half and reduces the duration of treatment.(Beukes et al., 2016). The bilateral sagittal split ramus osteotomy (BSSRO) is a popular and reliable procedure for symmetrical mandibular surgery. However, using BSSRO for asymmetrical correction may result in an asymmetrical mandible, even after correcting the chin position. Correction of laterognathia or cant may create interferences between the inner and outer tables of the sagittal splits, causing asymmetry at the level of the ramus and angles. To avoid these bony interferences, an additional cut to the inner table has been proposed, but it may maintain the existing asymmetry if the mandibular angles are already asymmetrical. Alternatively, asymmetrical bony contact may improve the symmetry at the level of the angles, but it is difficult to plan

accurately in advance. To address this issue, a possible solution is to use a unilateral sagittal split osteotomy (USSO) for correcting mandibular asymmetry. This approach allows the surgeon to use the opposite condyle as the center of rotation, which can control the yaw of the mandible during surgery and result in more predictable outcomes. Although there have been early descriptions and case reports on the effectiveness and complications of USSO, controversy remains. Unilateral sagittal split osteotomy greatly improves facial symmetry in patients with class III malocclusion and mandibular asymmetry affecting the chin and rami/angles. The correction of asymmetry at the level of the ramus and angles is a critical component in the design and execution of the USSO method.(Abou Chebel et al., 2020)

Several disadvantages, such as fracture, bleeding, infection, and TMD, were found after bilateral sagittal split ramus osteotomy (BSSRO). Some of these disadvantages were associated with the changes of stress in temporomandibular joint (TMJ) after osteotomy. Biomechanically, these changes in patients with facial asymmetry after BSSRO would affect the stress distributions within the TMJ. BSSRO could cause anterior disc displacement or other symptoms of TMD.(Shu et al., 2018)

D. Finite Element Analysis (FEA)

Orthodontists used mathematical calculations, such as force vectors and moments, to predict the resultant tooth movements due to a lack of exact knowledge about the reactions following the application of orthodontic forces. Despite its precision, this theoretical method ignores the biological setting in which these forces and moments are applied, resulting in clinical outcomes that deviate from expectations.

With the development of 3D imaging, it was possible to see the individual anatomy in great detail. This innovation resulted in dental clinical applications that made operations safer and more precise, particularly in implant dentistry. Dental experts used 3D reconstruction software to create detailed 3D models from precise 3D pictures of real anatomy. These models made it easier to alter force systems in vitro using "Finite Element Analysis," a previously utilized engineering tool for 2D models. The goal was to uncover and comprehend the origins of common undesirable reactions that result in longer orthodontic treatment durations.

However, because to the difficulties of creating complete accurate models of the jaws and teeth, FEA applicability has been limited, and most research have been confined to a specific model, disregarding the individual variances observed clinically. Despite these drawbacks, FEA is the sole tool that can help us get to a position where a "virtual patient," produced from a true individual 3D representation, may be subjected to specified clinical setups before being used in vivo with expected results.

1. Definition

FEA is a current tool for numerical stress analysis that approximates physical models into numerical mathematical equations. It was first developed in 1943 by R. Courant, who used the Ritz approach. The procedure begins with the discretization of the structure into its constituents, known as "finite elements," which are connected by nodes with well-defined physical properties (e.g., stiffness, elasticity). Then, to approximate the reactions and interactions inside each constituent, a quantitative analysis is performed. (Vasudeva et al., 2012). All of the elements' equations must be solved at the same time,

which is a work that can only be done by computers. Deflection, stress, strains, vibration, energy storage, and a variety of other engineering phenomena can all be estimated.

Complex mechanical issues can be solved using FEA. The method was first recognized as a tool for approximating physiologic and biologic problems that may be addressed by mathematical equations. It was first used to test design integrity and identify key spots in components without having to fabricate the part or assembly. Dentistry made advantage of FEA methods, focusing on mechanotherapy.

2. 3D imaging

a. Evolution towards 3D imaging

The evolution from 2D to 3D imaging has been a significant advancement in the field of medical imaging. 2D imaging, such as X-rays and ultrasound, provides a flat image of a two-dimensional cross-section of the body, while 3D imaging, such as CT scans and MRI, creates a three-dimensional image of the body.

The first step towards 3D imaging was the development of computed tomography (CT) in the 1970s. CT scans use X-rays to produce multiple cross-sectional images of the body, which can be combined to create a 3D image. The development of magnetic resonance imaging (MRI) in the 1980s was another major breakthrough in 3D imaging (Verdun et al., 2015). MRI uses magnetic fields and radio waves to create detailed images of the body's internal structures. Advancements in computer technology have also played a significant role in the evolution of 3D imaging. Computer-aided design (CAD) software is now widely used in the medical field to create 3D models of the body, which can be used for planning

surgeries and other medical procedures. In recent years, 3D printing has also emerged as a promising tool in medicine. Using 3D printing technology, doctors can create physical models of patient-specific anatomy, which can be used for surgical planning and medical education.

Overall, the evolution from 2D to 3D imaging has revolutionized the field of medical imaging, enabling doctors to visualize and diagnose medical conditions with greater accuracy and precision.

Despite various constraints that influenced their accuracy and prohibited their use to build 3D models for experimental and clinical analysis, traditional 2D diagnostic imaging records have long been the standard in orthodontics. Some of these restrictions are object magnification, distortion, projective displacement, and superimposition of structures. Medicine and, later, dentistry have used 3D technology to aid diagnostic and treatment planning throughout the last decade. There has been a debate in the medical field regarding the frequent use of cone beam computed tomography (CBCT) and CT scans in dentistry. In the orthodontic field, some experts have raised concerns about the usefulness of 3D imaging in routine clinical treatment and diagnosis. The American Association of Orthodontists (AAO) and the American Academy of Oral and Maxillofacial Radiology (AAOMR) do not encourage the frequent use of ionizing radiation for standard orthodontic diagnosis and treatment planning. However, they acknowledge the usefulness of 3D imaging in specific clinical situations, such as retained or impacted permanent teeth, facial asymmetries, craniofacial anomalies, severe skeletal discrepancies, and TMJ malformation and airway assessment. There has been a debate in the medical field regarding the frequent

use of cone beam computed tomography (CBCT) and CT scans in dentistry. In the orthodontic field, some experts have raised concerns about the usefulness of 3D imaging in routine clinical treatment and diagnosis. (L. Carter et al., 2008).

b. CBCT vs CT scans

Both CT scans and CBCT machines are types of computed tomography machines, but they differ significantly in terms of radiation doses, image capture, quality, and interpretation. Medical CT scans use a fan-shaped x-ray beam to collect data from image detectors arranged in an arc around the patient, resulting in a single slice per rotation. The spacing between the collected slices determines image resolution. In contrast, CBCT captures the entire volume of the object in a single-turn motion, which is faster and exposes the patient to less radiation.

A study by (Loubele et al., 2009) compared jaw dimensions and bone quality assessment between CBCT and MSCT scans. The measurements obtained from CBCT and MSCT were accurate but slightly underestimated the bone widths. CBCT scans were better at showing the lamina dura and PDL, while MSCT scans were better at showing the cortical bone and gingiva. Another study by (Scarfe & Farman, 2008) found that MSCT had better contrast resolution than CBCT. Micro CT was found to be the best source for precise tissue modeling, but it had increased radiation doses.

In MSCT, radiodensity is measured using the Hounsfield Unit scale (HU), which yields accurate measurements of tissue density. In CBCT, the grayscale displays the level of x-ray attenuation, but it is not an accurate measurement of HUs. The CBCT voxel value of an

organ depends on its location, so regions with identical densities may appear with varying grayscale values in the CBCT scan.

3. Development of FEA in dentistry

(Ledley & Huang, 1968) were the first to use FEA in dentistry by creating a linear model of a tooth based on experimental data and linear displacement force analysis. Since then, FEA has been used to investigate various aspects of dentistry, including teeth, bone, and oral tissues, as well as stress analysis of different restorative materials and implant designs (Gačnik et al., 2014).

Over time, FEA has advanced significantly in dental research. In the first era (1970-1990), dental models were two-dimensional and based on simplified geometry, and the large number of calculations needed for analysis made automation difficult. To overcome geometric discontinuity in the models, assumptions and constraints were imposed, which may have resulted in mathematical errors and questioned the models' validity (Ko et al., 2012).

In the second era (1990-2000), 3D models based on accurate human anatomy records were developed, and manual and automated meshing techniques improved. Poroelasticity, homogenization theory, and dynamic response solvers from the engineering field were adopted to examine dental issues. However, incorrect models and time-consuming model construction were still issues due to the large element sizes in the evolving meshing techniques (Hohmann et al., 2011).

Creating correct and appropriate FE meshes of the researched geometry is crucial, as the results of FE simulations are extremely sensitive to geometric modeling assumptions. The use of early anatomical records with improved resolution (CT images) and advancements in computer and software capabilities allowed for more intricate simulations of complex 3D structures, such as occlusal surfaces, pulp, dentin, and enamel, and improved FE solvers' meshing capabilities (Ko et al., 2012.).

4. Limitations and inaccurate assumptions

Finite Element Analysis (FEA) is a powerful numerical method that can be used to model and analyze complex structures, including dental structures. Biological tissues have a more intricate structure than engineering structures, and their mechanical behavior is not entirely understood due to factors such as their complex anatomy, limited experimental research, and insufficient technology to measure oral tissue properties (Qian et al., 2001). Consequently, certain assumptions are made in orthodontic FEA studies. However, there are several limitations of FEA in dentistry that should be taken into consideration. Here are some of them:

Simplified Models: FEA models are only as good as the input data used to create them. In dentistry, it can be challenging to create accurate models of dental structures due to their complex geometries and the difficulty of obtaining precise measurements. Tooth movement is influenced by the periodontal ligament, which underscores the significance of accurately defining its material properties. A systematic review of the mechanical assumptions made

in FEA studies regarding the periodontal ligament revealed a wide variety of modeling approaches, including linear-elastic, viscoelastic, hyperelastic, and multiphase methods.(Fill et al., 2012) In addition, the tendency to use simplified approaches or assumptions, such as linear-elastic modeling, may have resulted in an incomplete representation of the time-dependent behavior of the periodontal ligament. Consequently, simplifications may have to be made in the modeling process, which can lead to inaccuracies in the analysis (Vasudeva, 2008).

Material Properties: The accuracy of FEA results depends heavily on the accuracy of the material properties used in the analysis. In dentistry, it can be difficult to determine the precise material properties of teeth and dental materials, which can lead to inaccuracies in the analysis. Incorrect assumptions are not limited to the periodontal ligament, as bone material properties have been commonly assumed to be linear-elastic in most studies. In a study by (Schwartz-Dabney & Dechow, 2002a), it was demonstrated that there are differences in the material properties based on direction (known as material anisotropy) and the direction with the highest stiffness in various regions of 10 mandibles with teeth. The presence of anisotropy and regional variations in skeletal material properties can significantly impact the correlation between stress and strain, as described by (Cowin & Hart, 1989.)

Boundary Conditions: FEA models are typically based on assumptions about the boundary conditions of the system being analyzed. In dentistry, it can be challenging to accurately model the complex boundary conditions that occur in the oral environment, which can lead to inaccuracies in the analysis.

Neglecting Small Details: In some cases, small details of the system being analyzed may be neglected in the FEA model, such as small cracks or defects. However, these small details can have a significant impact on the behavior of the system and can lead to inaccuracies in the analysis.

Clinical Validation: FEA models should be validated against real-world clinical data to ensure their accuracy and relevance. However, there are limited clinical data available in dentistry to validate FEA models, which can limit their usefulness in clinical practice.

In summary, while FEA can be a valuable tool in dentistry, it has its limitations, and its results should be interpreted with caution, taking into consideration the potential inaccuracies and uncertainties associated with the modeling process (Geng Jian-Ping et al., 2001.).

a. Generalizability of results

The generalizability of Finite Element Analysis (FEA) results in dentistry refers to the ability to apply the results of FEA models to other similar dental structures or conditions beyond the specific system being analyzed. It is also the ability to apply findings from a study to real-world settings beyond the laboratory. Using Finite Element Analysis (FEA), data can be inferred and analyzed from a single mathematical solution for a particular setup. In the field of engineering, a single problem with predetermined settings and properties typically results in a single solution. However, in medical and dental fields, individual variations may lead to different outcomes for the same clinical problem.

Therefore, clinical trials should be conducted with representative samples of the population using well-defined research protocols and appropriate statistical analyses to ensure the validity and significance of the results. Unfortunately, most dental FEA studies have employed a "single model" engineering approach, raising questions about the clinical relevance of their findings. Future studies must consider the variations that exist between real patients to bridge the gap between virtual finite element models and actual clinical situations. While FEA can provide valuable insights into the behavior of dental structures, it's important to consider the limitations of generalizing the results.

Here are some factors to consider regarding the generalizability of FEA results in dentistry:

- System-specific: FEA models are specific to the system being analyzed, and the results may not be generalizable to other similar dental structures or conditions. For example, an FEA model of a specific tooth may not be directly applicable to another tooth with a different size or shape.
- Material properties: The material properties used in FEA models can significantly affect the results. However, the material properties of dental structures can vary significantly between individuals, making it challenging to generalize FEA results across the population.
- Clinical relevance: FEA models should be validated against real-world clinical data to ensure their relevance and applicability. However, there is limited clinical data available in dentistry to validate FEA models, which can limit their usefulness in clinical practice.

- Limitations of modeling: The accuracy of FEA results depends on the accuracy of the assumptions and simplifications made in the modeling process. However, it can be challenging to create accurate models of dental structures due to their complex geometries and the difficulty of obtaining precise measurements.

In summary, while FEA can provide valuable insights into the behavior of dental structures, the generalizability of the results should be considered in light of the limitations of FEA modeling and the variations in material properties and clinical conditions among individuals. It's essential to interpret FEA results with caution and consider their relevance and applicability to other similar dental structures or conditions.

b. 3D Modeling of human tissues

Three-dimensional (3D) modeling of human tissues involves creating digital representations of biological tissues in a 3D space. This technique has become increasingly popular in medical research and clinical applications as it allows for detailed visualization of complex anatomical structures and the simulation of biological processes.

Here are some of the techniques and applications of 3D modeling of human tissues:

Imaging modalities: 3D modeling of human tissues often begins with imaging data, such as computed tomography (CT), magnetic resonance imaging (MRI), or microscopy images.

These images are used to create a 3D model of the tissue, which can then be analyzed and manipulated.

Computational modeling: Once a 3D model has been created, it can be used to simulate biological processes, such as blood flow or tissue deformation. Computational modeling can provide insights into the behavior of tissues under different conditions and can be used to predict the outcomes of medical interventions.

Medical applications: 3D modeling of human tissues has numerous applications in clinical medicine. For example, it can be used to plan surgical procedures, such as the placement of implants or the removal of tumors. It can also be used to create custom prosthetics or orthotics that are tailored to the individual patient.

Research applications: 3D modeling of human tissues is also used in medical research. For example, it can be used to study the development of diseases or to test the effectiveness of new drugs. It can also be used to create models for medical education and training.

Overall, 3D modeling of human tissues is a powerful tool that allows for detailed visualization and simulation of biological processes. Its applications range from medical education and research to clinical decision-making and treatment planning.

A major limitation of using FEA simulation is the challenge of accurately modeling the complex anatomy of human hard and soft tissues. This is due to the significant amount of time and effort needed to create a realistic model. Although 3D modeling software has made significant advancements, the segmentation process is still primarily done manually. To create an accurate model of a maxillary or mandibular arch, including enamel, dentin, pulp, PDL, lamina dura, and distinct cortical and trabecular bones, it can take hundreds of hours (Pollei, 2009).

Due to their small size, it can be challenging to see the periodontal ligament (PDL) tissue and trabeculae of the spongy bone using standard resolution CT and CBCT scans, which creates a problem when building finite element (FE) models. To address this, different methods have been developed to create a layer between the teeth and the bone to represent the PDL. However, the thickness of this layer depends on the highest resolution that the 3D modeling software can handle, resulting in different PDL thicknesses being used in various studies (Fill et al., 2012).

(Carcedo, 2010.) conducted a study comparing various digital reconstruction software packages and found that only four of them (Mimics, Simpleware/ScanIP, Amira, and 3D Slicer) were capable of analyzing medical images. All except 3D Slicer were considered easy to moderately easy to use and included tools for data preparation, image noise reduction, manual and semi-automatic segmentation, angular and linear measurements, mesh generation, editing and refinement, creation of a 3D preview model, and exporting the meshed model in various formats such as Patran, Ansys, Abaqus, Fluent, Nastran, and Comsol.

5. FEA in orthodontics

In orthodontics, FEA can be used to study the biomechanical response of teeth, bones, and surrounding soft tissues during orthodontic treatment. Although FEA has its limitations, it still holds great promise in the field of orthodontic research, making up a substantial portion of dental applications. Its non-invasive nature and accuracy make it an ideal tool for obtaining detailed, quantitative information about the physiological responses of internal structures, like the periodontal ligament and the alveolar bone. Additionally,

FEA allows researchers to study a homogeneous sample while controlling all variables and predicting how tissues will respond to orthodontic mechanical forces. The introduction of FEA into orthodontics was pioneered by (Tanne et al., 1987). Previous research had focused on the application of force in a single tooth system, which was based on the average anatomical structure and revealed stress levels (Cobo et al., 1993). As software technology improved and 3D radiography became available in dentistry, more advanced models were created to examine stress levels in multiple teeth (C. Liu et al., 2015). Here are some applications of FEA in orthodontics:

Orthodontic appliance design: FEA can be used to evaluate the performance of different orthodontic appliances, such as braces, wires, and aligners. By simulating the biomechanics of the orthodontic system, FEA can help to optimize the design of these appliances to improve their effectiveness and efficiency.

Biomechanical analysis: FEA can be used to study the biomechanical response of teeth, bones, and surrounding soft tissues during orthodontic treatment. This can help to predict:

1. The movement of teeth and the amount of force needed to achieve the desired tooth movement.
2. Stress distribution areas in the periodontal ligament (PDL) and alveolar bone during different types of tooth movements: canine and incisors retraction, molar and incisors intrusion, torque expression, distalization...

Material selection: FEA can be used to evaluate the performance of different materials used in orthodontic treatment, such as brackets, wires, and aligners. By simulating the biomechanics of the orthodontic system with different materials, FEA can help to identify the best materials for specific treatment goals.

Treatment planning: FEA can be used to simulate different treatment setups and predict the outcomes of orthodontic treatment. This can help to optimize treatment planning and reduce the risk of complications during treatment.

Overall, FEA is a valuable tool in orthodontics that can help to optimize treatment planning and improve the effectiveness and efficiency of orthodontic treatment. By simulating the biomechanics of the orthodontic system, FEA can provide valuable insights into the behavior of teeth, bones, and surrounding soft tissues during treatment, helping to improve treatment outcomes and reduce the risk of complications.

6. Significance

FEA can help orthodontists to better understand the biomechanical response of the orthodontic system and make more informed treatment decisions, leading to better patient care.

One of the most significant applications of FEA in orthodontics is in predicting tooth movement. FEA can help to predict the biomechanical response of teeth, bones, and surrounding soft tissues during orthodontic treatment. By simulating the biomechanics of the orthodontic system, FEA can help to determine the amount and direction of force needed to achieve the desired tooth movement. This can help orthodontists to plan and execute treatment more effectively, reducing the risk of complications and improving treatment outcomes.

FEA can also be used to optimize orthodontic appliance design. By simulating the biomechanics of the orthodontic system, FEA can help to evaluate the performance of

different orthodontic appliances, such as braces, wires, and aligners. This can help to optimize the design of these appliances to improve their effectiveness and efficiency. For example, FEA can be used to determine the optimal bracket position and angulation, the appropriate wire size and shape, and the best material for each component.

Another significant application of FEA in orthodontics is in material selection. FEA can be used to evaluate the performance of different materials used in orthodontic treatment, such as brackets, wires, and aligners. By simulating the biomechanics of the orthodontic system with different materials, FEA can help to identify the best materials for specific treatment goals. For example, FEA can be used to compare the performance of different types of brackets, such as metal brackets and ceramic brackets, to determine which is best suited for a particular patient.

FEA can also be used to optimize treatment planning. By simulating different treatment setups and predicting the outcomes of orthodontic treatment, FEA can help to optimize treatment planning and reduce the risk of complications during treatment. For example, FEA can be used to simulate the effects of different types and amounts of force on tooth movement, allowing orthodontists to plan treatment that is more efficient and effective.

Overall, FEA is a valuable tool in orthodontics that can help to improve treatment outcomes, reduce the risk of complications, and make treatment more efficient and cost-effective. FEA can help orthodontists to better understand the biomechanical response of the orthodontic system and make more informed treatment decisions, leading to better patient care. By predicting tooth movement, optimizing appliance design and material

selection, and optimizing treatment planning, FEA can help to make orthodontic treatment more effective, efficient, and affordable for patients.

E. Specific aims

The aims of this study are to evaluate:

1. The stress distribution and displacement on the contralateral and ipsilateral condyles and condylar necks in USSO patients following graded movements of the mandible in advancement and setback (4-6-8-10-12 mm)
2. The stress on the contralateral and ipsilateral menisci in USSO patients following graded movements of the mandible in advancement and setback (4-6-8-10-12 mm)
3. The effect of condylar volume variation on displacement

F. Hypothesis

The main hypothesis is that in USSO there is more stress on the non-operated condyle than the operated condyle.

Subordinate hypothesis is that the morphology of the condyles affects the stress distribution.

CHAPTER III

MATERIAL AND METHODS

A. Material

This research was approved by the institutional review board (IRB) of the American University of Beirut (date of approval: March 18, 2022).

1. Anatomical record

8 Pretreatment cranial CT scans (in DICOM format) of adult asymmetrical patients seeking combined orthognathic-orthodontic treatment at the Division of Orthodontics and Dentofacial Orthopedics at the American University of Beirut Medical Center were used for 3D model generation. Two groups comprised of 4 patients each underwent either mandibular advancement or setback.

The Following inclusion criteria were used to select the patient pool:

- Facial asymmetry due to true mandibular asymmetry
- Healthy patient
- Mild skeletal discrepancy
- Non-growing adult patient
- CT of face, with mandibular arch and TMJ apparatus properly imaged.

Exclusion characteristics were:

- Severe maxillo-mandibular skeletal discrepancies
- Craniofacial syndromes (Crouzon, Hemifacial microsomia...)

- Psychological problems
- CT is of non-diagnostic quality.

In the present study, CT scans were used for better visualization and differentiation of the distinctive bony structures and densities through different cross sections, allowing better anatomical duplication during the 3D model re-construction. The patient names were blinded and the DICOM image was imported for image processing.

B. Methods

1. 3D model

Different softwares were used from computer tomography image reconstruction to finite element simulations. Simpleware Scan IP corresponds to the development of the 3D model; Abaqus CAE relates to the FE analysis.

a. Model segmentation

The CT image was imported and segmented using the image processing and digital reconstruction software ScanIPTM 7.0 (Simpleware Ltd., Exeter UK). The region of interest included the part of the temporal bone related to the temporomandibular joint and the mandibular bone and teeth (using the crop tool in ScanIPTM).

Masks of the menisci and of the cortical bone of the body of the mandible including the teeth, ramus, condyle, and the temporal bone were created using manual and automated tools (Figure 3.1). Cortical and trabecular bone were unified to simplify the complex

model. Manual segmentation was minimized, as much as possible in order to save time and obtain reproducible and consistent outcomes.

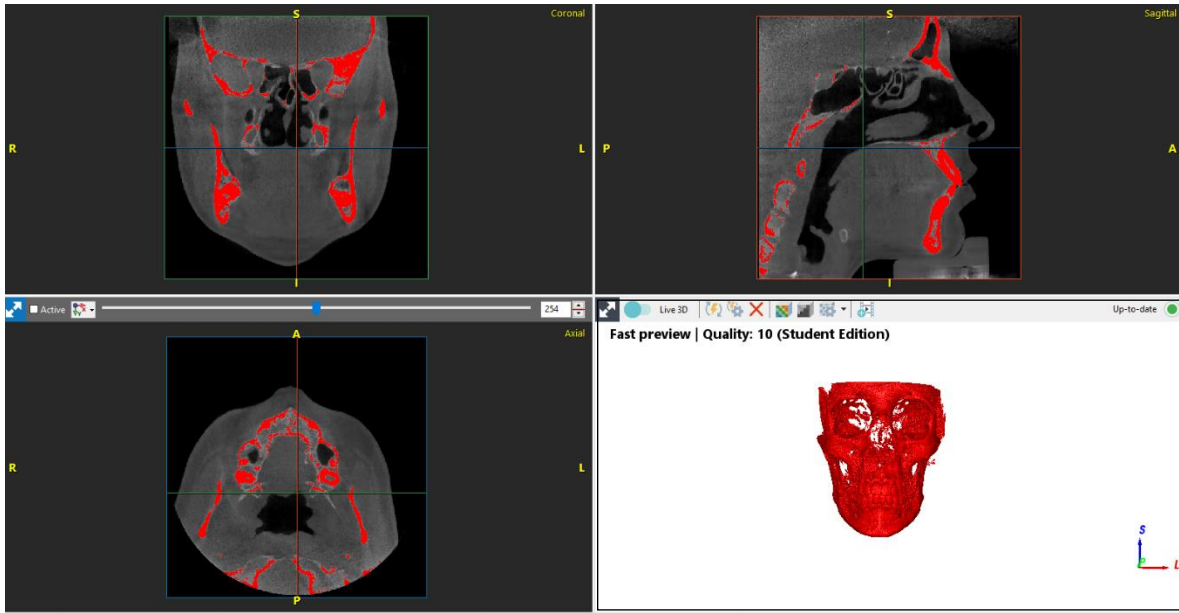


Figure 3.1. Mask creation from a skull CT scan in Simpleware Scan IP.

i. Bone/teeth masks

In CT scans, a Hounsfield Unit (HU) is proportional to the degree of x-ray attenuation and is allocated to each pixel to show the image that represents the density of the tissue. The cortical bone and the teeth cause similar attenuation of the x-rays thus have similar Hounsfield unit. For this reason, it is appropriate to first use the ‘Segmentation with Threshold’ tool that identifies voxels with Hounsfield units in a specific range to capture the voxels associated to the teeth. A HU range between 347 and 3069 was used to detect all teeth voxels and the dense cortical bone (Figure 3.2). Bone density may differ among various regions of the same jaw and areas of differing densities may only be separated by

millimeters (Alper et al., 2012). As a result, bone segmentation demands precise manual work. In a first step, we created a mask called “cortical bone of the mandible” using the ‘Segmentation with Threshold tool’ and manual segmentation with ‘paint/unpaint tool’. This mask does not represent the cortical bone yet because it does not include all the voxels related to it and is perforated in the areas opposing the teeth (which will increase after smoothing). It is only a tool to generate a cortical mask. The gaps were closed using the ‘morphological close’, ‘cavity fill’ and ‘paint tool. No separation between the cortical and trabecular bone was done for model simplification. The temporal bone mask was created with the same tools as the mandibular mask with only cortical bone properties.

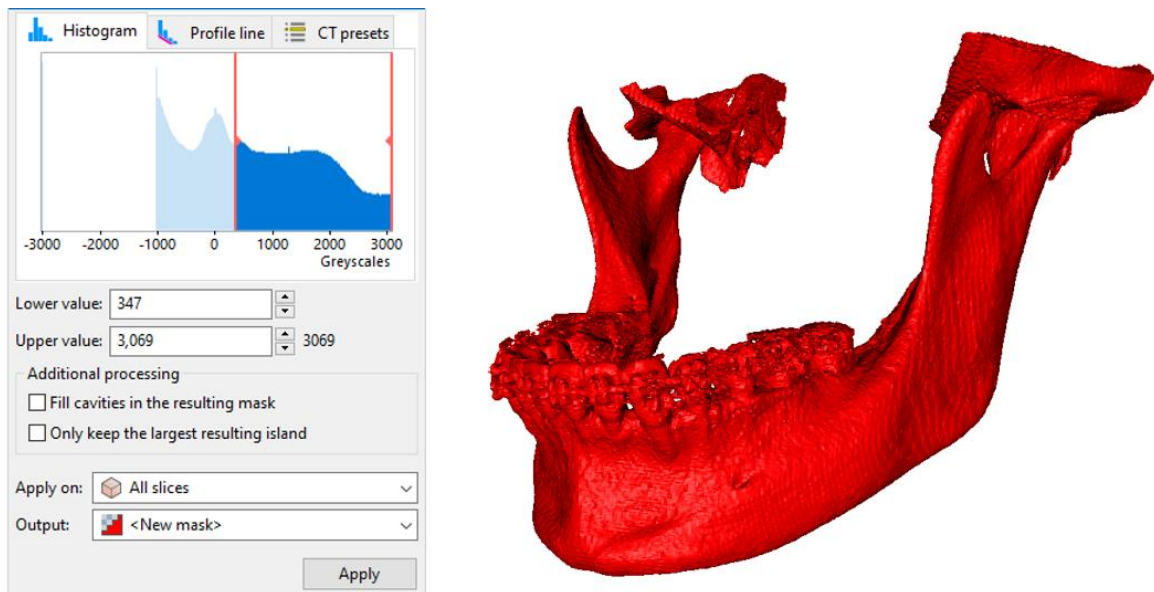


Figure 3.2. Paint with threshold tool for the creation of the mandibular mask.

ii. Articular disk/Meniscus Mask

The articular disk is a cartilage which cannot be captured on the CT scan.

Consequently, the meniscus mask was created by filling the space between the temporal bone and the condyle (Figure 3.3). The construction included 3 steps:

- Duplication of the temporal bone mask
- Expansion of the new temporal bone mask by 1 voxel (0.3 to 0.4 mm) away from the glenoid fossa using the morphological dilate tool.
- Selecting the common area between the condylar bone mask and the expanded temporal bone mask area, which will eventually represent the meniscus, using the *‘Intersection Boolean operation tool’*.



Figure 3.3. Masks of the menisci

iii. Smoothing

The Recursive Gaussian filter (Intensity 2) was used to smoothen all masks.

Smoothing with this filter implies:

- “Shaving” of the masks, thus removing pixels from the outer surfaces leading to

their shrinkage (1 pixel of shrinkage for a Recursive Gaussian intensity 2).

- Formation of unassigned pixels at the interface between the masks.

To counteract the shrinkage, all masks were enlarged by 1 pixel using the ‘morphological dilate’ tool. Further smoothing using the “smart mask smoothing option” was done prior to the generation of the FE Model. In the model configuration, ‘Smart mask smoothing option’ employs the underlying greyscale information to improve a model’s smoothness and accuracy while preserving volume algorithm. The smoothed model is seen in Figure 3.4.

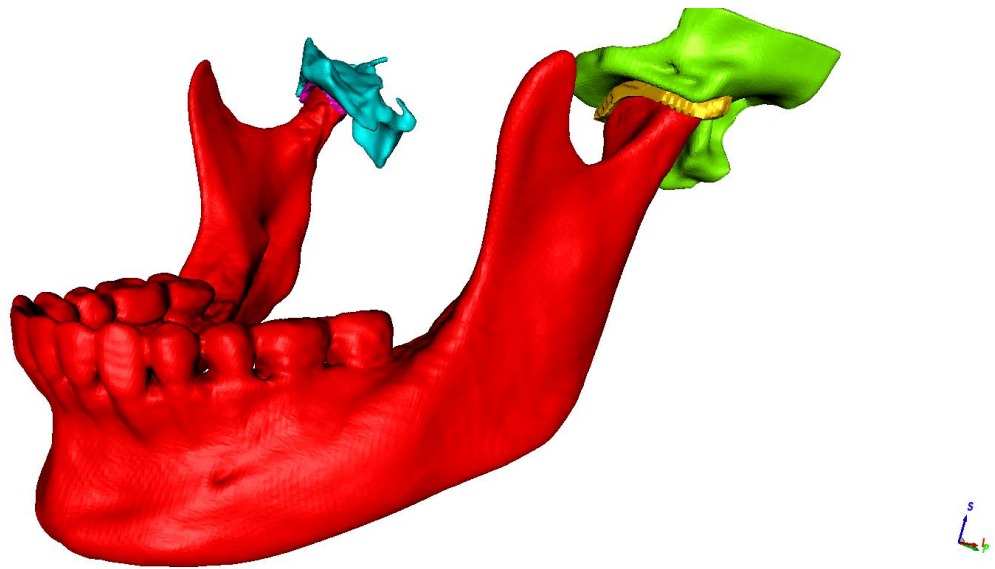


Figure 3.4. Mandibular Model with the different masks (temporal, meniscus, mandible).

iv. Surgical cut

The mandible masks of all the models were duplicated; all the other masks were suppressed so the editing tools would not interfere and alter their geometry. Using the “simple 3D editing tool” a major part of the duplicated mandible was cut by the “delete operation” to minimize and render the work easier on the 2D view. In the case of unilateral sagittal osteotomy on the left side, the duplicated mask consisted of the left ramus, similarly, for a unilateral sagittal osteotomy on the right side, the duplicated mask consisted of the right ramus. On each slice of the 2D CT scan, the duplicated mask would be edited using the “paint with threshold” tool to achieve the Obwegeser-Dal Pont cut and to recreate the separated right or left ramus for the rest of the mandible (Figure 3.5). To finalize the surgical cut, “Boolean operations” was used to subtract the two mandibular masks from each other to achieve smooth surfaces at the level of the cut. The resulting smooth interface at the cut would minimize the errors in the model during the meshing process and eventually when running the FEA simulation on ABAQUS. For reproducibility, the cut followed the anatomical structures, the first cut made through the lingual cortex above the mandibular foramen parallel to the occlusion Corticotomy extended from anterior border of ramus behind lingula (entrance of the inferior alveolar nerve). The second corticotomy was done through buccal cortex in a vertical direction at the level of the first or second molar. A Connecting cut between the first two osteotomies was done with a final split detaching the entire ramus.

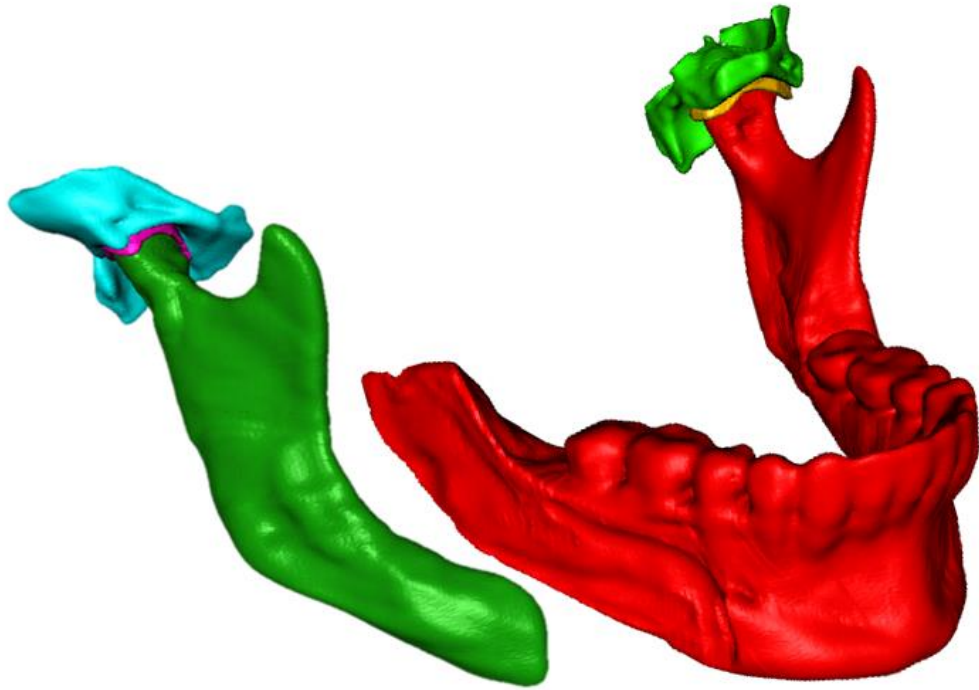


Figure 3.5. Simulation of the unilateral sagittal split osteotomy

b. Individual variation

To incorporate individual variation, 8 CT scans corresponding to 8 different patients were used in this study. Anatomical features differing between the patients were: condylar size and morphology and mandibular shape and size. Each CT scan was segmented as described above to obtain 8 new 3D models each one corresponding to a specific asymmetrical patient. The effect of the condylar size will be highlighted by correlating the condylar size to the amount von mises stress distributed and the amount of displacement achieved with the different incremental surgical movements in the advancement and setback scenarios (Figure 3.6)

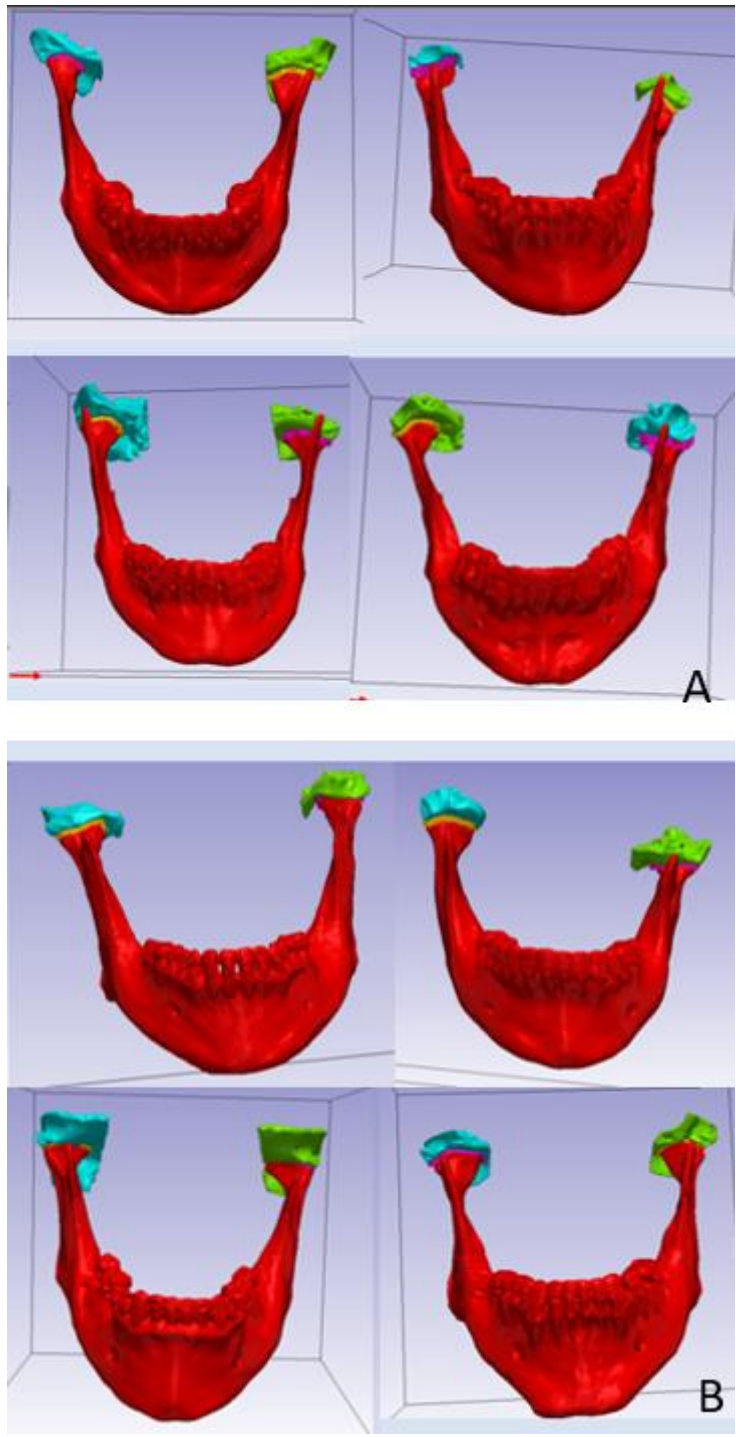


Figure 3.6. Finite element model of the 8 different CT scans. A: patients that underwent advancement surgery. B: patients that underwent setback surgery.

b. Meshing Process

Meshing in Finite Element Analysis (FEA) is the division of a complicated geometry into smaller, more manageable elements known as finite elements. The mesh is made by connecting these finite pieces at predetermined locations known as nodes (Figure 3.7). Mesh creation serves to discretize continuous domains to enable numerical analysis with FEA tools. The accuracy of the FEA results depends heavily on the mesh quality. The quality of the mesh is critical to the accuracy of the FEA results. A good mesh should have the following properties:

- Element size: The size of the elements should be small enough to accurately capture the variations in the solution, but not to the level to significantly increase the computation time.
- Element shape: The shape of the elements should be regular and consistent to avoid numerical errors.
- Element connectivity: The elements should be connected properly at the nodes to ensure a continuous solution.
- Mesh density: The mesh density should be high in areas where there are significant changes in the solution, such as stress concentrations or areas of high deformation.

The meshing process involves several steps, including:

- Geometry cleanup: The geometry of the model is cleaned up to remove any inconsistencies, such as small gaps or overlaps, that may cause issues during meshing.

- Mesh size determination: The size of the elements is determined based on the geometry and the requirements of the analysis. This may involve using automatic mesh generation tools or manually specifying the element size.
- Element type selection: The type of element used in the mesh is selected based on the requirements of the analysis. Common element types include linear or quadratic triangular or quadrilateral elements for two-dimensional analysis, and tetrahedral or hexahedral elements for three-dimensional analysis.
- Mesh generation: The mesh is generated using software tools that divide the model into the specified elements and connect them at the nodes.
- Mesh refinement: The mesh is refined in areas where higher accuracy is required, such as regions of high stress or deformation.
- Mesh quality check: The quality of the mesh is checked using metrics such as element distortion and aspect ratio to ensure that it meets the desired criteria.

Mesh size of 0.6 mm (corresponding to coarseness level -40) was chosen to avoid large size models that would increase simulation time, without compromising on the accuracy of the results. The models comprised an average of 125 343 tetrahedral elements.

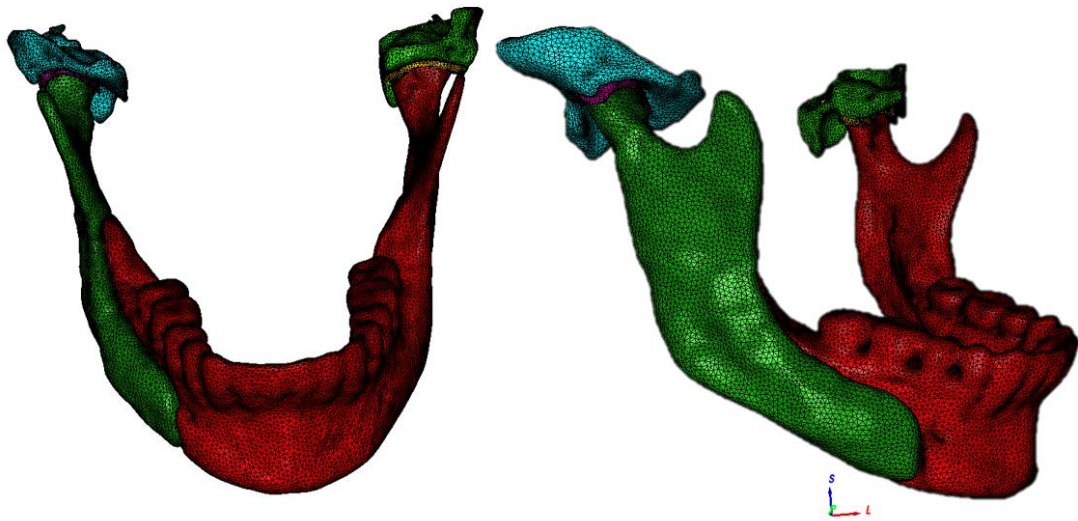


Figure 3.7. Meshed model of the mandible.

2. *Finite Element Analysis (FEA)*

a. Definition of material properties

Most FEA investigations concentrate on verifying the material properties assumption. It is assumed that oral tissues exhibit homogeneous isotropic material properties. From the available literature, material properties (Young's Modulus of Elasticity and Poisson's ratios) of trabecular bone, teeth, articular disk, and PDL ligament were defined (Table 3.1).

The values utilized in the present study are drawn from the logic and usage shared by many writers who have studied the material characteristics of the mandible and the TMJ complex. (D. R. Carter & Spengler, 1978.);(J. Chen et al., 1998); (Tanaka et al., 2004); It is assumed that all of the materials employed in this study are homogenous, isotropic, and linearly elastic. (Tanne et al., 1996).

Table 3.1. Material properties of the different components of the models.

Material	Elastic Modulus (MPa)	Poisson's ratio
Cortical Bone	13700	0.3
Trabecular Bone	7900	0.3
Articular Disk	44.1	0.45
Teeth	20000	0.3
PDL	0.68	0.45

b. Interactions

After creating individual masks of each component of the model such as the temporal bone, menisci, the ramus and the body of the mandible on the operated and non-operated sides, these masks were imported individually into ABAQUS CAE. The “find contact pair” tool, which is an automatic tool that locates the different types of interactions between the various imported masks, is used to identify the different interactions between the various masks/components. Using the “edit contact property” tool (Figure 3.8), tangential behavior was rearranged to have a frictionless contact at the level of the surgical cut between the ramus and the body of the mandible; and penalty with a friction coefficient of 0.001 (The disc-condyle, disc-temporal bone, interaction was regarded as contact with a frictional coefficient of 0.001 in previous finite element analyses) (Shu et al., 2018).

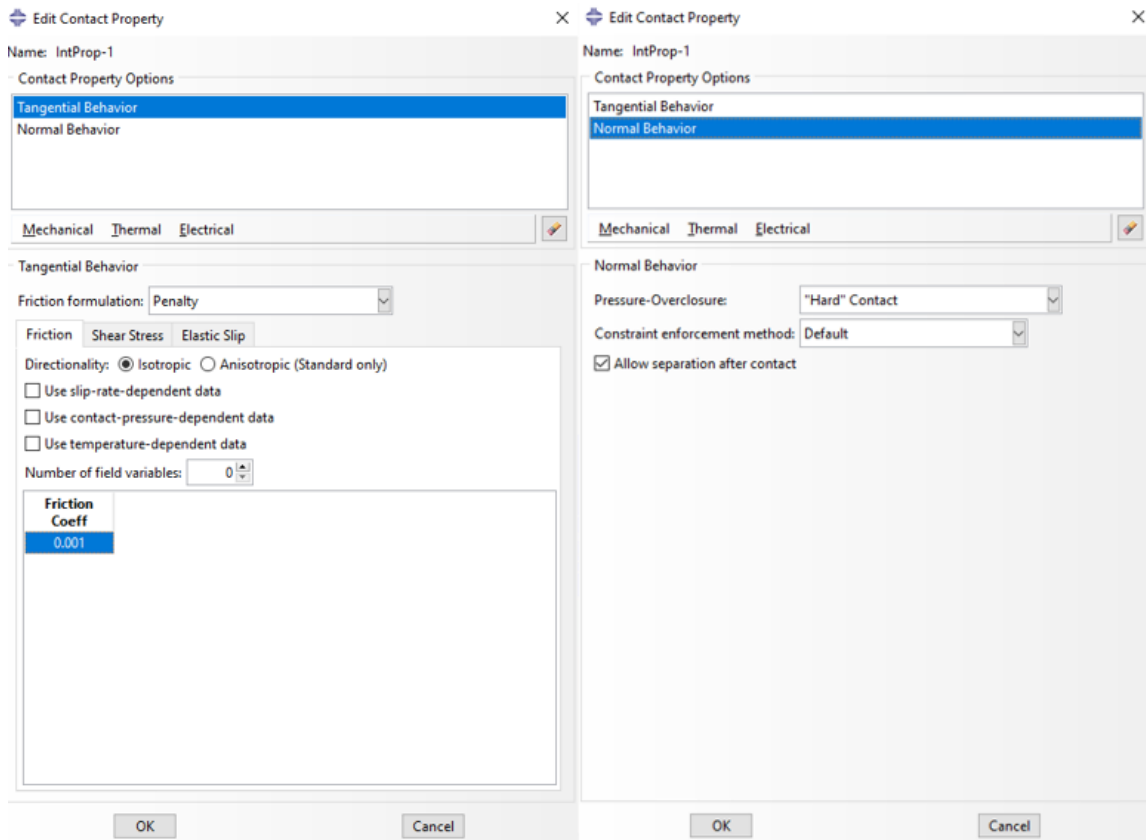


Figure 3.8. Tangential and normal behavior contact properties.

In order to limit the atypical lateral condylar movement during the USSO simulation in ABAQUS CAE and to simulate the articular capsule to keep the condyles in the articular fossa, “connectors” from the interaction module was used with a hinge type (Figure 3.9).

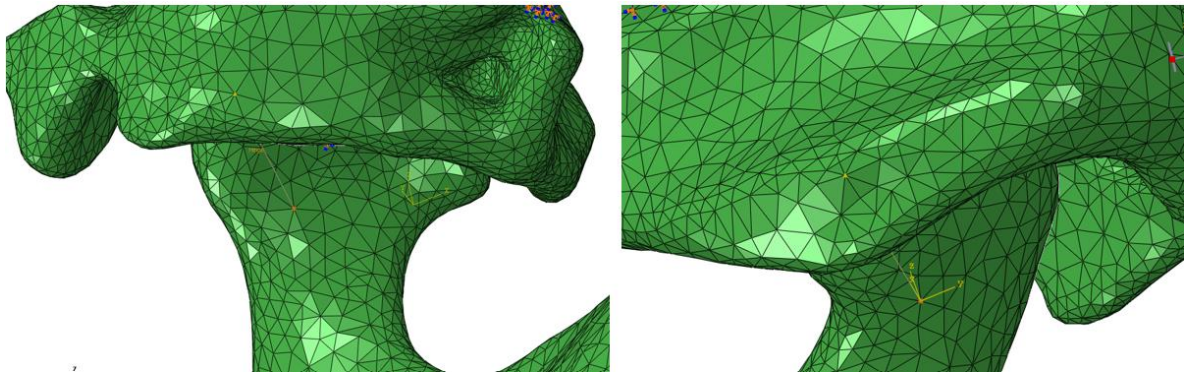


Figure 3.9. Hinge type connectors at the level of the condyles.

c. Loading setups

To simplify the experiments, certain initial and loading conditions are used that do not fully replicate all the factors present in real surgical movements. (there is no friction while doing a surgical movement). However, despite these simplifications, the experiments still reflect the fundamental surgical steps that is similar to what occurs in clinical situations.

i. Load/displacement

The 8 models were divided into 2 categories comprising 4 patients each on which advancement or setback movements were done. The amount of displacement in both groups ranged from 4 to 12 mm in increments of 2 mm. As a result, for each patient the mandible was advanced or set back by 4,6,8,10 and 12 mm resulting in a total of 5 FEA runs for each patient.

Since surgical movements are done in a single setting and not extended over time, displacements rather than forces were applied to the FEA models to simulate the surgical advancement or setback movements. The displacements were applied on 30 nodes selected

from the mandibular body mesial to the surgical cut. The displacement application was replicated at the same location for each patient. (Figure 3.10).

In ABAQUS, a mechanical boundary condition was created with the type “displacement/rotation” from which a datum axis was constructed using 3 points of origin to replicate the direction of the displacement in both surgical setups. The direction of the displacement followed the X axis with no components in the Y and Z axes (X=U1=4/6/8/10/12 mm).

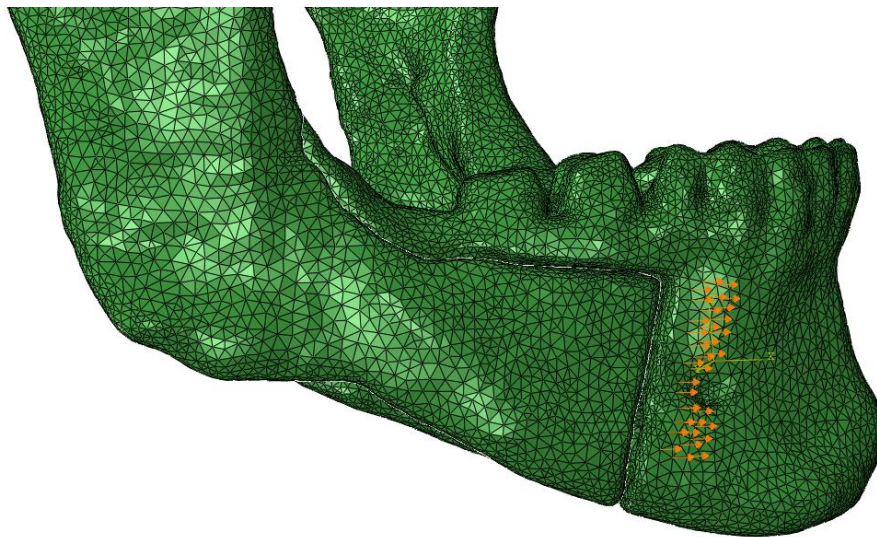


Figure 3.10. Direction vectors of the displacement with the Datum axis.

ii. Boundary conditions

Most FEA studies have considered any part of the cranial base such as the temporal bone as fully restrained. This assumption is logical because the bones of the cranial base are fused together and therefore restricted in all directions. Thus, in our study, the top

surfaces of the modeled temporal bones were selected using 200 nodes on each side left and right, where the “ENCASTRE” option was selected to restrict the selected body or part in all planes of space in both translation and rotation ($U1=U2=U3=UR1=UR2=UR3=0$) (Figure 3.11).

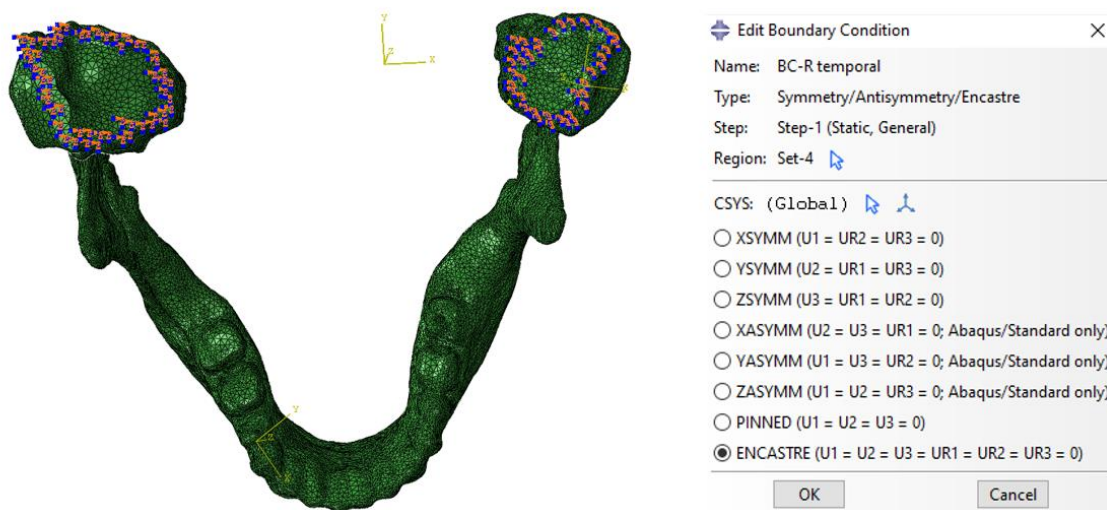


Figure 3.11. Boundary conditions settings.

e. Data collection

i. Measures

Deflection, stress, stresses, vibration, displacement, energy storage, and many more phenomena can all be calculated using FEA. The most frequently assessed metrics in dental FEA investigations are displacement of the crowns and stress evaluation at the PDL. In orthodontics, the area where tooth movement occurs is indicated by the stress distribution caused by forces between the periodontal ligament and the bone. As a result, it is assumed

that stress at the PDL will increase proportionally to the pace of bone remodeling (Kojima et al., 2012). Also, it suggests the locations where root resorption is more likely to occur. Not only the forces at the level of the teeth are studied but also displacement in different surgical setups at the level of the maxilla or mandible. Total displacement is the sum of the initial translation movements of a node in the X, Y, and Z axes plus the rotation movements about the same axes. A measurement of a material's elasticity, von Mises stresses at an element represents the point at which the elastic limit is surpassed, and permanent deformation occurs.

FEA results are typically presented using color-mapped diagrams and arrows. Yet, statistical analysis using numerical data is necessary to be able to show individual variances. The ability to gather numerical stresses, displacement, and other events at each node or element is provided by Abaqus. For stress data collection, a set containing randomly selected elements uniformly dispersed along each surface of the neck of the condyle and the different surfaces of the menisci (anterior, posterior, lateral, medial) each containing 60 elements was created. Figure 3.12 shows the method used to separate the 4 surfaces of the meniscus and the condyles (anterior, posterior, medial and lateral). For displacement data collection, 100 nodes were selected uniformly at the surfaces of the condyle and the neck of the condyle. Running the finite element analysis, the stress and displacement results were exported as DAT. files into excel where the averages were calculated. Finally, the averages were put in final data sheets (need to define the measurements used before describing how they were done)

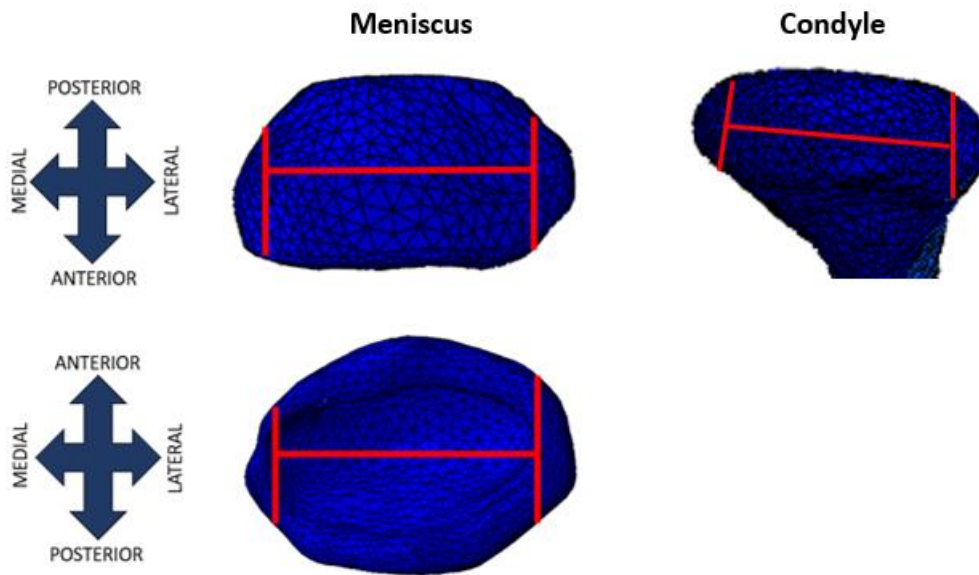


Figure 3.12. separation method for the different surface of the meniscus and condyles.

The condylar volume was measured using Simpleware Scan IP, where the “measurements/volume” tool was used to deliver accurate numbers (Figure 3.13).

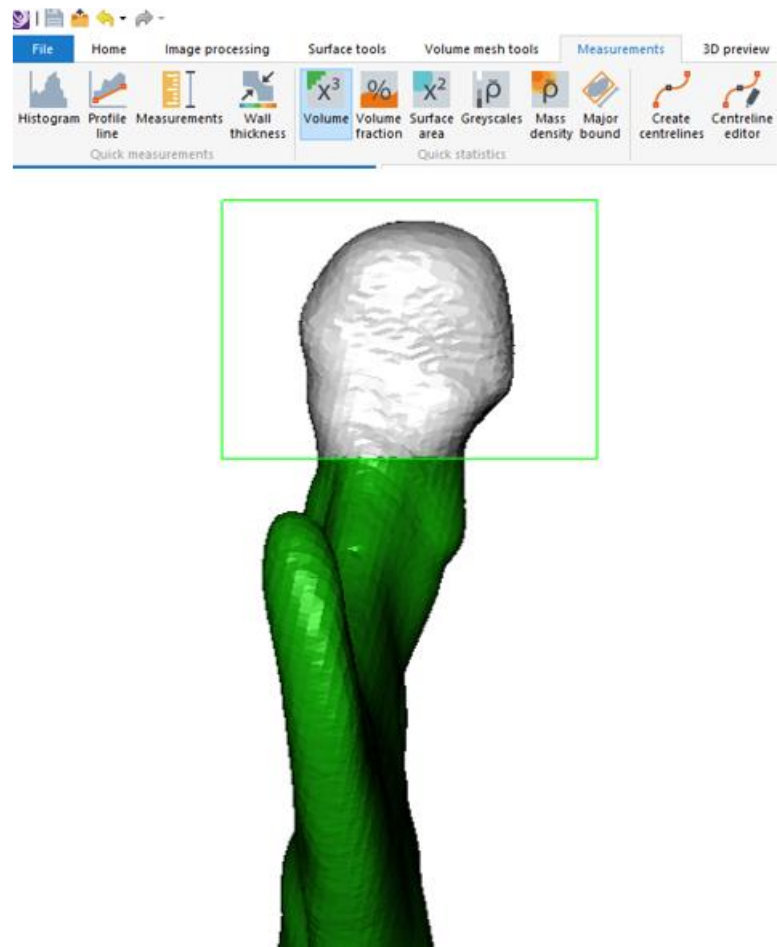


Figure 3.13. Condylar volume calculation in Simpleware Scan IP.

3. *Statistical analysis*

Within the study design adopted, three independent variables can be defined:

1. The between-subjects variable represented by the advancement vs setback at the operated side of the mandible
2. The within-subjects variables represented by the increment of movement (4,6,8,10,12 mm) and the operated vs non-operated side factor

Four outcomes are assessed and measured relatively to the different variables:

Displacement at condyles

1. Displacement at neck of condyles
2. Stress at neck of condyles
3. Stress at the level of menisci (medial, lateral, anterior and posterior)

For every outcome, a three-way ANOVA test was applied with two within-subjects and one between-subjects factors. The correlations between the different interactions were analyzed using the Pearson test. Significance was set at 0.001.

Descriptive statistics (means and standard deviations) were generated for all the outcome variables: displacement and stress distribution at condyles, condylar necks and stress at the level of menisci (medial, lateral, anterior and posterior). They were all normally distributed (Shapiro-Wilk's p value > 0.05).

A three-way mixed ANOVA test was used to investigate the effects of three independent variables: one between-subjects (advancement vs. setback) and 2 within-subjects (degree of movement and side -operated vs. non-operated) on each outcome variable. Among all the outcome variables, only the posterior stress at the level of menisci presented a three-way interaction between side, amount and group. All other variables showed a statistically significant 2-way interaction between side and amount. The ANOVA test was followed by reporting of simple main effects and Bonferroni adjustments were applied throughout the tests.

In addition, Pearson product moment correlation coefficients were used to assess the correlation between displacement and stress at the neck of the condyles, displacement, and

condylar volume with different surgical movements (4, 6, 8, 10, 12 mm) in operated vs non-operated sides.

The IBM® SPSS® statistics 24.0 statistical package was used to carry out all statistical analyses. Statistical significance was set at 0.05.

CHAPTER IV

RESULTS

In this section, the findings on stress and displacement are compared accounting for differences between operated and non-operated sides, type of USSO (advancement vs. setback), and increments of surgical movements. Moreover, outcomes will be displayed at the level of the condylar surfaces, meniscus, and condylar neck.

Considering the number of patients with the 2 diverging USSO procedures, each patient will be considered separately in the first part of this section and justified combined statistics in a second part.

A. PART 1: change in stress and displacement relative to surgical movement: case series

To determine the pattern of change between operated and non-operated side, each individual patient was considered separately. First, the comparison was a display of changes in stress or displacement plotted against ranges of surgical movements. The outcome was a display that allowed the determination of trends between the sides at various anatomical levels. In the next sections, the velocity curves of the mean stresses at the neck of the condyles represent the differences between the incremental surgical values (from 4 to 6, 6 to 8, 8 to 10 and 10 to 12 mm) displayed relative to stress and displacement.

1. Stress at the neck of the condyles

The stress distribution at the level of the condylar neck reveals the activity at the non-operated side of either advancement or setback (Fig. 4.1), with a progression of stress as the surgical movement was increased. The stresses were more intense and diffused at the non-operated setback condylar neck.

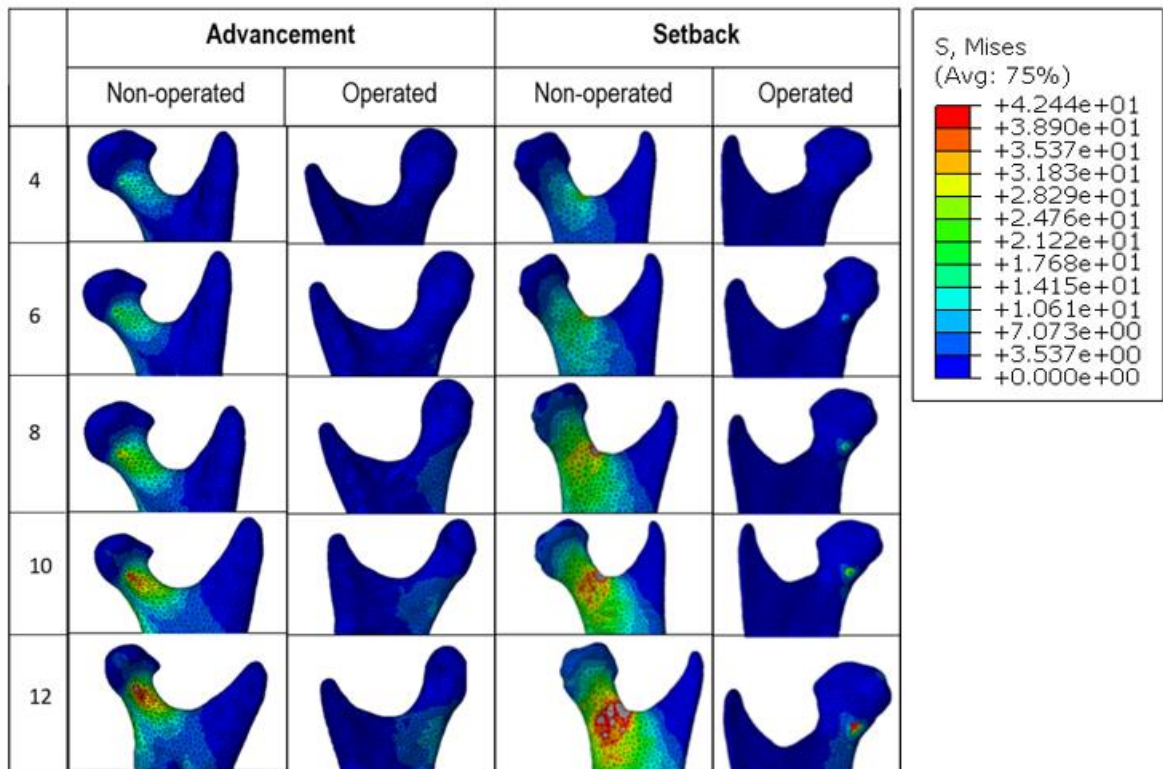


Figure 4.1. Finite element analysis visual representation of the stress increase at the level of the neck of the condyles in one patient whose USSO involved mandibular advancement, and another with mandibular setback. Note the higher stresses on the non-operated side, more intense and diffused in the setback operation.

The computation of velocity revealed that the largest response to the surgical displacement was from 0 to 4 mm, whether advancement or setback (Fig. 4.2;). Whereas

the operated side displayed minor changes in stress, the non-operated side disclosed most reactions, apparently stabilizing between 4 to 6mm of surgical movement (4.024 MPa in advancement; 3.957 MPa in setback), before further increase between 6 to 8mm, and decline thereafter.

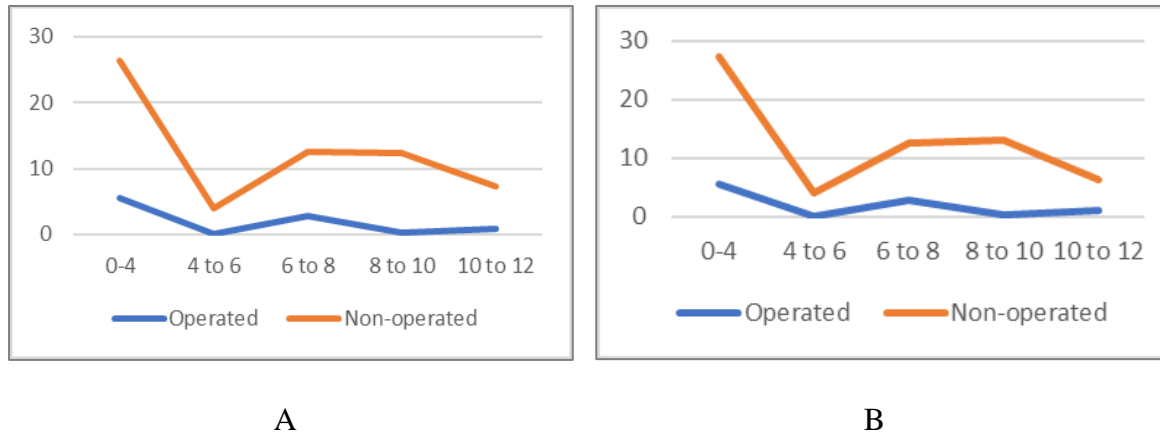


Figure 4.2. Velocity curves illustrating stress (y axis) at the neck of the condyles relative to incremental surgical advancement (A) and setback (B) movements (x axis) on the operated and non-operated sides.

2. *Stress at the anterior surface of the meniscus*

The stress distribution at the anterior surface of the meniscus also was greater at the non-operated side of either advancement or setback (Fig. 4.3), increasing in intensity as either movement was greater. The anterior surface of the menisci was subjected to more stress than the other parts of the disc.

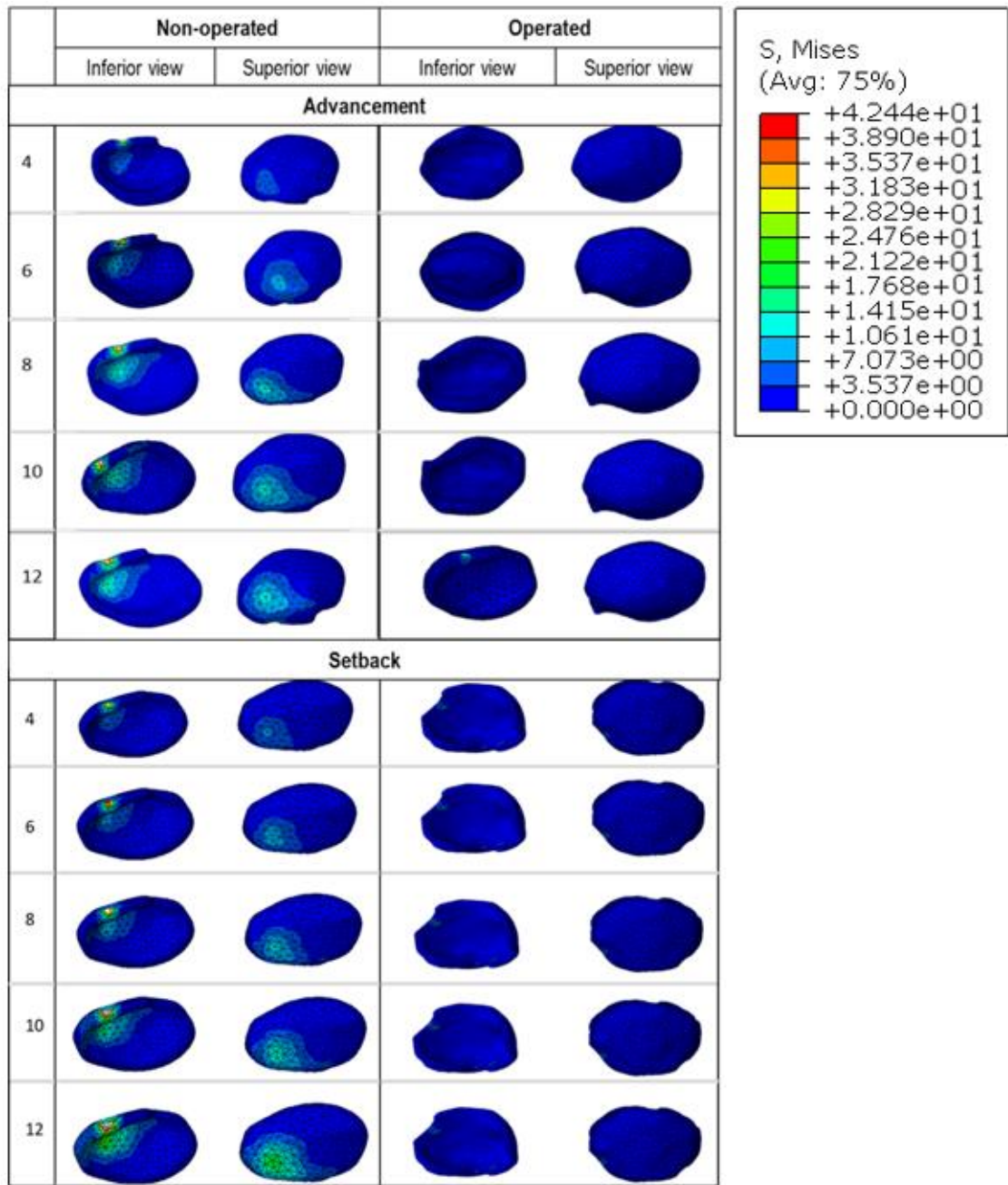


Figure 4.3. Finite element analysis visual representation of the stress increase at the level of the menisci in one patient with advancement USSO and another with mandibular setback. Note the higher stresses on the non-operated side increased with the surgical movement and more intense in the setback operation.

The same pattern was observed in the response at the anterior surface of the meniscus, but the change occurred at different surgical brackets. The greatest response to

the surgical displacement was also from 4 to 6 mm (Fig. 4.4). The operated side displayed nearly no changes in stress. The stress on the non-operated side decreased the most between 6 to 8mm of surgical movement (0.21781MPa in advancement; 0.340179 MPa in setback), then increased between 8 to 10mm to nearly half of the initial increase between 0 to 4mm.

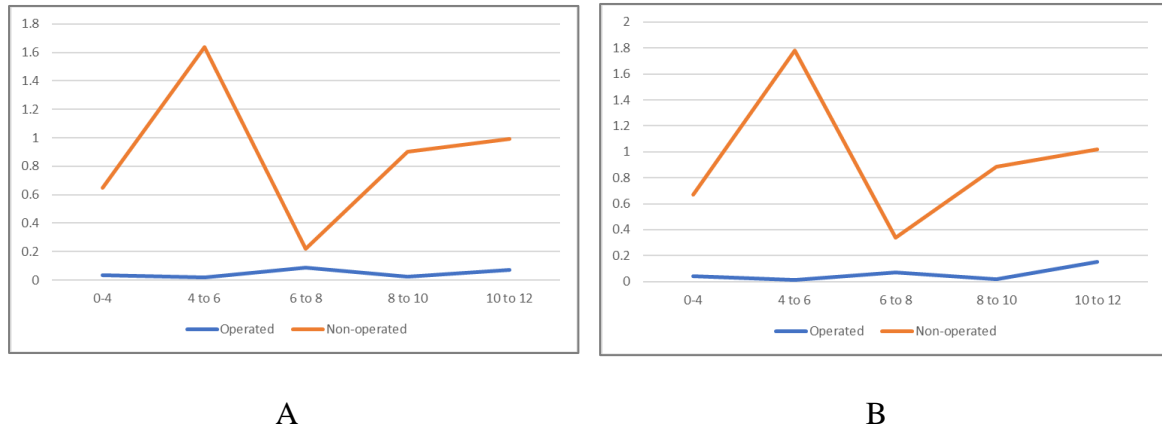


Figure 4.4. Velocity curves illustrating stress (y axis) at the anterior surface of the meniscus relative to incremental surgical advancement (A) and setback (B) movements (x axis) on the operated and non-operated sides.

3. Stress at the different condylar surfaces

The stress distribution was at the anterior, posterior and lateral surface of the condyle with the highest value at the posterior surface at the non-operated side in advancement (Fig. 4.5), increasing in intensity as either movement was greater. The same pattern emerges at setback for the non-operated condyle but with a higher value at the anterior surface.

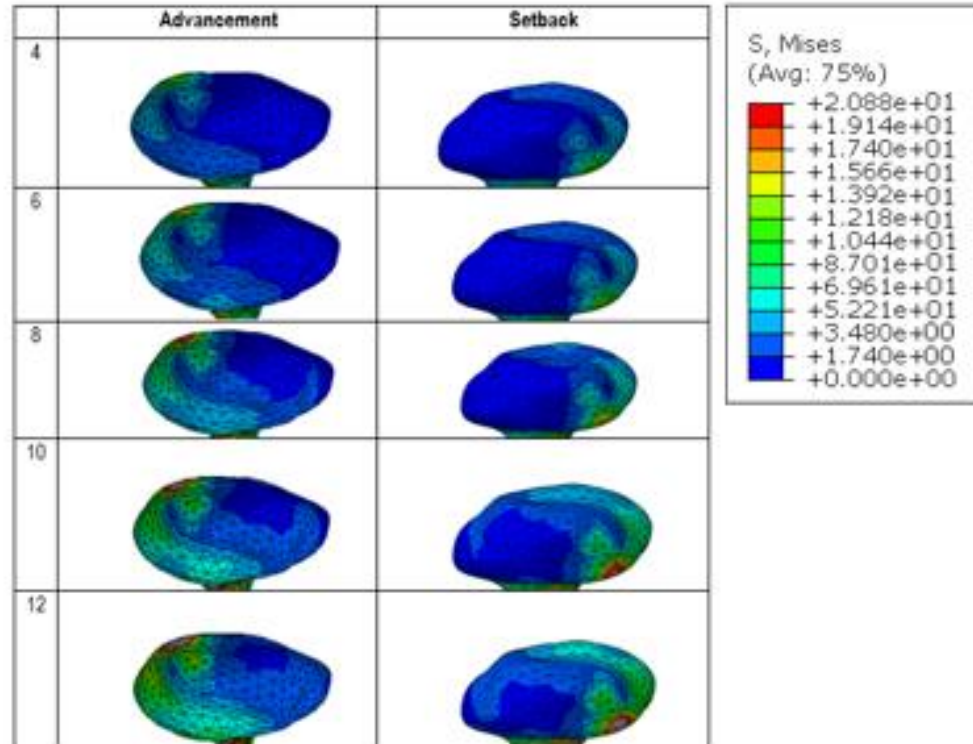


Figure 4.5. Finite element analysis visual representation of the stress increase at the level of the non-operated condyle in one patient with advancement USSO and another with mandibular setback. Note the higher stresses on the non-operated side increased with the surgical movement.

The patients in this group presented similar plots of stress relative to surgical advancement or setback yet differing from the neck of the condyle (Figs. 4.6, 4.7). On the operated side, the velocity of changes remained minimal. On the non-operated side, the anterior and posterior surfaces exhibited the highest stresses, stabilizing between 4 to 6mm until 10 to 12mm. The lateral surface followed the same trend but at a lower stress level.

In Figs 4.6 and 4.7, the actual advancement or setback that the respective patients underwent is represented by a black arrow. In all patients, the surgical movement was equal to or smaller than 4mm.

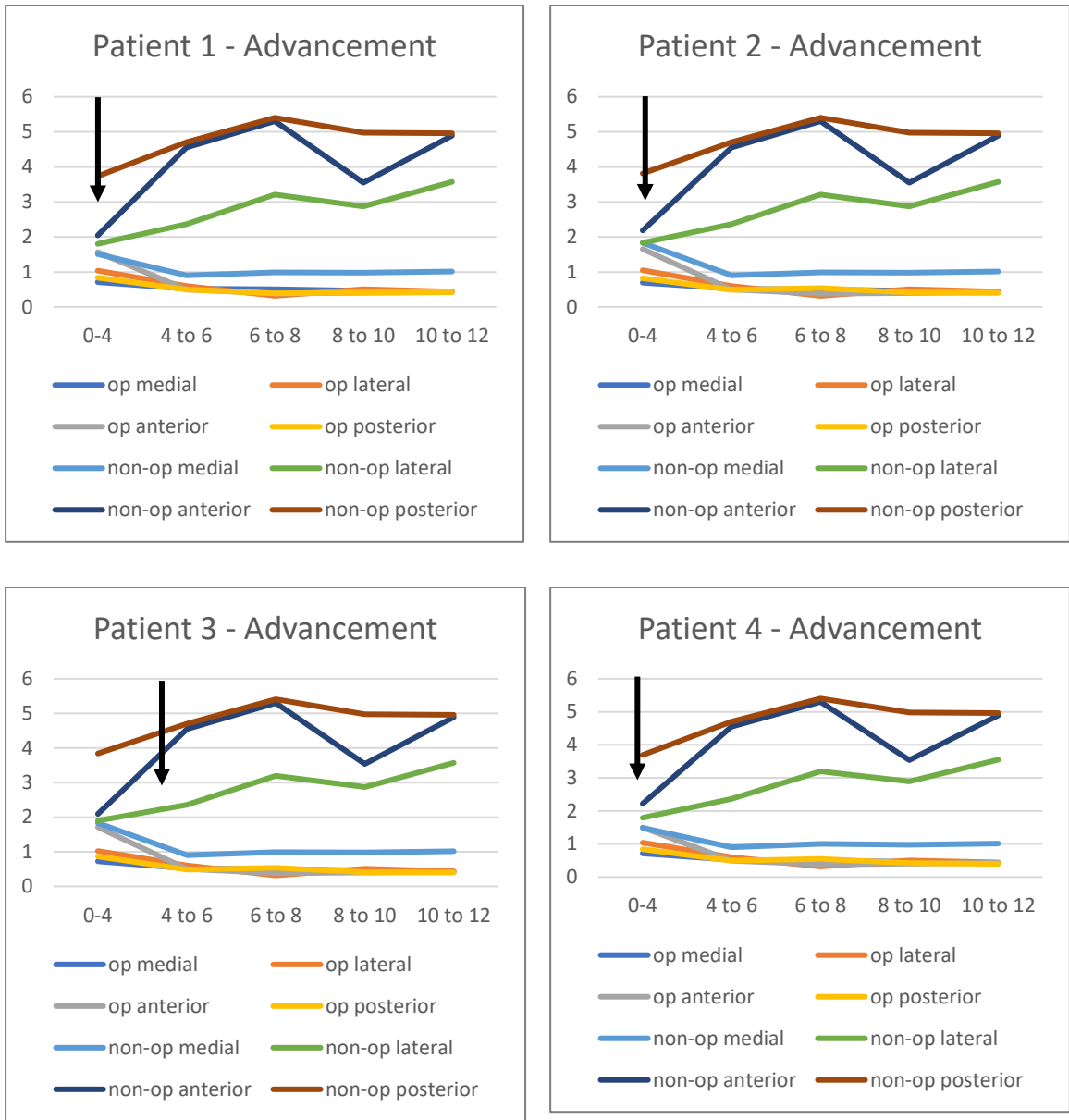


Figure 4.6. Velocity curves of individual advancement patients plotting stress at the condyles relative to the incremental surgical movements ranges with the black arrow showing actual surgical movements done by the surgeon.

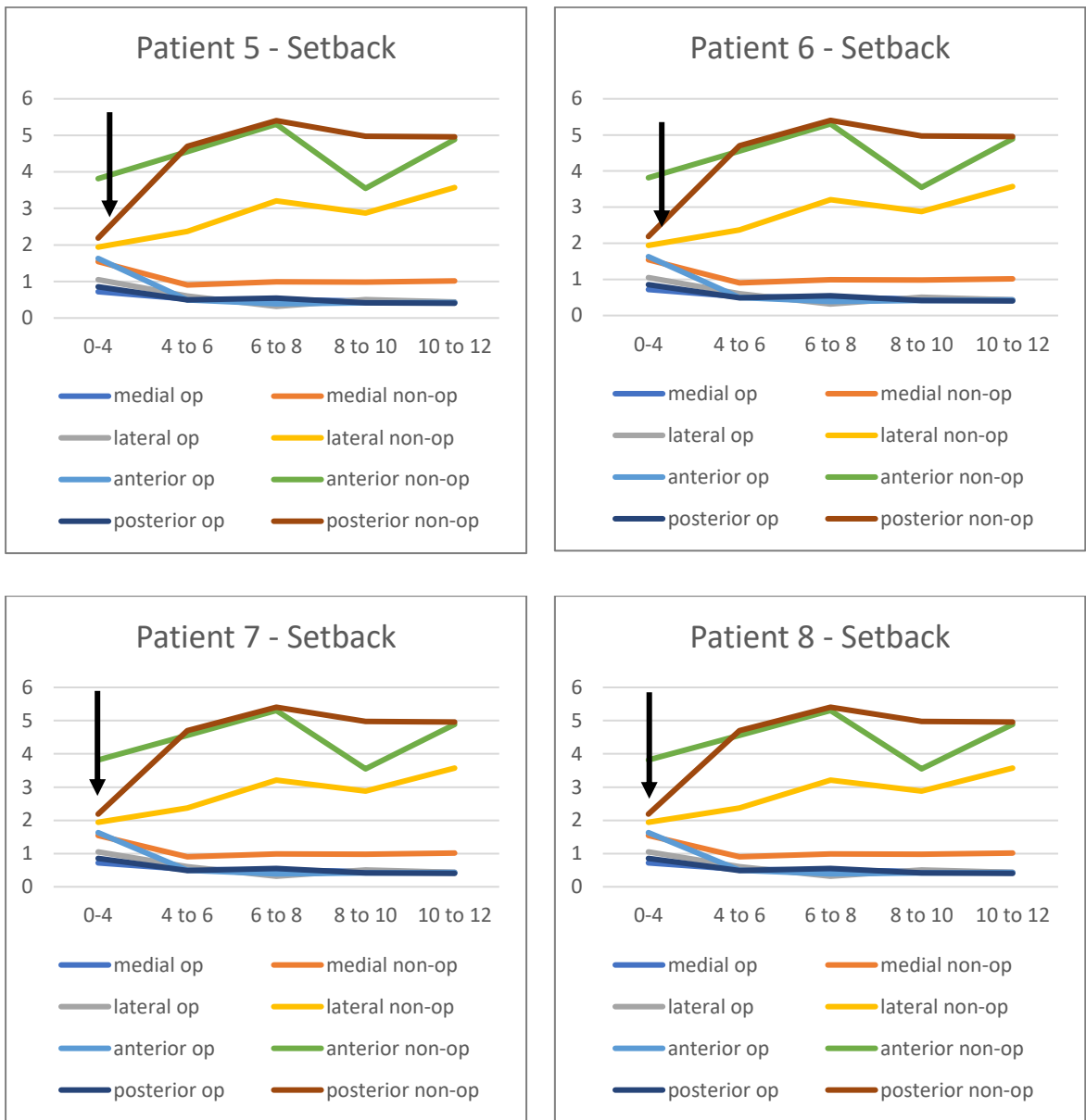


Figure 4.7. Velocity curves of individual setback patients plotting stress at the condyles relative to the incremental surgical movements ranges with the black arrow showing actual surgical movements done by the surgeon.

Because the same pattern emerged in all patients, the means of the movements were computed and plotted to display the general trends (Figs. 4.8)

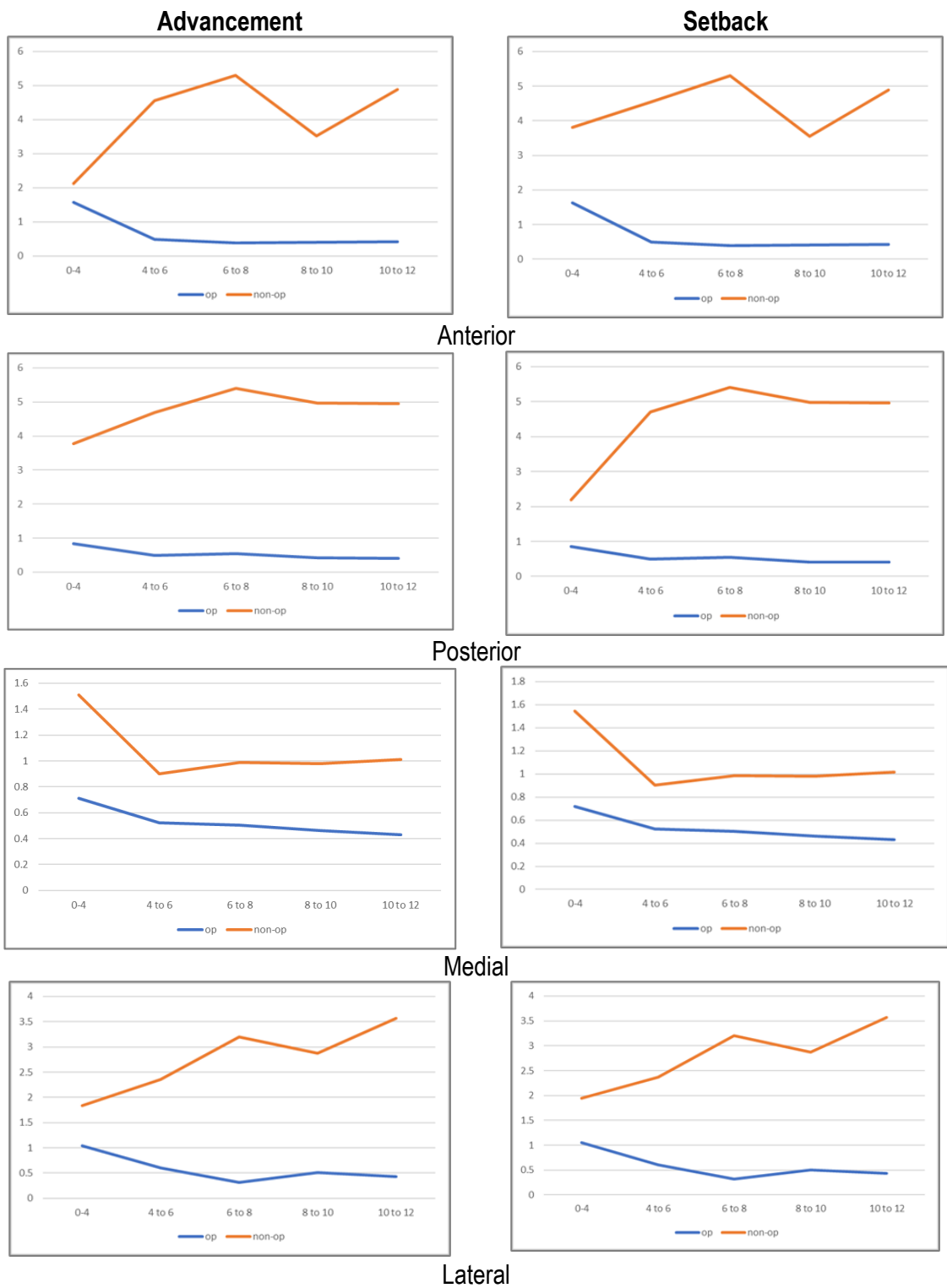


Figure 4.8. Graphs representing the velocity curves of mean stresses at various condylar surfaces relative to incremental surgical advancement and setback movements.

4. Displacement at the condyles and condylar necks

A similar trend was observed of a decrease in the velocity of displacement between the operated and non-operated sides in the advancement and setback categories, albeit averaged for 4 patients in each (Fig. 4.9). However, the non-operated side displayed greater values than the operated side. Whereas the operated side seemingly reached a plateau at the range of surgical movement 4 to 6mm (within 0.1mm), the non-operated side kept moving on a downward slope until the 8 to 10mm level.

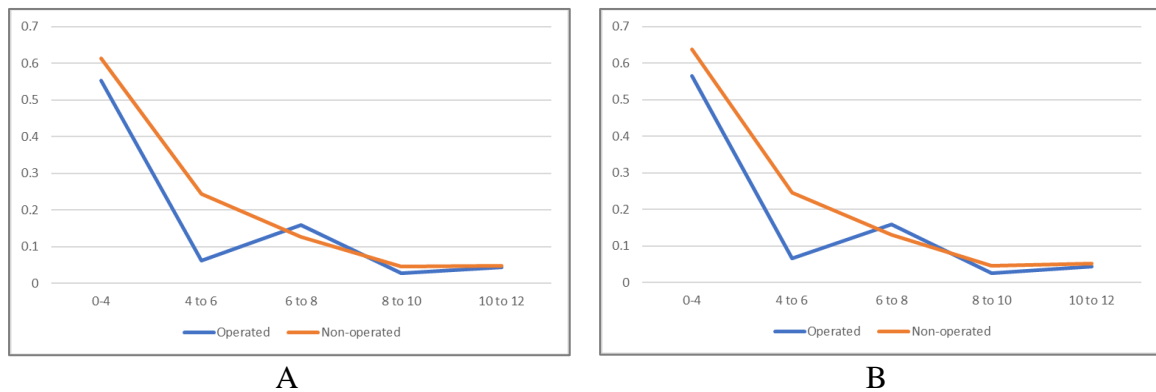


Figure 4.9. Graphs representing the velocity curve of the displacement at the condyles relative to surgical advancement (A) and setback (B) movements.

The same pattern emerged for the condylar neck as for the condyles, however the non-operated side seemed to plateau, like the operated side, at 6 to 8mm (Fig. 4.10).

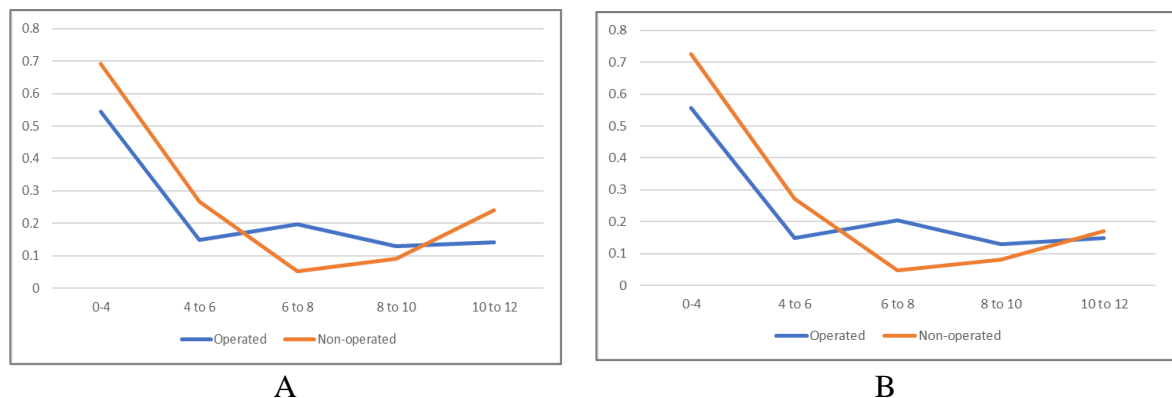


Figure 4.10. Graph representing the velocity curve of the displacement at the neck of the condyles relative to surgical advancement (A) and setback (B) movements.

B. PART 2: Comparisons of the outcome variables between surgical groups, degree of movements and sides

Although the sample size was very limited (n=4 in advancement and n=4 in setback groups), the similar pattern of movements was a basis for the more involved statistics to explore emerging trends, with the realization that any conclusion may not be generalized and would require larger sample sizes. Such exploration would warrant countless hours of work, considering the time invested in the present constructions and computations.

The data met the assumptions of a three-way mixed ANOVA, the optimal test to use to investigate the effects of 3 independent variables: one between-subjects (advancement vs. setback) and 2 within-subjects (degree of movement and side -operated vs. non-operated) on each outcome variable.

The three-way interaction was not significant for any of the outcome variables except for the stress at the neck of condyle ($p=0.04$) and stress at the level of menisci on the posterior side ($p<0.001$) (Table 4.1). Therefore, comparisons were made for each subgroup separately. All the other variables exhibited a two-way interaction between side and amount; and the results of the variables were compared accordingly.

Table 4.1. Three-way mixed ANOVA interactions for the different variables.

Variable	df	Str-Neck cond		Disp- cond		Disp- Neck cond	
		F	p	F	p	F	p
Side*Group	4	0.046	0.837	0.452	0.527	1.095	0.336
Amount*Group	4	2.490	0.162	0.553	0.698	0.996	0.357
Side*Amount	4	3129.33	<0.001**	697.099	<0.001**	32.529	0.001**
Side*Amount*Group	4	5.966	0.04*	0.521	0.721	1.002	0.359

Stress at menisci									
Variable	df	Medial		Lateral		Anterior		Posterior	
		F	p	F	p	F	p	F	p
Side*Group	4	1.375	0.285	0.020	0.893	3.107	0.128	8.826	0.025*
Amount*Group	4	1.757	0.231	1.735	0.233	1.740	0.221	17.336	0.001**
Side*Amount	4	799.95	<0.001**	52.969	<0.001**	8119.88	<0.001**	74.397	<0.001**
Side*Amount*Group	4	1.504	0.267	1.243	0.309	1.169	0.340	44.666	<0.001**

* Significant at the 0.05 level, **Significant at the 0.01 level

1. Difference between advancement and setback

When controlling for other variables, there was no statistically significant difference between advancement and setback in all different outcomes: displacement at the level of the condyles ($p=0.137$), neck of the condyles ($p=0.062$), stress at the neck of the menisci on the medial ($p=0.243$), lateral ($p=0.843$) and anterior ($p=0.082$) sides.

The stress at the level of the neck of the condyle also was not statistically significantly different for both operated and non-operated sides ($p=0.489$ and 0.092 respectively). The stress at the posterior side of the menisci was only significant on the non-operated side ($p=0.028$). Stress in the setback group (0.627 ± 0.037 MPa) was significantly greater than in the advancement group (0.477 ± 0.037 MPa) (Table 4.2).

Table 4.2. Comparison of the outcome variables between advancement and setback.

	Advancement N=4		Setback N=4		Difference		3-way mixed ANOVA	
	EMM	SE	EMM	SE	EMM	SE	F	P
Displacement condyle	0.814	0.009	0.837	0.009	-0.023	0.013	2.936	0.137
Displacement neck of condyle	0.926	0.010	0.958	0.010	-0.032	0.014	5.228	0.062
Stress neck of condyle								
Operated	7.396	0.151	7.554	0.151	-0.157	0.213	0.544	0.489
Non-operated	43.576	0.364	44.608	0.364	-1.031	0.515	4.006	0.092
Stress meniscus								
Medial	1.390	0.059	1.497	0.059	-0.108	0.083	1.679	0.243
Lateral	0.207	0.009	0.209	0.009	-0.003	0.012	0.043	0.843
Anterior	3.486	0.090	3.219	0.090	0.267	0.128	4.366	0.082
Posterior								
Operated	0.145	0.007	0.143	0.007	0.002	0.010	0.039	0.850
Non-operated	0.477	0.037	0.627	0.037	-0.150	0.052	8.236	0.028*

EMM: Estimated Marginal Mean; SE: Standard Error. Significant at *0.05 and **0.01

2. *Effect of amount of surgical movement and side (operated vs non-operated)*

a. Stress at the condylar necks

In the advancement group, a statistically significant increase in stress among incremental changes (4,6,8,10 and 12 mm) was recorded on both the operated and non-operated sides ($p < 0.001$) (Table 4.3). Comparisons between the different increments of displacement also revealed that stress increased significantly on the operated side from 4 to 6 ($p = 0.002$), 6 to 8 ($p < 0.001$), 8 to 10 ($p = 0.034$) and 10 to 12 mm ($p < 0.001$). On the non-operated side, stress also increased significantly among the different increments of displacement (p values < 0.001). At the level of the neck of the condyle, higher stress level was found on the non-operated side compared with the opposite side with each amount of surgical movement (4,6,8,10, 12 mm) ($p < 0.001$).

In the setback group, a statistically significant increase in stress among 4, 6, 8, 10, and 12 mms was recorded ($p < 0.001$). Increases in stress from 6 to 8, 8 to 10, and 10 to 12 mm were statistically significant ($p < 0.001$) on the operated side. On the non-operated

side, stress increases were statistically significant ($p < 0.001$) for each increment increase (4 vs 6, 6 vs 8, 8 vs 10, and 10 vs 12 mm). Stress differences between the operated and non-operated sides were statistically significant ($p < 0.001$), with values greater on the non-operated side with each increase in movement (4,6,8,10, and 12) (Table 4.4).

Table 4.3. Stress at the condylar neck in the advancement group (n=4)

	Operated		Non-operated		Difference		3-way mixed ANOVA	
	EMM	SE	EMM	SE	EMM	SE	F	P
4 mm	5.454	0.142	26.437	0.320	-20.983	0.405	2687.776	<0.001**
6 mm	5.545	0.143	30.461	0.328	-24.916	0.415	3609.865	<0.001**
8 mm	8.242	0.143	42.974	0.366	-34.732	0.459	5737.346	<0.001**
10 mm	8.409	0.160	55.409	0.628	-47.000	0.702	4488.442	<0.001**
12 mm	9.332	0.176	62.601	0.368	-53.269	0.444	14394.08	<0.001**
F	13143.892		11217.270					
p	<0.001**		<0.001**					
4 vs 6	0.002**		<0.001**					
6 vs 8	<0.001**		<0.001**					
8 vs 10	0.034*		<0.001**					
10 vs 12	<0.001**		0.001**					

EMM: Estimated Marginal Mean; SE: Standard Error. Significant at *0.05 and **0.01

The association between the amount of surgical movement performed in the advancement setup, ranging from 4 to 12 mm, and the stress at the level of the condylar neck is shown in Fig 4.11 (A). The Von Mises stresses were greater on the non-operated side, ranging from 27.420 to 63.219 and lower on the operated side, ranging from 5.601 to 9.484. In the setback group, stress at the surgical neck of the condyles relative to surgical movement increased (Fig. 4.11-B). The Von Mises stresses were higher on the contralateral side (range: 26.347 to 62.601) compared with the ipsilateral side (range: 5.454 to 9.332), also increasing with the amount of advancement from 4 to 12 mm.

Table 4.4. Stress at the condylar neck in the setback group (n=4)

	Operated		Non-operated		Difference		3-way mixed ANOVA	
	EMM	SE	EMM	SE	EMM	SE	F	P
4 mm	5.601	0.149	27.420	0.306	-21.818	0.211	5839.403	<0.001**
6 mm	5.716	0.151	31.377	0.353	-25.661	0.240	11410.11	<0.001**
8 mm	8.395	0.149	43.968	0.347	-35.573	0.253	19745.40	<0.001**
10 mm	8.571	0.149	57.054	0.307	-48.483	0.216	50152.4	<0.001**
12 mm	9.484	0.148	63.219	0.347	-53.735	0.240	49927.62	<0.001**
F	32649.044		74669.280					
p	<0.001**		<0.001**					
4 vs 6	0.145		<0.001**					
6 vs 8	<0.001**		<0.001**					
8 vs 10	<0.001**		<0.001**					
10 vs 12	<0.001**		<0.001**					

EMM: Estimated Marginal Mean; SE: Standard Error. Significant at *0.05 and **0.01

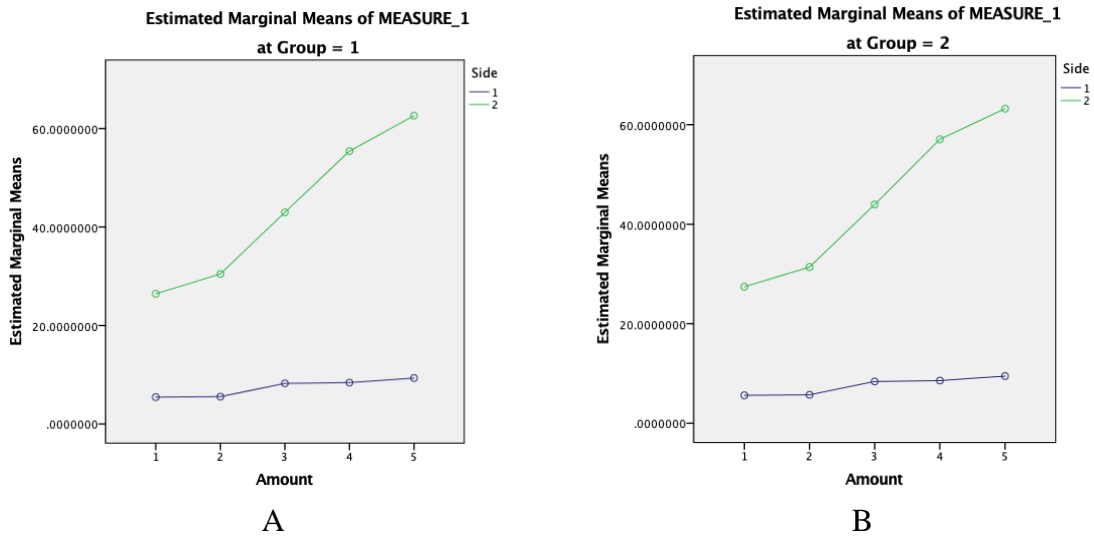


Figure 4.11. Stress at the level of the neck of the condyle: **A**. Advancement; **B**: Setback. Side 1= operated, Side 2= non-operated. (Amount 1 = 4mm; 2= 6mm; 3= 8mm; 4= 10mm; 5= 12mm).

b. Stress at the medial surface of the menisci

In the advancement group, an increase of stress among incremental changes (4, 6, 8, 10, and 12 mm) was observed in both operated and non-operated sides (p= 0.002, p< 0.001). Increase in stress from 10 to 12 mm was statistically significant on the operated side

(p=0.033). On the non-operated side, statistical significance ($0.004 < p < 0.001$) was observed between all pairs of increments. Stresses were higher on the non-operated side (Table 4.5).

Statistically significantly higher Von Mises stresses at the non-operated side (range: 0.650 to 4.404) compared to the stresses on the operated side was lower (range: 0.034 to 0.237). The Von Mises stresses increased as the surgical movement increased from 4 mm to 12 mm.

Table 4.5. Stress at the medial surface of the menisci in the advancement group (n=4)

	Operated		Non-operated		Difference		3-way mixed ANOVA	
	EMM	SE	EMM	SE	EMM	SE	F	P
4 mm	0.034	0.002	0.650	0.011	-0.616	0.012	2686.489	<0.001**
6 mm	0.055	0.006	2.291	0.052	-2.236	0.049	2059.215	<0.001**
8 mm	0.140	0.017	2.508	0.064	-2.368	0.056	1818.481	<0.001**
10 mm	0.165	0.023	3.411	0.049	-3.245	0.045	5164.882	<0.001**
12 mm	0.237	0.025	4.404	0.044	-4.167	0.037	12687.28	<0.001**
F	56.636		3599.98					
p	0.002**		<0.001**					
4 vs 6	0.496		<0.001**					
6 vs 8	0.050*		0.004**					
8 vs 10	0.489		0.001**					
10 vs 12	0.033*		<0.001**					

EMM: Estimated Marginal Mean; SE: Standard Error. Significant at *0.05 and **0.01

In the setback group, stress levels were statistically significant between 4 and 6 mm ($p=0.012$) and 10 and 12 mm ($p=0.033$) increments on the operated side, and between all pairs of increments on the non-operated side. Higher stress was found at the non-operated side with each increment of surgical setback (Table 4.6). The Von Mises stress increased from 0.670 to 4.708 and was noticeably higher on the non-operated side than the operated side (ranging from 0.044 to 0.29).

Table 4.6. Stress at the medial surface of the menisci in the setback group (n=4)

	Operated		Non-operated		Difference		3-way mixed ANOVA	
	EMM	SE	EMM	SE	EMM	SE	F	P
4 mm	0.044	0.002	0.670	0.021	-0.626	0.023	773.124	<0.001**
6 mm	0.055	0.003	2.453	0.139	-2.397	0.141	287.181	<0.001**
8 mm	0.127	0.011	2.793	0.210	-2.666	0.216	151.883	0.001**
10 mm	0.146	0.002	3.677	0.211	-3.531	0.212	276.272	<0.001**
12 mm	0.299	0.010	4.708	0.238	-4.409	0.245	323.029	<0.001**
F	1440.7		265.433					
p	<0.001**		<0.001**					
4 vs 6	0.012*		0.006**					
6 vs 8	0.050*		0.384					
8 vs 10	0.489		<0.001**					
10 vs 12	0.033*		<0.001**					

EMM: Estimated Marginal Mean; SE: Standard Error. Significant at *0.05 and **0.01

The relationships between the stress at the medial surface of the menisci and the amount of surgical advancements and setbacks are illustrated in Fig. 4.12.

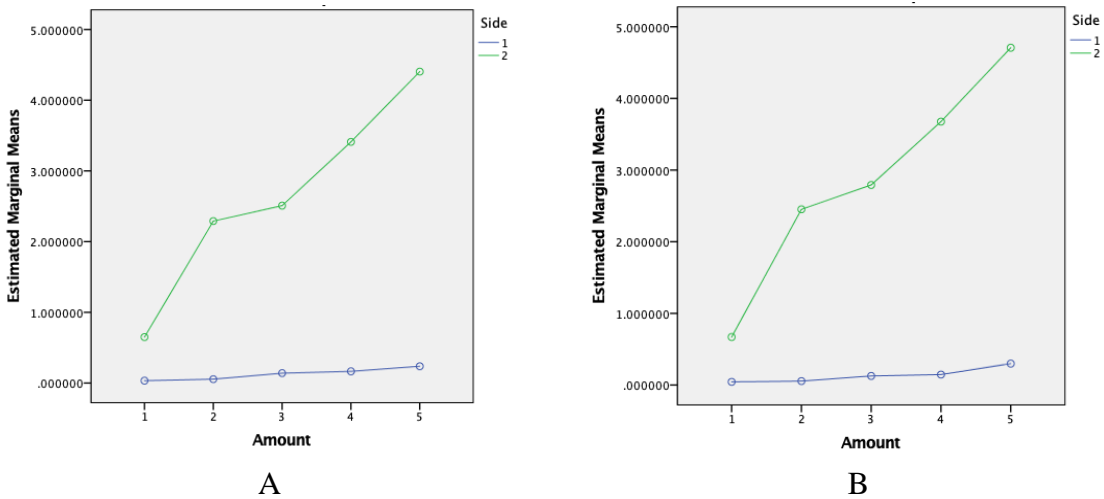


Figure 4.12. Von mises stresses (y axis) at the level of the medial surface of the meniscus in the advancement (A) and setback (B) groups.

Amounts of movements (x axis): 1 = 4mm; 2= 6mm; 3= 8mm; 4= 10mm; 5= 12mm.

Condylar sides: 1- operated, 2- non-operated.

c. Stress at the lateral surface of the menisci

In the advancement group, a statistically significant increase of stress among incremental changes (4,6,8,10 and 12 mm) was recorded on the operated ($p = 0.001$) and non-operated ($p=0.005$) sides. Stress increased significantly on the operated side from 4 to 6 ($p <0.001$), 6 to 8 ($p =0.019$). The stress increase on the non-operated side was statistically significant in each of the increments except for 8 vs 10 mm. Higher stress levels were found on the operated side than on the non-operated side with every increment of surgical movement (Table 4.7).

Table 4.7. Stress at the lateral surface of the menisci in the advancement group (n=4)

	Operated		Non-operated		Difference		3-way mixed ANOVA	
	EMM	SE	EMM	SE	EMM	SE	F	P
4 mm	0.076	0.001	0.028	0.003	0.048	0.002	452.222	<0.001**
6 mm	0.227	0.003	0.062	0.006	0.165	0.004	2023.406	<0.001**
8 mm	0.364	0.012	0.073	0.005	0.292	0.009	341.078	<0.001**
10 mm	0.405	0.016	0.131	0.024	0.274	0.020	73.232	0.003**
12 mm	0.468	0.026	0.234	0.024	0.234	0.025	31.766	0.011*
F	181.712		55.829					
p	<0.001**		0.005**					
4 vs 6	<0.001**		0.022*					
6 vs 8	0.019*		0.007**					
8 vs 10	0.219		0.506					
10 vs 12	0.081		<0.001**					

EMM: Estimated Marginal Mean; SE: Standard Error. Significant at *0.05 and **0.01

In the setback group, stress levels also increased significantly on the operated and non-operated sides with the incremental changes. The increase was higher on the operated side between 4 and 6 mm ($p = 0.001$) and 6 and 8 mm ($p=0.006$) setbacks, whereas significance was recorded on the non-operated side between all sets of increments except for 8 vs 10 mm. Significantly greater stress levels were observed on the operated side compared to the non-operated side (Table 4.8).

Table 4.8. Stress at the lateral surface of the menisci in the setback group (n=4)

	Operated		Non-operated		Difference		3-way mixed ANOVA	
	EMM	SE	EMM	SE	EMM	SE	F	P
4 mm	0.075	0.002	0.027	0.002	0.048	0.002	225.609	0.001**
6 mm	0.213	0.006	0.062	0.004	0.151	0.005	320.306	<0.001**
8 mm	0.329	0.014	0.073	0.004	0.257	0.009	294.233	<0.001**
10 mm	0.446	0.033	0.133	0.021	0.313	0.027	64.161	0.004**
12 mm	0.501	0.046	0.236	0.020	0.265	0.033	24.323	0.016*
F	83.981		73.862					
p	0.002**		0.003**					
4 vs 6	0.001**		0.004**					
6 vs 8	0.006**		<0.001**					
8 vs 10	0.089		0.400					
10 vs 12	0.426		<0.001**					

EMM: Estimated Marginal Mean; SE: Standard Error. Significant at *0.05 and **0.01

The association between the stress at the lateral surface of the menisci and the amount of surgical advancements and setbacks is shown in Fig. 4.13.

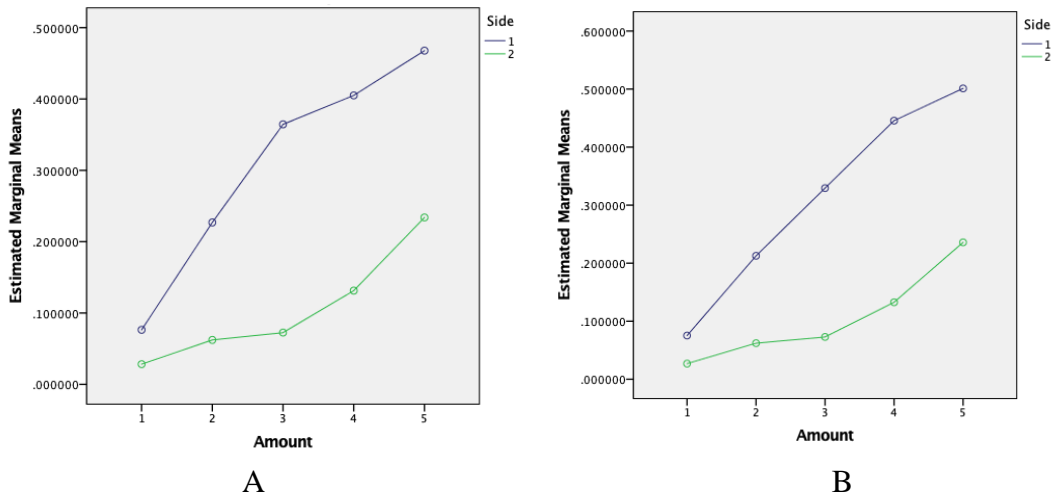


Figure 4.13. Von mises stresses (y axis) at the lateral surface of the meniscus in the advancement (A) and setback (B) groups.

Amounts of movements (x axis): 1 = 4mm; 2= 6mm; 3= 8mm; 4= 10mm; 5= 12mm.

Condylar sides: 1- operated, 2- non-operated.

d. Stress at the anterior surface of the menisci

In the advancement group, statistically significant increase of stress with the incremental movements was recorded on the operated and non-operated sides ($p < 0.001$). The difference in stress increase on the operated side was significant between 6 and 8 mm ($p = 0.033$), while between all incremental pairs on the non-operated side (Table 4.9).

Table 4.9. Stress at the anterior surface of the menisci in the advancement group (n=4)

	Operated		Non-operated		Difference		3-way mixed ANOVA	
	EMM	SE	EMM	SE	EMM	SE	F	P
4 mm	0.233	0.031	3.764	0.141	-3.531*	0.160	488.040	<0.001**
6 mm	0.258	0.030	5.080	0.151	-4.821*	0.170	799.933	<0.001**
8 mm	0.370	0.017	6.580	0.150	-6.211*	0.160	1508.698	<0.001**
10 mm	0.384	0.019	7.294	0.141	-6.910*	0.151	2105.669	<0.001**
12 mm	0.489	0.042	10.406	0.163	-9.917*	0.201	2435.027	<0.001**
F	67.106		11764.209					
p	0.001**		<0.001**					
4 vs 6	0.265		0.001**					
6 vs 8	0.033*		<0.001**					
8 vs 10	0.090		<0.001**					
10 vs 12	0.343		<0.001**					

EMM: Estimated Marginal Mean; SE: Standard Error. Significant at *0.05 and **0.01

Higher stresses were detected on the non-operated side for each incremental advancement compared to the operated side ($p < 0.001$).

During setback, stress increased significantly at all increments on the operated ($p = 0.007$) and non-operated ($p < 0.001$) sides, specifically between 10 and 12 mm on the operated side ($p = 0.003$), and between all pairs of increments on the non-operated side (Table 4.10). Stresses were higher on the non-operated side ($p < 0.001$).

Graphical representations of the findings are shown in Figure 4.14.

Table 4.10. Stress at the anterior surface of the menisci in the setback group (n=4)

	Operated		Non-operated		Difference		3-way mixed ANOVA	
	EMM	SE	EMM	SE	EMM	SE	F	P
4 mm	0.224	0.011	3.321	0.196	-3.098*	0.194	255.629	0.001**
6 mm	0.261	0.020	4.509	0.241	-4.248*	0.238	318.963	<0.001**
8 mm	0.356	0.028	6.040	0.239	-5.685*	0.260	478.396	<0.001**
10 mm	0.390	0.041	6.725	0.248	-6.335*	0.279	513.931	<0.001**
12 mm	0.489	0.045	9.871	0.246	-9.382*	0.279	1131.813	<0.001**
F	31.248		6079.318					
p	0.007**		<0.001**					
4 vs 6	0.290		0.002**					
6 vs 8	0.382		<0.001**					
8 vs 10	0.813		0.002**					
10 vs 12	0.003**		<0.001**					

EMM: Estimated Marginal Mean; SE: Standard Error. Significant at *0.05 and **0.01

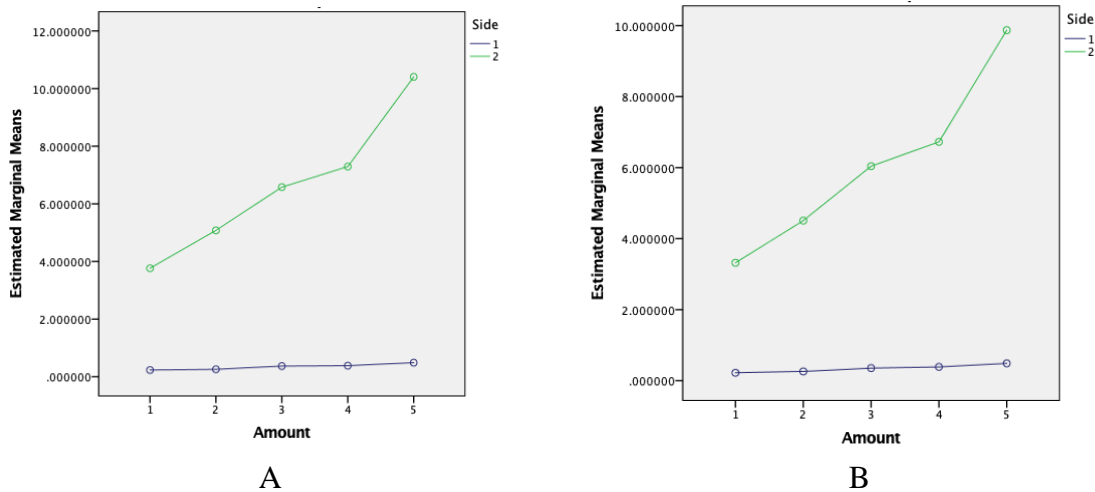


Figure 4.14. Von mises stresses (y axis) at the anterior surface of the menisci in the advancement (A) and setback (B) groups.

Amounts of movements (x axis): 1 = 4mm; 2= 6mm; 3= 8mm; 4= 10mm; 5= 12mm.

Condylar sides: 1- operated, 2- non-operated.

e. Stress at the posterior surface of the menisci

In the advancement group, a statistically significant increase in stress among incremental changes (4,6,8,10 and 12 mm) was recorded ($0.001 < p < 0.003$) (Table 4.11).

Stress increase at the operated side was statistically significant from 4 to 6mm ($p < 0.001$),

6 to 8mm ($p = 0.003$), 8 to 10mm ($p = 0.004$), and 10 to 12 mm ($p = 0.004$). The stress increase on the non-operated side was statistically significant between the increment increases 6 and 8mm ($p < 0.001$) and 8 to 10mm ($p = 0.001$). Stress was significantly higher in each amount of surgical advancement on the non-operated side (Table 4.11).

Higher Von Mises stresses were recorded on the contralateral side (range: 0.284 to 0.697) than on the operated side (range: 0.024 to 0.310). Stresses on both sides increased as the surgical advancement increased.

Table 4.11. Stress at the posterior surface of the menisci in the advancement group (n=4)

	Operated		Non-operated		Difference		3-way mixed ANOVA	
	EMM	SE	EMM	SE	EMM	SE	F	P
4 mm	0.024	0.001	0.284	0.014	-.261*	0.014	355.562	<0.001**
6 mm	0.032	0.001	0.374	0.046	-.343*	0.046	55.883	0.005**
8 mm	0.066	0.003	0.444	0.045	-.378*	0.045	71.078	0.004**
10 mm	0.295	0.015	0.588	0.049	-.293*	0.052	31.161	0.011*
12 mm	0.310	0.017	0.697	0.068	-.387*	0.067	32.933	0.011*
F	323.965		63.137					
p	<0.001**		0.003**					
4 vs 6	<0.001**		0.733					
6 vs 8	0.002**		<0.001**					
8 vs 10	0.004**		0.001**					
10 vs 12	0.004**		0.173					

EMM: Estimated Marginal Mean; SE: Standard Error. Significant at *0.05 and **0.01

In the setback group, a statistically significant increase ($p < 0.001$) in stress among the graded setbacks was registered on both operated and non-operated sides (Table 4.12). With incremental displacements, the increase in stress was statistically significant between the different incremental changes on the operated side ($0.021 < p < 0.002$). The stress increase on the non-operated side was statistically significant in each increment of 6 to 8 ($p < 0.001$), 8 vs 10 ($p < 0.001$) and 10 vs 12 ($p = 0.01$). Statistically significantly greater stress on the

non-operated side (range: 0.283 to 0.964) with each amount of movement (4,6,8,10,12) (p = 0.001) was recorded.

Table 4.12. Stress at the posterior surface of the menisci in the setback group (n=4)

	Operated		Non-operated		Difference		3-way mixed ANOVA	
	EMM	SE	EMM	SE	EMM	SE	F	P
4 mm	0.025	0.002	0.283	0.017	-.257*	0.017	222.356	0.001**
6 mm	0.032	0.002	0.435	0.037	-.402*	0.036	127.498	0.001**
8 mm	0.065	0.004	0.655	0.034	-.589*	0.032	336.662	<0.001**
10 mm	0.286	0.014	0.800	0.032	-.514*	0.027	374.723	<0.001**
12 mm	0.309	0.012	0.964	0.022	-.656*	0.020	1091.133	<0.001**
F	622.777		652.238					
p	<0.001**		<0.001**					
4 vs 6	0.012*		0.086					
6 vs 8	0.005**		<0.001**					
8 vs 10	0.002**		<0.001**					
10 vs 12	0.021*		0.010*					

EMM: Estimated Marginal Mean; SE: Standard Error. Significant at *0.05 and **0.01

The association between surgical movements and stress are illustrated graphically in

Fig. 4.15 (A).

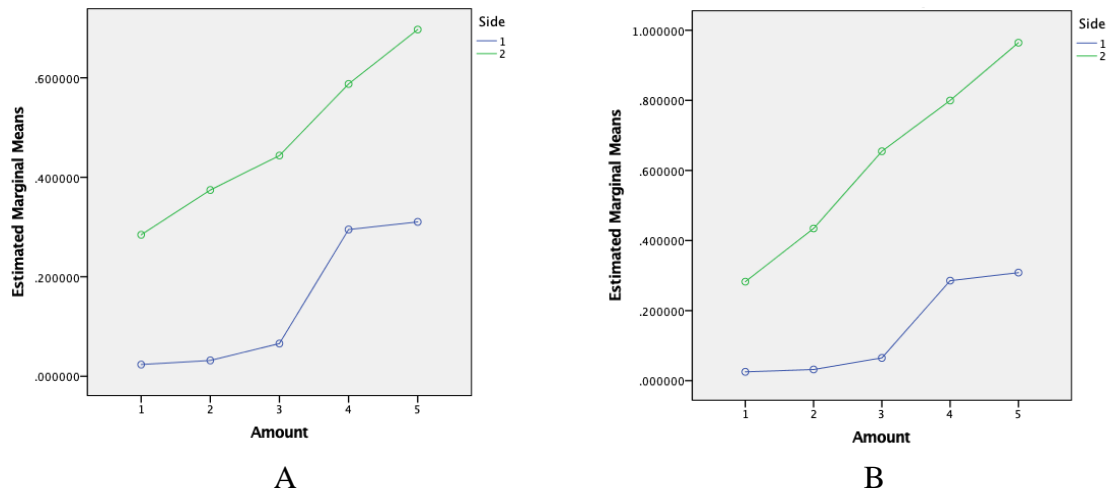


Figure 4.15. Von mises stresses (y axis) at the level of the posterior surface of the menisci in the advancement (A) and setback (B) groups.

Amounts of movements (x axis): 1 = 4mm; 2= 6mm; 3= 8mm; 4= 10mm; 5= 12mm.

Condylar sides: 1- operated, 2- non-operated.

f. Displacement of the condyles

In the USSO advancement group, the increase in displacement was statistically significantly different between the incremental surgery (p values < 0.001; Table 4.13). On the operated side, the increase in displacement was statistically significant between 8 and 10mm (p= 0.014) and 10 and 12 mm (p=0.004). The displacement increase was statistically significant between each pair of surgical increment on the non-operated side (0.033<p<0.001) except between 8 and 10mm. A statistically significant greater displacement was observed on the non-operated side for each incremental advancement (Table 4.13, Fig. 4.16).

Table 4.13. Displacement of the condyle in the advancement group (n=4)

	Operated		Non-operated		Difference		3-way mixed ANOVA	
	EMM	SE	EMM	SE	EMM	SE	F	P
4 mm	0.553	0.012	0.613	0.008	-0.06	0.018	11.231	0.044*
6 mm	0.614	0.014	0.857	0.009	-.243*	0.018	188.01	0.001**
8 mm	0.772	0.013	0.983	0.018	-.211*	0.024	78.808	0.003**
10 mm	0.800	0.013	1.028	0.011	-.228*	0.021	122.74	0.002**
12 mm	0.843	0.011	1.076	0.007	-.233*	0.015	227.65	0.001**
F	146142.7		1382.072					
p	<0.001**		<0.001**					
4 vs 6	0.001**		<0.001**					
6 vs 8	<0.001**		0.008**					
8 vs 10	0.014*		0.091					
10 vs 12	0.004**		0.033*					

EMM: Estimated Marginal Mean; SE: Standard Error. Significant at *0.05 and **0.01

In the setback group, a significant increase in displacement among incremental surgical movements was observed on the operated and non-operated sides (p < 0.001; Table 4.14). The increase was statistically significant between all pairs of increments (0.014< p<

0.000) on the operated and non-operated sides. Greater displacement was recorded on the non-operated side at each incremental surgical movement (Table 4.14, Fig. 4.16).

Table 4.14. Displacement of the condyle in the setback group (n=4)

	Operated		Non-operated		Difference		3-way mixed ANOVA	
	Mean	SD	Mean	SD	EMM	SE	F	P
4 mm	0.566	0.015	0.638	0.008	-0.072	0.012	38.585	0.008**
6 mm	0.631	0.016	0.884	0.011	-.253*	0.015	291.323	<0.001**
8 mm	0.789	0.015	1.015	0.013	-.226*	0.010	534.781	<0.001**
10 mm	0.815	0.014	1.061	0.009	-.246*	0.013	369.894	<0.001**
12 mm	0.859	0.015	1.112	0.014	-.253*	0.012	471.348	<0.001**
F	53017.861		3821.278					
p	<0.001**		<0.001**					
4 vs 6	0.001**		<0.001**					
6 vs 8	<0.001**		0.002**					
8 vs 10	0.014*		0.020*					
10 vs 12	0.004**		0.024*					

EMM: Estimated Marginal Mean; SE: Standard Error. Significant at *0.05 and **0.01

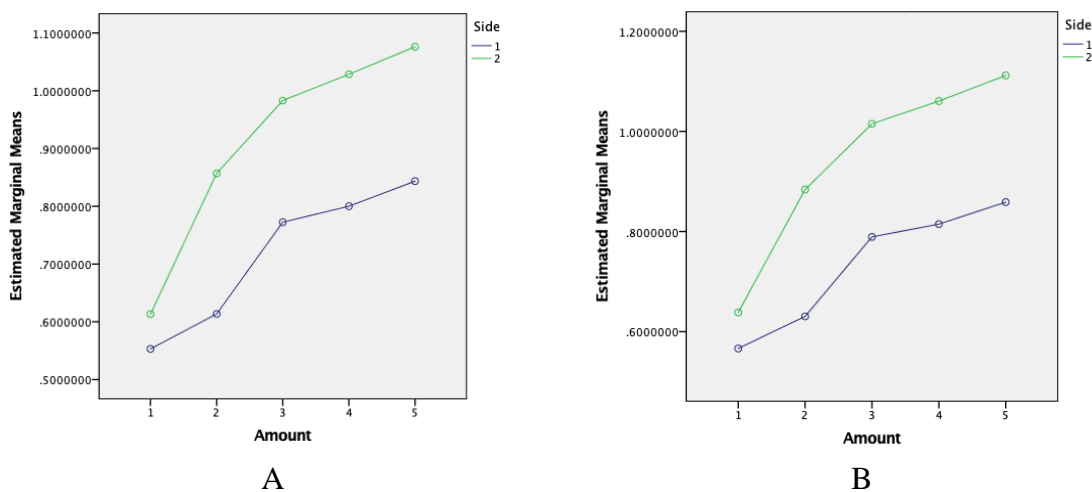


Figure 4.16. Displacement at the level of the condyles in the advancement (A) and setback (B) groups.

Amounts of movements (x axis): 1 = 4mm; 2= 6mm; 3= 8mm; 4= 10mm; 5= 12mm.
 Condylar sides: 1- operated, 2- non-operated.

g. Displacement of the neck of the condyles

Displacement at the neck of the condyles increased significantly in the advancement group among the incremental changes on both the operated and non-operated sides ($p < 0.001$) (Table 4.15). The increase was statistically significant on the non-operated side between 4 and 12 mm ($p < 0.001$), and on the operated side 4 vs 6mm, 6 vs 8mm and 10 vs 12 mm ($p < 0.001$). Moreover, the increase was seen on the operated and non-operated sides and statistically significant between all pairs of incremental surgeries on the operated side, also similarly on the non-operated side except between 8 and 10mm ($p < 0.001$). The displacement was statistically greater on the non-operated side across the incremental surgeries except between 8 and 10 mm.

Table 4.15. Displacement of the neck of the condyle in the advancement group (n=4)

	Operated		Non-operated		Difference		3-way mixed ANOVA	
	EMM	SE	EMM	SE	EMM	SE	F	P
4 mm	0.545	0.009	0.693	0.012	-.148 [*]	0.019	61.061	0.004 ^{**}
6 mm	0.693	0.008	0.960	0.013	-.267 [*]	0.020	182.824	0.001 ^{**}
8 mm	0.891	0.008	1.013	0.013	-.123 [*]	0.020	36.503	0.009 ^{**}
10 mm	1.021	0.010	1.022	0.012	-0.001	0.020	0.002	0.966
12 mm	1.163	0.007	1.262	0.011	-.099 [*]	0.017	35.373	0.010 ^{**}
F	20260.866		23089.668					
p	<0.001 ^{**}		<0.001 ^{**}					
4 vs 6	<0.001 ^{**}		<0.001 ^{**}					
6 vs 8	<0.001 ^{**}		<0.001 ^{**}					
8 vs 10	<0.001 ^{**}		0.168					
10 vs 12	<0.001 ^{**}		<0.001 ^{**}					

EMM: Estimated Marginal Mean; SE: Standard Error. Significant at *0.05 and **0.01

The same pattern was seen in the setback group, with a statistically significant increase in displacement on the operated and non-operated sides ($p < 0.001$, $p = 0.006$) (Table 4.16). For the different setback increments, displacement increased significantly on

the operated side for all increments ($0.009 < p < 0.000$), but only between 4 and 6mm and between 6 and 8mm on non-operated side ($p < 0.001$).

Table 4.16. Displacement of the neck of the condyle in the setback group (n=4)

	Operated		Non-operated		Difference		3-way mixed ANOVA	
	Mean	SE	Mean	SD	EMM	EMM	F	P
4 mm	0.557	0.011	0.726	0.010	-.169*	0.008	426.481	<0.001**
6 mm	0.705	0.010	0.998	0.009	-.293*	0.008	1514.92	<0.001**
8 mm	0.909	0.012	1.044	0.008	-.135*	0.009	214.210	0.001**
10 mm	1.039	0.012	1.124	0.075	-0.085	0.075	1.284	0.340
12 mm	1.187	0.021	1.295	0.008	-.109*	0.018	34.653	0.010**
F	2168.534		46.415					
p	<0.001**		0.006**					
4 vs 6	<0.001**		<0.001**					
6 vs 8	<0.001**		<0.001**					
8 vs 10	<0.001**		1					
10 vs 12	0.009**		0.893					

EMM: Estimated Marginal Mean; SE: Standard Error. Significant at *0.05 and **0.01

The relationship between the incremental surgical movements and the displacement at the neck of the condyles is shown in Fig. 4.17 (A).

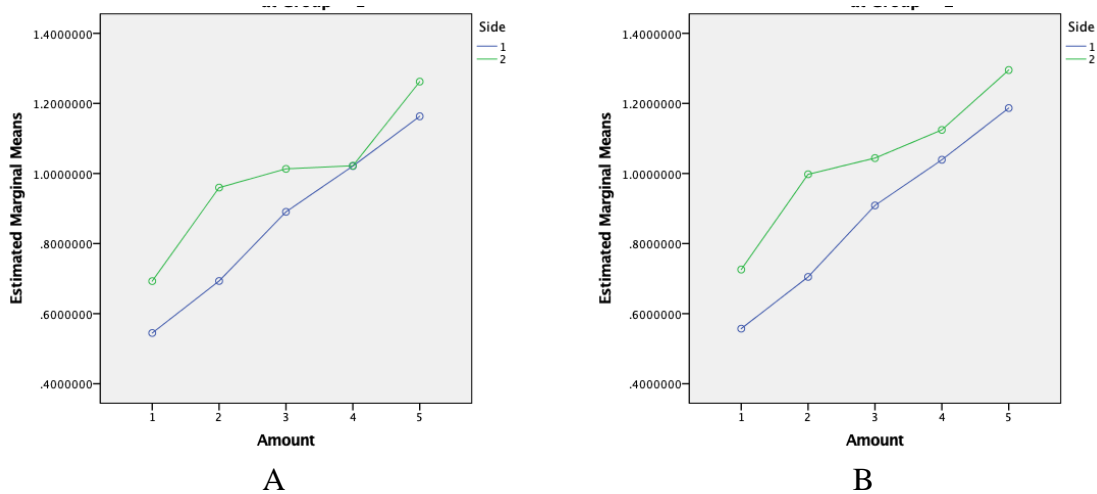


Figure 4.17. Displacement at the level of the neck of the condyles in the advancement (A) and setback (B) groups.

Amounts of movements (x axis): 1 = 4mm; 2= 6mm; 3= 8mm; 4= 10mm; 5= 12mm.

Condylar sides: 1- operated, 2- non-operated.

C. Correlations

1. Correlations between displacement and stress with the incremental surgical movements (4, 6, 8, 10, 12 mm) at the neck of the condyle

Statistically significant ($p < 0.01$) correlations between displacement and stress at the different incremental surgical movements ranged from 0.820 to 0.971 on the operated side, and from 0.916 to 0.984 on the non-operated side (Table 4.18).

Table 4.17. Pearson's correlation coefficients between displacement and stress at the neck of the condyles in the operated and non-operated sides.

	Operated	Non-Operated
4 mm	0.971**	0.974**
6 mm	0.945**	0.970**
8 mm	0.956**	0.984**
10 mm	0.956**	0.965**
12 mm	0.820*	0.916**

* Significant at the 0.05 level, **Significant at the 0.01 level

The correlation coefficients for the non-operated side were typically greater than on the operated side. The statistical significance of the correlation coefficients indicated that the association between displacement and stress was not random.

2. Correlations between displacement and condylar volume with the incremental surgical movements (4, 6, 8, 10, 12 mm)

Theses correlations were negative and higher on the operated side ($-0.992 < r < -0.979$) than the non-operated side ($-0.518 < r < -0.626$) (Table 4.19), indicating that the displacement decreased as the condylar volume increased, and that this association was stronger in the operated group.

Table 4.18. Pearson's correlation coefficients between displacement and condylar volume in operated and non-operated sides.

	Operated	Non-Operated
4 mm	-0.979**	-0.623
6 mm	-0.992**	-0.518
8 mm	-0.986**	-0.626
10 mm	-0.981**	-0.598
12 mm	-0.990**	-0.615

* Significant at the 0.05 level, **Significant at the 0.01 level

CHAPTER V

DISCUSSION

In this research, we have introduced finite element modeling of the unilateral sagittal split osteotomy, which was previously a rarely used or unrecorded surgery. Important information on the effect of this osteotomy on the operated and non-operated condyles emerged, two of which most significant:

1. Stress on the operated side was nearly negligible relative to the non-operated side at various increments of mandibular unilateral advancement or setback.
2. A threshold of advancement or setback at about 6mm or less associated with the present real surgical setups might represent a guideline to be further tested.
3. At a methodological level, actual treatment records of patients undergoing the USSO were used to determine the generated stresses and displacement under the FE modeling tests. Accordingly, the results reflect realistic assessments of the surgical impact.

More characteristic outcomes are explored in this discussion, including strengths and limitations of the research.

A. Strengths

1. Individual variation

Most FEA studies used in orthodontics formulated conclusions based on a single mathematical solution, which was equivalent to a single setup or a fractionalized, simplified clinical setup. However, researchers from our institution introduced a novel approach to account for individual variation in FE analysis of tooth movement (Ammoury et al, 2019) that could have direct clinical application (Ghafari and Ammoury, 2020). These studies indicated that individual variances in the medical and dental fields provide varied outcomes for the same clinical condition, necessitating the analysis of larger samples to identify both central tendencies and probable outliers.(Ammoury et al., 2019).

We included 8 different mandibles from patients who underwent the unilateral osteotomy. Thus, we accounted for the various individual anatomical traits, such as condylar size and shape, then subjecting them to FE analysis that cannot be performed on live tissue. This strategy, rarely applied to date, brings the engineering generated outcomes closer to actual clinical conditions. In addition, this exercise in time consuming build-up of 8 models, essentially reflecting 8 case reports, revealed consistent outcomes that allowed statistical computations of variances and identification of trends that could be further tested on larger samples, and allowing the formulation of novel hypotheses for further testing to reach more conclusive evidence.

2. Complete 3D model

Building a complete and accurate FE model requires significant effort and time.

Modelling of the investigated structures may then be compromised. In some studies, incomplete models were used containing a segment of the mandible or hemimandible assuming fixed boundary conditions all around (Hassan, 2018).

Some authors have constructed complete FE models based on a dry skull rather than radiographic three-dimensional images, therefore harboring anatomical flaws. Dry skulls might have different physical characteristics resulting from post-mortem modifications such as dehydration and changes to the collagen matrix. Such modifications may impact the skull's mechanical characteristics, compromising its similarity to the skull of a living person. Also, dry skulls could have structural flaws like cracks or fractures that would alter their mechanical behavior and make them unsuitable for FEA (Rodrigo D, 2000). In comparison, our model was more complete, constructed from CT scans of 8 patients and containing all structures, but excluding the trabecular bone for simplification purposes.

B. FEA Studies

Finite element analysis was most frequently used in studying bilateral sagittal split osteotomy and rigid fixations. The main reasons were:

1. Optimization of surgical planning with FEA to generate information about the mandible's biomechanical response to BSSO and rigid fixation, which can be used to streamline surgical planning and reduce problems. In this perspective, the size and placement of the fixation plates and screws, as well as the ideal location and angle of the osteotomy cuts could be developed through FEA. Accordingly, the chance of postoperative problems such as malocclusion, nerve damage, and implant failure can be decreased (Choi Jong-Woo & Lee Jang Yeol, 2021).

2. Stability assessment under different stress circumstances. FEA can help evaluate the mandibular stability after BSSO and rigid fixation, revealing information on the displacement and distortion of the bone and implants, and the distribution of stresses and strains within the mandible. Accordingly, the best fixing procedure could be selected and the possibility of postoperative instability or displacement assessed (Ming-Yih et al., 2010).
3. Comparison of various fixation method. FEA facilitates testing the biomechanical behavior of various BSSO fixation methods, such as conventional versus bioresorbable plates or bicortical versus monocortical screws. By determining the respective benefits and drawbacks, FEA becomes a clinical decision-making tool (M. Y. C. Chen et al., 2020).

Few studies addressed the indications, geometry (Beukes et al., 2016) and stability of USSO and its effect on the TMJ (S.-G. Lee et al., 2015a), and others focused on the methods rotational effect on the condyles (Kim et al., 2015; Ryu et al., 2015; Wohlwender et al., 2011). However, the study through FEA of the forces, stresses and displacements on the TMJ and surrounding tissues, and the incorporation of patients with different condylar anatomies was needed. Our study addressed these lacunae on the less used USSO, further contributing to the integration of this less morbid technique in the treatment of mandibular asymmetry.

The methodological differences and similarities with other studies are outlined below.

C. Assessment of the methods

The surgical cut or the fracture was performed with medial bone cut extending towards the posterior border of the ramus as originally described as Obwegeser/Dal Pont modification, which proved to be more resilient clinically. Other authors described the same procedure with variations in the extension of the lingual split (Hyu et al., 2020). Ours corresponded to their type III lingual split pattern.

Our 3D model was similar to that created by Luo et al. (2023) who used an image processing and digital reconstruction software (MIMICS; Materialise, Leuven, Belgium) to extract a 3D model from computed tomography (CT) images of patients. They modeled not only the mandible but also the maxillary complex with the different bones. We modeled the temporal bone for simplification. In an approach similar to Takahashi et al.'s (2009), the mandibular bone was considered as cortical bone with single homogenous phase with 13.7 GPa and Poisson's ratio of 0.3 for further model simplification.

The anatomical features and the design of the articular surfaces used to establish the articular discs were similar to Shu et al.'s description (2018). Luo et al (2023) also followed the same scheme. The findings demonstrated that the model was close to the clinical setup, allowing the assessment of stresses at all surfaces, and associated conclusions. Moreover, the reconstruction of the disk within the TMJ area with five contact candidate surfaces that were needed to define their interaction, closely simulated the anatomical structures. The superior and inferior surfaces of the disk were constructed to touch the corresponding surfaces of the temporal bone and condyle. Pérez Del Palomar & Doblaré (2006) described a similar setup. While the interaction setting at the level of the surgical cut was not

described in FEA studies of BSSO, we set it between the mandibular body and the operated ramus.

D. Assessment of the findings

Considering that this is the first FEA study investigating the USSO, all findings are practically novel. We focus on selected results in this context, including comparison with pertinent outcomes of other studies, particularly BSSO investigations.

Higher stress was present on the non-operated condyle than the operated side for all increments of advancement and setback, a finding in contrast to previous clinical studies in which USSO with mandibular advancement was reported to result in increased stress on the non-operated side because of the rotation of the mandibular condyle within 3 to 4 degrees when the mandible was setback 7 mm (S.G. Lee et al., 2015).

Although it would be expected for stresses and displacements to increase when the surgical advancement or setback rises from 4 to 12mm, this association is first documented in this research at the level of the neck of the condyles and condyles. Only stresses were documented at the menisci.

Higher amounts of stress and displacement were evident at the level of the neck of the condyle. The reason for this finding is probably because this region was identified as the weakest region in the mandible that endures high fracture rates (Halazonetis, 1968). Additionally, the association between stress and displacement at the level of the condyles and neck of the condyles, suggests that when the condyle rotates in response to mandibular advancement or setback, the displacement increases the stress distribution in this area.

The relationship between displacement and stress in bone is described by Hooke's law, which stipulates that stress is proportional to strain. Strain would be proportional to the displacement of the bone under a given load. The relationship between displacement and stress in bone using FEA has been addressed in numerous studies, such as stress distribution in the proximal femur during simulated fall loading (Kaku et al., 2023). The authors found that stress increased with displacement in the femoral neck, indicating that the femoral neck is a critical region for fracture during a fall, a setup that may be parallel to the condyle and condylar neck in the mandible.

We found that the larger the condyles, the less the displacement. Volume changes after orthognathic surgery have not been assessed in the literature. This high correlation on the operated side may explain the lower stress registered at the level of the meniscus and the condyle. With more leeway of movement for the condyle, the ligaments that connect to the meniscal disk might stretch less, thus less stress.

The stress at the level of the posterior section of the menisci was statistically significant. This finding intersects with the report by Luo et al., 2023 that the average peak principal stress following BSSO surgery was located at the posterior surface of the articular cartilage. However, in our study, the main stress was on the anterior surface of the menisci, possibly because of a difference between the unilateral and bilateral osteotomies. However, more focused research is needed to sort out the different variables in these surgeries.

An important aspect of assessing our results relates to condylar rotation, which is a salient point in BSSO as well. Our findings that stress on the non-operated condyles was mainly identified on the posterior, anterior, and lateral sides, but minimal on the medial side, indicate an outward condylar rotation. More clinical studies are available on BSSO

than the USSO (a more recent method to gain acceptance). We include a summary from a publication by Pachnicz & Ramos (2021) that includes information on condylar behavior in studies on BSSO (Table 5.1).

Table 5.1. Summary of aims and conclusions from articles on post BSSO condylar changes (Reproduced from Pachnicz & Ramos, 2021)

Author	Study purpose	Outcome and conclusions
He <i>et al.</i> (37)	Characterization of the condylar displacement and surface remodeling after bimaxillary orthognathic surgery in adult patients with skeletal Class III malocclusion treated by the surgery-first or the orthodontic-first approach	Condyle translated in inferolateral direction, inward and anterior rotation was observed. After surgery condyle tends to return to original position. Displacements were within the patient's adaptation range. SFA and OFA results with similar condyle displacement and remodeling
Park <i>et al.</i> (38)	Evaluation of movement of the posteriorly displaced proximal segment after Intraoral Vertical Ramus Osteotomy IVRO	Proximal segment returns from posteriorly displaced position to its original position during healing. Posterior displacement of proximal segment results with favorable bone union
Wan <i>et al.</i> (39)	Assessment of the virtual surgery planning effect on the condylar seating during BSSO comparison of results between actual and virtual planned surgery	The outcomes resulting from the virtual and conventional planned surgeries are significantly different. Virtual planning in majority of cases seems not to be helpful in predicting surgery outcomes, assisting with condylar seating and might be beneficial only for novice clinicians
Xue <i>et al.</i> (40)	Evaluation of the clinical use of a surgical guide and CAD/CAM prebent titanium plate	The measured deviation of position and condyle orientation were lower than 1 mm and 1°, that is clinically significant. The occlusion was stable after 3 months and one year after surgery. In any patient pain or sound was found postoperatively. The guide is found to be useful tool for improve treatment with orthognathic surgery
Zupnik <i>et al.</i> (41)	Quantification of the condylar displacement in three planes of space after correction of open bite in II and III class malocclusion	After mandibular advancement condyles tend to displace: laterally, posteriorly and superiorly, rotated medially both for yaw and roll, clockwise pitch. Mandibular setback in majority of cases results with medial, posterior and superior translations and medial yaw, medial roll and counterclockwise rotational pattern
Rokutanda <i>et al.</i> (42)	Evaluation of the effects of changes in the condylar long axis and position on temporomandibular symptoms with respect proximal segment position after IVRO	Lateral opening of the condylar long axis and the anteroinferior movement may be beneficial for TMJ condition
Ma <i>et al.</i> (43)	The aim was to establish the method for quantitative evaluation of condyle positional changes and assessment of the usefulness of 3D images for this purpose	3D images can be used in condyle positional changes evaluation. Most of the condyles did not return to their preoperative position during 1-year follow-up. Condyles rotated posteriorly, cranially, and laterally

E. Clinical implications

Several inferences may be made from this research that relate to clinical applications, although needing complementary investigation.

1. Plotting velocity curves allowed a better visualization of the changes in stress and displacement over the increase in surgical movement. In this process, a hypothesis emerged stipulating that a threshold of 6mm might be a limit for balanced homeostasis whereby the stress at the non-operated side nearly equals that on the operated side. The biological underpinning of this hypothesis needs investigation, along with computation of clinical treatments to determine the range of movements in serial USSO operations and the significance of a threshold when the unilateral surgery is indicated.
2. This finding and its clinical corollary is agreeable with the report by Beukes et al., (2016) that USSO should be considered in patients with moderate mandibular asymmetry and a dental midline disparity of less than 5 mm. Abou Chebel et al. (2020) and Ammourey et al. (2022) published findings and treatment reports with surgical movements within the 5 to 6 mm limits.
3. Although available evidence does not include reports of advancement or setback with USSO beyond this amount, two points must be considered:
 - a. The nature of the asymmetry may not be of greater severity
 - b. Greater amounts of movement may be stable.Thus, judicious research is required to sort out these issues.
4. The fact that the highest stresses were observed in the 12mm advancement (23.8 MPa) and setback (22.7 MPa) setups, would indicate avoiding such major movements. In the

conditions of the material available in this study (no surgery beyond 6mm), the amount of 12mm may not be in the realm of regular USSO operations.

5. An important question relates to the health of the TMJ and whether post-surgical symptoms might develop from the unilateral surgery. Abou Chebel et al (2020) investigated TM dysfunction and found it in only 1 patient out of 30 that resolved 2 years post-surgically.
6. The high negative correlations between condylar volume and displacement indicates that the wider or larger the condyle the less the displacement is occurring thus lesser stress on the larger condyle. This finding would suggest that larger condyles would tolerate more displacement, thus greater surgical movement. This premise should be tested clinically through 3D imaging before and after unilateral osteotomy.

F. Limitations and research considerations

As in most dental FEA studies, we used an isotropic and homogeneous material property for the bone, which might produce simplified results. Also, FEA studies mostly represent a snapshot of a beginning condition (such as stresses and displacement), excluding modifications that develop over time such as bone remodeling, healing, and friction. These initial results represent the initial displacement of the condyles in the glenoid fossa and stress on the different structures under study.

The conclusions relate only to the analysis of the data, but verification would require additional research. When all factors have been investigated, including the definition of cortical bone thickness, stiffness, ligaments and muscular activity, the conditions should ideally be included in treatment planning. Subsequent clinical results

may not be like the initial ones. To reach the stage when FEA is a crucial component of surgical treatment planning, extensive research should be invested in time-dependent (continuous/dynamic) finite element models that would duplicate the clinical settings. Although this model has been around since 1996 (Middleton et al., 1996), FEA has not yet been able to accurately simulate the biological process of the bony reactions (resorption and apposition) over time. This important area of research should receive significant support.

CHAPTER VI

CONCLUSION

1. This study was the first to contribute FE modeling and findings based on the individual variations among 8 human subjects who underwent USSO surgery. Because of similar trends, central tendencies of the stress values and displacements could be formulated that should be validated with larger samples.
2. The non-operated side disclosed most differences with incremental surgical movements.
3. Individual velocity changes suggested a balance of stress between operated and non-operated sides between 4 and 6 mm of mandibular advancement or setback, which corresponded to the actual amount of surgical movement in the 8 patients under study.
4. Comparisons of advancement and setback outcomes, including stress and displacement at the level of the condyles and neck of the condyles revealed statistically significant differences between operated and non-operated sides.
5. With increased surgical movements, statistically significant increase in stress was observed at the level of the condyles, condylar necks, and menisci (especially the anterior surface).
6. The highest amount of stress was observed at the posterior surface of the non-operated condyle in the advancement surgery and on the anterior surface of the non-operated condyle in the setback osteotomy.

7. Stress at the level of the meniscus was statistically significantly greater on the non-operated side in both advancement and setback modalities, with greater stress observed in the setback group. The highest stress was recorded on the anterior surface of the meniscus.
8. Increase in displacement was associated with increase in stress. More displacement (up to 1.3mm) occurred at the non-operated than operated condyle. When condylar volume increased the displacement decreased.
9. This research yielded clinically testable hypothesis that should be explored in future FE models and direct clinical investigations.

APPENDIX

Figure 4.2

Advancement	Operated	Non-operated	Setback	Operated	Non-operated
0-4	5.454	26.437	0-4	5.601	27.42
4 to 6	0.091	4.024	4 to 6	0.115	3.957
6 to 8	2.697	12.513	6 to 8	2.679	12.591
8 to 10	0.167	12.435	8 to 10	0.176	13.086
10 to 12	0.923	7.192	10 to 12	0.913	6.165

Figure 4.4

Advancement	Operated	Non-operated	Setback	Operated	Non-operated
0-4	0.03406225	0.65002	0-4	0.0443005	0.6699725
4 to 6	0.02102425	1.6405825	4 to 6	0.01077325	1.7825275
6 to 8	0.084999	0.217813	6 to 8	0.07166875	0.34017925
8 to 10	0.0252715	0.902403	8 to 10	0.01948675	0.884123
10 to 12	0.07178925	0.99323	10 to 12	0.152902	1.020955

Figure 4.5

Setback	Operated	Non-operated	Setback	Operated	Non-operated
0-4	0.03408246	0.65078	0-4	0.0443121	0.6699887
4 to 6	0.02103128	1.6406028	4 to 6	0.01077429	1.7825309
6 to 8	0.0850034	0.217906	6 to 8	0.07167087	0.34018021
8 to 10	0.0252916	0.902632	8 to 10	0.01949804	0.884314
10 to 12	0.0718037	0.99415	10 to 12	0.152988	1.021038

Figure 4.8

	anterior		posterior	
adv	op	non-op	op	non-op
0-4	1.40195	2.04394	0.835766	3.73314
4 to 6	0.49834	4.55231	0.492984	4.70392
6 to 8	0.3878	5.30515	0.54713	5.40324
8 to 10	0.41311	3.5493	0.41435	4.9742
10 to 12	0.42244	4.8901	0.403784	4.9576
	posterior		lateral	
adv	op	non-op	op	non-op
0-4	0.835766	3.73314	1.03643	1.80301
4 to 6	0.492984	4.70392	0.60318	2.36476
6 to 8	0.54713	5.40324	0.31833	3.20909
8 to 10	0.41435	4.9742	0.50677	2.87584
10 to 12	0.403784	4.9576	0.43526	3.5719

Figure 4.9

Advancement	Operated	Non-operated	Setback	Operated	Non-operated
0-4	0.553	0.613	0-4	0.566	0.638
4 to 6	0.061	0.244	4 to 6	0.065	0.246
6 to 8	0.158	0.126	6 to 8	0.158	0.131
8 to 10	0.028	0.045	8 to 10	0.026	0.046
10 to 12	0.043	0.048	10 to 12	0.044	0.051

Figure 4.10

Advancement	Operated	Non-operated	Setback	Operated	Non-operated
0-4	0.545	0.693	0-4	0.557	0.726
4 to 6	0.148	0.267	4 to 6	0.148	0.272
6 to 8	0.198	0.053	6 to 8	0.204	0.046
8 to 10	0.13	0.09	8 to 10	0.13	0.08
10 to 12	0.142	0.24	10 to 12	0.148	0.171

REFERENCES

- A K Hegtvedt, M L Ollins, R P White Jr, T. A. T. (1987). Minimizing the risk of transfusions in orthognathic surgery: use of predeposited autologous blood. *Int J Adult Orthodon Orthognath Surg*, 2(4), 185–192.
- Abou Chebel, N., Saadeh, M., & Haddad, R. (2020). Unilateral sagittal split osteotomy: effect on mandibular symmetry in the treatment of class III with laterognathia. *Progress in Orthodontics*, 21(1). <https://doi.org/10.1186/s40510-020-00319-3>
- Alper, B., Gultekin, P., & Yalci, S. (2012). Application of Finite Element Analysis in Implant Dentistry. In *Finite Element Analysis - New Trends and Developments*. InTech. <https://doi.org/10.5772/48339>
- Amini B. (2015, May 7). Temporomandibular joint MRI anatomy. Case study. *Radiopaedia.Org* .
- Ammoury, M. J., Abou Chebel, N., & Macari, A. T. (2022). Three-dimensional surgical management of a patient with Pruzansky I hemifacial microsomia and severe facial asymmetry: A 4-year follow-up. *American Journal of Orthodontics and Dentofacial Orthopedics*, 161(5), 708–726. <https://doi.org/10.1016/j.ajodo.2020.11.046>
- Ammoury, M. J., Mustapha, S., Dechow, P. C., & Ghafari, J. G. (2019). Two distalization methods compared in a novel patient-specific finite element analysis. *American Journal of Orthodontics and Dentofacial Orthopedics*, 156(3), 326–336. <https://doi.org/10.1016/j.ajodo.2018.09.017>
- Angle, E. H. (1899). Classification of malocclusion.
- Bell, R. B. (2018). A History of Orthognathic Surgery in North America. *Journal of Oral and Maxillofacial Surgery*, 76(12), 2466–2481. <https://doi.org/10.1016/j.joms.2018.09.006>
- Berg, R. (1979). Post-retention analysis of treatment problems and failures in 264 consecutively treated cases. *European Journal of Orthodontics*, 1(1), 55–68. <https://doi.org/10.1093/ejo/1.1.55>
- Beukes, J., Reyneke, J. P., & Damstra, J. (2016). Unilateral sagittal split mandibular ramus osteotomy: Indications and geometry. *British Journal of Oral and Maxillofacial Surgery*, 54(2), 219–223. <https://doi.org/10.1016/j.bjoms.2015.10.029>
- Böckmann, R., Meyns, J., Dik, E., & Kessler, P. (2014). The modifications of the sagittal ramus split osteotomy: A literature review. *Plastic and Reconstructive Surgery - Global Open*, 2(12). <https://doi.org/10.1097/GOX.0000000000000127>
- Carcedo, M. G. (2010). Anthropometric Characterization of Human Subjects.
- Carter, D. R., & Spengler, D. M. (1978). basic science and pathology *Mechanical Properties and Composition of Cortical Bone*.
- Carter, L., Farman, A. G., Geist, J., Scarfe, W. C., Angelopoulos, C., Nair, M. K., Hildebolt, C. F., Tyndall, D., & Shrout, M. (2008). American Academy of Oral and Maxillofacial Radiology executive opinion statement on performing and interpreting diagnostic cone beam computed tomography. In *Oral Surgery, Oral Medicine, Oral Pathology, Oral Radiology and Endodontology* (Vol. 106, Issue 4, pp. 561–562). <https://doi.org/10.1016/j.tripleo.2008.07.007>

- Chen, J., Akyuz, U., Xu, L., & Pidaparti, R. M. V. (1998). Stress analysis of the human temporomandibular joint. In *Medical Engineering & Physics* (Vol. 20).
- Chen, M. Y. C., Wu, Y. F., Huang, H. L., & Hsu, J. T. (2020). Biomechanical evaluation of sagittal split ramus osteotomy fixation techniques in Mandibular setback. *Applied Sciences* (Switzerland), 10(9). <https://doi.org/10.3390/app10093031>
- Choi Jong-Woo & Lee Jang Yeol. (2021). Virtual Surgical Planning and Three-Dimensional Simulation in Orthognathic Surgery. In *The Surgery-First Orthognathic Approach: With discussion of occlusal plane-altering orthognathic surgery*, (pp. 159–183). SpringerLink.
- Chugh, T., Ganeshkar, S. V., Revankar, A. V., & Jain, A. K. (2013). Quantitative assessment of interradicular bone density in the maxilla and mandible: Implications in clinical orthodontics. *Progress in Orthodontics*, 14(1). <https://doi.org/10.1186/2196-1042-14-38>
- Cobo, J., Sicilia, A., Argfielles, J., Suarez, D., & Vijande, M. (1993). Initial stress induced in periodontal tissue with diverse degrees of bone loss by an orthodontic force: Tridimensional analysis by means of the finite element method.
- Cowin, S. C., & Hart, R. T. (1990). technicalnote-errors in the orientation of the principal stress axes if bone tissue is modeled as isotropic.
- de Leeuw, R. ; K. G. D. A. A. of O. P. (2018). *Orofacial pain: Guidelines for assessment, diagnosis and management* (Sixth edit). quintessence publishing Co. Ltd.
- Fang, B., Shen, G. F., Yang, C., Wu, Y., Feng, Y. M., Mao, L. X., & Xia, Y. H. (2009). Changes in condylar and joint disc positions after bilateral sagittal split ramus osteotomy for correction of mandibular prognathism. *International Journal of Oral and Maxillofacial Surgery*, 38(7), 726–730. <https://doi.org/10.1016/j.ijom.2009.03.001>
- Fill, T. S., Toogood, R. W., Major, P. W., & Carey, J. P. (2012). Analytically determined mechanical properties of, and models for the periodontal ligament: Critical review of literature. In *Journal of Biomechanics* (Vol. 45, Issue 1, pp. 9–16). <https://doi.org/10.1016/j.jbiomech.2011.09.020>
- Fonseca R.J. (2017). *Oral and Maxillofacial Surgery-Inkling Enhanced E-Book: 3-Volume Set*. Elsevier Health Sciences.
- Gačnik, F., Ren, Z., & Hren, N. I. (2014). Modified bone density-dependent orthotropic material model of human mandibular bone. *Medical Engineering and Physics*, 36(12), 1684–1692. <https://doi.org/10.1016/j.medengphy.2014.09.013>
- Geng Jian-Ping, Tan Keson B. C, & Lui Gui-Rong. (2001). Application of finite element analysis in implant dentistry: A review of the literature.
- Ghafoor, H. (2018). Reverse engineering in orthodontics. *Turkish Journal of Orthodontics*, 31(4), 139–144. <https://doi.org/10.5152/TurkJOrthod.2018.18027>
- Guyer, E. C., Ellis, E. E., McNamara, J. A., & Behrents, R. G. (1986). Components of class III malocclusion in juveniles and adolescents. In *The Angle orthodontist* (Vol. 56, Issue 1, pp. 7–30). [https://doi.org/10.1043/0003-3219\(1986\)056<0007:COCIMI>2.0.CO;2](https://doi.org/10.1043/0003-3219(1986)056<0007:COCIMI>2.0.CO;2)
- Halazonetis, J. A. (1968). the “weak” regions of the mandible.
- Hassan, M. K. R. M. S. L. F. A. (2018). A Finite Element Analysis Study Comparing 3 Internal Fixation Techniques in Mandibular Sagittal Split Osteotomy. *International Journal of Otolaryngology and Head & Neck Surgery*, 298–311.

- Henderson, D. (1981). the vertical dimension in orthognathic surgery Introduction In the assessment of cases for orthognathic surgery individuals are encountered who exhibit imbalance between the vertical and horizontal components of the facial skeleton and other parts of the f. March.
- Hohmann, A., Kober, C., Young, P., Dorow, C., Geiger, M., Boryor, A., Sander, F. M., Sander, C., & Sander, F. G. (2011). Influence of different modeling strategies for the periodontal ligament on finite element simulation results. *American Journal of Orthodontics and Dentofacial Orthopedics*, 139(6), 775–783. <https://doi.org/10.1016/j.ajodo.2009.11.014>
- Hu, J., Song, Y., Wang, D., Yuan, H., Jiang, H., & Cheng, J. (2020). Patterns of lingual split and lateral bone cut end and their associations with neurosensory disturbance after bilateral sagittal split osteotomy. *International Journal of Oral and Maxillofacial Surgery*, 49(5), 595–601. <https://doi.org/10.1016/j.ijom.2019.09.003>
- Jacobs, J. D., Bell, W. H., Williams, C. E., & Kennedy, J. W. (1980). Control of the transverse dimension with surgery and orthodontics. *American Journal of Orthodontics*, 77(3), 284–306. [https://doi.org/10.1016/0002-9416\(80\)90083-4](https://doi.org/10.1016/0002-9416(80)90083-4)
- Jacobs, J. D., & Sinclair, P. M. (1983). Principles of orthodontic mechanics in orthognathic surgery cases. *American Journal of Orthodontics*, 84(5), 399–407. [https://doi.org/10.1016/0002-9416\(93\)90003-P](https://doi.org/10.1016/0002-9416(93)90003-P)
- Jakobsone, G., Stenvik, A., Sandvik, L., & Espeland, L. (2011). Three-year follow-up of bimaxillary surgery to correct skeletal Class III malocclusion: Stability and risk factors for relapse. *American Journal of Orthodontics and Dentofacial Orthopedics*, 139(1), 80–89. <https://doi.org/10.1016/j.ajodo.2009.03.050>
- Jaradat, M. (2018). An Overview of Class III Malocclusion (Prevalence, Etiology and Management). *Journal of Advances in Medicine and Medical Research*, 25(7), 1–13. <https://doi.org/10.9734/jammr/2018/39927>
- Kaku, N., Hosoyama, T., Shibuta, Y., Kimura, M., & Tsumura, H. (2023). Influence of femoral bowing on stress distribution of the proximal femur: a three-dimensional finite element analysis. *Journal of Orthopaedic Surgery and Research*, 18(1). <https://doi.org/10.1186/s13018-023-03559-1>
- Kim, M. I., Kim, J. H., Jung, S., Park, H. J., Oh, H. K., Ryu, S. Y., & Kook, M. S. (2015). Condylar positioning changes following unilateral sagittal split ramus osteotomy in patients with mandibular prognathism. *Maxillofacial Plastic and Reconstructive Surgery*, 37(1). <https://doi.org/10.1186/s40902-015-0036-y>
- Klein, K. P., Kaban, L. B., & Masoud, M. I. (2020). Orthognathic Surgery and Orthodontics: Inadequate Planning Leading to Complications or Unfavorable Results. *Oral and Maxillofacial Surgery Clinics of North America*, 32(1), 71–82. <https://doi.org/10.1016/j.coms.2019.08.008>
- Ko, C.-C., Rocha, E. P., & Larson, M. (2012). Past, Present and Future of Finite Element Analysis in Dentistry. www.intechopen.com
- Kojima, Y., Kawamura, J., & Fukui, H. (2012). Finite element analysis of the effect of force directions on tooth movement in extraction space closure with miniscrew sliding mechanics. *American Journal of Orthodontics and Dentofacial Orthopedics*, 142(4), 501–508. <https://doi.org/10.1016/j.ajodo.2012.05.014>

- Ledley, R. S., & Huang, H. K. (1968). Linear Model of Tooth Displacement by Applied Forces.
- Lee, K. J. (2014). Pre-orthodontic Orthognathic Surgery (POGS) Using TADs: Evidences and Applications. In *Temporary Skeletal Anchorage Devices: A Guide to Design and Evidence-Based Solution* (pp. 209–229).
- Lee, S.-G., Kang, Y.-H., Byun, J.-H., Kim, U.-K., Kim, J.-R., & Park, B.-W. (2015a). Stability of unilateral sagittal split ramus osteotomy for correction of facial asymmetry: long-term case series and literature review. *Journal of the Korean Association of Oral and Maxillofacial Surgeons*, 41(3), 156. <https://doi.org/10.5125/jkaoms.2015.41.3.156>
- Lee, S.-G., Kang, Y.-H., Byun, J.-H., Kim, U.-K., Kim, J.-R., & Park, B.-W. (2015b). Stability of unilateral sagittal split ramus osteotomy for correction of facial asymmetry: long-term case series and literature review. *Journal of the Korean Association of Oral and Maxillofacial Surgeons*, 41(3), 156. <https://doi.org/10.5125/jkaoms.2015.41.3.156>
- Li, H., Zhou, N., Huang, X., Zhang, T., He, S., & Guo, P. (2020). Biomechanical effect of asymmetric mandibular prognathism treated with BSSRO and USSRO on temporomandibular joints: a three-dimensional finite element analysis. *British Journal of Oral and Maxillofacial Surgery*, 58(9), 1103–1109. <https://doi.org/10.1016/j.bjoms.2020.06.006>
- Lindorf, H. H., & Steinhäuser, E. W. (1978). Correction of jaw deformities involving simultaneous osteotomy of the mandible and maxilla. *Journal of Maxillofacial Surgery*, 6(C), 239–244. [https://doi.org/10.1016/S0301-0503\(78\)80099-X](https://doi.org/10.1016/S0301-0503(78)80099-X)
- Liu, C., Zhu, X., & Zhang, X. (2015). Three-dimensional finite element analysis of maxillary protraction with labiolingual arches and implants. *American Journal of Orthodontics and Dentofacial Orthopedics*, 148(3), 466–478. <https://doi.org/10.1016/j.ajodo.2015.04.028>
- Liu, Z., Shu, J., Zhang, Y., & Fan, Y. (2018). The Biomechanical Effects of Sagittal Split Ramus Osteotomy on Temporomandibular Joint. *Computer Methods in Biomechanics and Biomedical Engineering*, 21(11), 617–624. <https://doi.org/10.1080/10255842.2018.1504034>
- Loubele, M., Bogaerts, R., van Dijck, E., Pauwels, R., Vanheusden, S., Suetens, P., Marchal, G., Sanderink, G., & Jacobs, R. (2009). Comparison between effective radiation dose of CBCT and MSCT scanners for dentomaxillofacial applications. *European Journal of Radiology*, 71(3), 461–468. <https://doi.org/10.1016/j.ejrad.2008.06.002>
- Luo, H., Teng, H., Chong, D. Y. R., & Liu, Z. (2023). Effects of bilateral sagittal split ramus osteotomy and bimaxillary osteotomies on stress distribution of temporomandibular joints in patients with maxillofacial deformity under asymmetric occlusions. *Medical & Biological Engineering & Computing*. <https://doi.org/10.1007/s11517-023-02785-3>
- McNeil, C., McIntyre, G. T., & Laverick, S. (2014). How much incisor decompensation is achieved prior to orthognathic surgery? *Journal of Clinical and Experimental Dentistry*, 6(3), 225–229. <https://doi.org/10.4317/jced.51310>

- Middleton, J., Jones, M., & Wilson, A. (1996). The role of the periodontal ligament in bone modeling: The initial development of a time-dependent finite element model.
- Ming-Yih, L., Chun-Li, L., Wen-Da, T., & Lun-Jou, L. (2010). Biomechanical stability analysis of rigid intraoral fixation for bilateral sagittal split osteotomy. *Journal of Plastic, Reconstructive and Aesthetic Surgery*, 63(3), 451–455. <https://doi.org/10.1016/j.bjps.2008.11.057>
- Möhlhenrich, S. C., Kamal, M., Peters, F., Fritz, U., Hölzle, F., & Modabber, A. (2016). Bony contact area and displacement of the temporomandibular joint after high-oblique and bilateral sagittal split osteotomy: A computer-simulated comparison. *British Journal of Oral and Maxillofacial Surgery*, 54(3), 306–311. <https://doi.org/10.1016/j.bjoms.2015.12.020>
- Moss, M. L., & Salentijn, L. (1969). The primary role of functional matrices in facial growth. *American Journal of Orthodontics*, 55(6), 566–577. [https://doi.org/10.1016/0002-9416\(69\)90034-7](https://doi.org/10.1016/0002-9416(69)90034-7)
- Netter, Frank H; Norton, Neil Scott; Machado, C. A. G. (2017). *Netter's head and neck anatomy for dentistry* (3rd editio). Elsevier.
- Pachnicz, D., & Ramos, A. (2021). Mandibular condyle displacements after orthognathic surgery-an overview of quantitative studies. In *Quantitative Imaging in Medicine and Surgery* (Vol. 11, Issue 4, pp. 1628–1650). AME Publishing Company. <https://doi.org/10.21037/qims-20-677>
- Pérez Del Palomar, A., & Doblaré, M. (2006). 3D finite element simulation of the opening movement of the mandible in healthy and pathologic situations. *Journal of Biomechanical Engineering*, 128(2), 242–249. <https://doi.org/10.1115/1.2165697>
- Pollei, J. K. (2009). finite element analysis of miniscrew placement in maxillary alveolar bone with varied angulation and material type.
- Proffit, W.R., Fields Jr, H. W. & Sarver, D. M. (2012). *Contemporary Orthodontics*, 5e. Elsevier.
- Qian, H., Chen, J., & Katona, T. R. (2001). The influence of PDL principal fibers in a 3-dimensional analysis of orthodontic tooth movement. *American Journal of Orthodontics and Dentofacial Orthopedics*, 120(3), 272–279. <https://doi.org/10.1067/mod.2001.116085>
- Raposo, R., Peleteiro, B., Paço, M., & Pinho, T. (2018). Orthodontic camouflage versus orthodontic-orthognathic surgical treatment in class II malocclusion: a systematic review and meta-analysis. *International Journal of Oral and Maxillofacial Surgery*, 47(4), 445–455. <https://doi.org/10.1016/j.ijom.2017.09.003>
- Richard, Drake; Vogl, A. Wayne; Mitchell, A. (2020). *Gray's Atlas of Anatomy* (3rd editio).
- Rodrigo D, P. (2000). Stress distribution in the temporomandibular joint affected by anterior disc displacement: a three-dimensional analytic approach with the finite-element method. In *Journal of Oral Rehabilitation*.
- Ryu, H. S., An, K. Y., & Kang, K. H. (2015). Cone-beam computed tomography based evaluation of rotational patterns of dentofacial structures in skeletal class iii deformity with mandibular asymmetry. *Korean Journal of Orthodontics*, 45(4), 153–163. <https://doi.org/10.4041/kjod.2015.45.4.153>

- Scarfe, W. C., & Farman, A. G. (2008). What is Cone-Beam CT and How Does it Work? In *Dental Clinics of North America* (Vol. 52, Issue 4, pp. 707–730).
<https://doi.org/10.1016/j.cden.2008.05.005>
- Schwartz-Dabney, C. L., & Dechow, P. C. (2002a). Edentulation alters material properties of cortical bone in the human mandible. *Journal of Dental Research*, 81(9), 613–617.
<https://doi.org/10.1177/154405910208100907>
- Schwartz-Dabney, C. L., & Dechow, P. C. (2002b). Edentulation alters material properties of cortical bone in the human mandible. *Journal of Dental Research*, 81(9), 613–617.
<https://doi.org/10.1177/154405910208100907>
- Sevillano, M. G. C., Diaz, G. J. F., De Menezes, L. M., Nunes, L. K. F., Miguel, J. A. M., & Quintão, C. C. A. (2020). Management of the Vertical Dimension in the Camouflage Treatment of an Adult Skeletal Class III Malocclusion. *Case Reports in Dentistry*, 2020. <https://doi.org/10.1155/2020/8854588>
- Shu, J. H., Yao, J., Zhang, Y. L., Chong, D. Y. R., & Liu, Z. (2018a). The influence of bilateral sagittal split ramus osteotomy on the stress distributions in the temporomandibular joints of the patients with facial asymmetry under symmetric occlusions. *Medicine (United States)*, 97(25), 1–7.
<https://doi.org/10.1097/MD.00000000000011204>
- Shu, J. H., Yao, J., Zhang, Y. L., Chong, D. Y. R., & Liu, Z. (2018b). The influence of bilateral sagittal split ramus osteotomy on the stress distributions in the temporomandibular joints of the patients with facial asymmetry under symmetric occlusions. *Medicine (United States)*, 97(25).
<https://doi.org/10.1097/MD.00000000000011204>
- Stokbro, K., Aagaard, E., Torkov, P., Bell, R. B., & Thygesen, T. (2014). Virtual planning in orthognathic surgery. *International Journal of Oral and Maxillofacial Surgery*, 43(8), 957–965. <https://doi.org/10.1016/j.ijom.2014.03.011>
- Takahashi, Hiromasa, Furuta, H., Moriyama, S., Sakamoto, Y., Matsunaga, H., & Kikuta, T. (2009). Assessment of three bilateral sagittal split osteotomy techniques with respect to mandibular biomechanical stability by experimental study and finite element analysis simulation. *Medical Bulletin of Fukuoka University*, 181–192.
- Tanaka, E., Del Pozo, R., Tanaka, M., Asai, D., Hirose, M., Iwabe, T., & Tanne, K. (2004). Three-dimensional finite element analysis of human temporomandibular joint with and without disc displacement during jaw opening. *Medical Engineering and Physics*, 26(6), 503–511. <https://doi.org/10.1016/j.medengphy.2004.03.001>
- Tanne, K., Sc, D. D., & Sakuda, M. (1987). Tissue By Orthodontic Forces. *Am J Orthod Dentofacial Orthop* . [https://doi.org/doi:10.1016/0889-5406\(87\)90232-0](https://doi.org/doi:10.1016/0889-5406(87)90232-0).
- Tanne, K., Tanaka, E., Sakuda, M., & Osaka, J. (1996). Stress distribution in the temporomandibular joint produced by orthopedic chincup forces applied in varying directions: A three-dimensional analytic approach with the finite element method. In *Am J Orthod Dentofac Orthop* (Vol. 110).
- Vasudeva, G. (2008). Finite element analysis: A Boon To Dental Research. In *The Internet Journal of Dental Science* (Vol. 6, Issue 2).
- Vasudeva, G., Finite, G. V., To, A. B., Internet, T., & Science, D. (2012). Finite element analysis: A Boon To Dental Research. *The Internet Journal of Dental Science*, 6(2), 1–6. <https://doi.org/10.5580/2626>

- Verdun, F. R., Racine, D., Ott, J. G., Tapiovaara, M. J., Toroi, P., Bochud, F. O., Veldkamp, W. J. H., Schegerer, A., Bouwman, R. W., Hernandez-Giron, I., Marshall, N. W., & Edyvean, S. (2015). Image quality in CT: From physical measurements to model observers. In *Physica Medica* (Vol. 31, Issue 8, pp. 823–843). Associazione Italiana di Fisica Medica. <https://doi.org/10.1016/j.ejmp.2015.08.007>
- Wang, D. (2002). Orthognathic surgery. In *Zhonghua yi xue za zhi* (Vol. 82, Issue 24).
- Wohlwender, I., Daake, G., Weingart, D., Brandsttter, A., Kessler, P., & Lethaus, B. (2011). Condylar resorption and functional outcome after unilateral sagittal split osteotomy. *Oral Surgery, Oral Medicine, Oral Pathology, Oral Radiology and Endodontology*, 112(3), 315–321. <https://doi.org/10.1016/j.tripleo.2010.10.030>
- Wright, E. F. (2014). *Manual of Temporomandibular Disorders* (3rd editio). John Wiley & sons.